Quelques contributions dans la conception de “régions sûres” et “tests d’élagages sûrs” en optimisation convexe

Thu Le Tran

COLLEGE MATHS, TELECOMS
DOCTORAL INFORMATIQUE, SIGNAL
BRETAGNE SYSTEMES, ELECTRONIQUE

Université de Rennes

THÈSE DE DOCTORAT DE

L'UNIVERSITÉ DE RENNES

ÉCOLE DOCTORALE N° 601
Mathématiques, Télécommunications,
Informatique, Signal, Systèmes, Électronique
Spécialité : *Mathématiques et leurs Interactions*

Par

TRAN Thu Le

Some Contributions on Safe Regions and Safe Screening in Convex Optimization

Thèse présentée et soutenue à Rennes, le 14 Décembre 2023
Unité de recherche : IRMAR - UMR CNRS 6625

Rapporteurs avant soutenance :

Vincent DUVAL Directeur de recherche, Inria, Paris
Olivier FERCOQ Professeur, Telecom Paris

Composition du Jury :

Président :	Charles SOUSSEN	Professeur, CentraleSupélec, Paris
Examinateurs :	Luc LE MAGOAROU	Maître de conférences, INSA, Rennes
	Barbara PASCAL	Chargée de recherche, CNRS Nantes
Dir. de thèse :	Cédric HERZET	Chargé de recherche - HDR, Inria, Rennes

Invité(s) :

Co-encadrant de thèse : Hong-Phuong DANG Enseignante-chercheuse, ECAM Rennes - Louis de Broglie
Co-encadrant de thèse : Clément ELVIRA Enseignant-chercheur, CentraleSupélec, Rennes

Acknowledgement

I am sincerely grateful to all those who have played a pivotal role in shaping my academic journey in France, starting from my one-year master's program to my three-year PhD, the journey began in September 2019 and has now reached its culmination with the completion of my PhD thesis in the end of 2023.

Foremost, my heartfelt gratitude go to my main supervisor, Cédric Herzet. His guidance has been instrumental since my master's thesis, steadfastly supporting me throughout the last three years of my doctoral research. During the initial year, I encountered challenges in producing results and publications. I am genuinely appreciative that my supervisors, especially Cédric, chose understanding over pressure. He consistently exhibited patience, provided motivation, and meticulously reviewed my reports, even during times when progress seemed limited. Furthermore, I am grateful for his mentorship in approaching research systematically, steering me in the right direction. The elegance of this thesis is indebted to his invaluable perspectives, significantly enhancing both the results and overall organization. His exceptional teaching skills, adeptly clarifying intricate mathematical concepts and offering insights into technical details, have left an indelible mark on my academic journey. Undoubtedly, Cédric stands out as one of the most influential teachers I've had the privilege to learn from, profoundly shaping my future path as a dedicated researcher.

I would also like to extend my heartfelt gratitude to my supervisor, Clément Elvira. I distinctly recall his patient guidance, ranging from explaining fundamental mathematical concepts to engaging in discussions on the most technical details in the Fenchel-Rockafellar duality theory. His mentorship has been invaluable, characterized by fruitful discussions that sparked new ideas. Furthermore, I appreciate his pivotal role in broadening my skill set, providing guidance in both programming and the art of "storytelling" in academic writing. Alongside Cédric, Clément also played a significant role in shaping my academic journey.

I would also like to express my thanks to my supervisor, Hong-Phuong Dang, who has been a steadfast supporter since my master's studies. I am thankful for her mentorship, both in my personal and academic life. Additionally, I highly appreciate her consistent guidance at every step of my PhD journey, as she has continuously encouraged me and enhanced my confidence.

A special acknowledgment is owed to Valérie Monbet, who played a crucial role in nearly every stage of my study in France. She supervised my master's internship and thesis, proposed the PhD position, and provided total support for my postdoc applications. The moment she informed me

about successfully securing funding for my PhD remains unforgettable. I deeply appreciate her unwavering support and belief in my potential, serving as a significant source of motivation for my ongoing and future research endeavors.

I greatly appreciate the two reviewers, Vincent Duval and Olivier Fercoq, and the examiners, Barbara Pascal, Luc Le Magoarou, and the president, Charles Soussen, who formed the thesis committee for my PhD defense. A special thanks to Vincent for insightful discussions that opened up various potential applications of my results. I am grateful to Olivier for his thorough reading and valuable suggestions, significantly enhancing the quality and rigor of this work. Thanks to Barbara for her encouragement and fruitful discussions. Lastly, my appreciation extends to Luc and Charles for dedicating their time and agreeing to join my committee, as well as for their feedback in improving my thesis.

I would also like to express my thanks to the University of Rennes, Ecole doctorant MATISSE, ENSAI, and, in particular, IRMAR and Inria for enabling me to conduct my PhD research and for their financial support in participating in conferences. Additionally, I extend my thanks to Xhenxila Lachambre, Marie-Aude Verger, and Elodie Cottrel for their valuable administrative support.

I would like to express my gratitude to Hai and Yves, dear friends from our time together in the master's program. Thank you for our insightful discussions and enduring friendship. Special thanks to Ali and Émeric, my office mates, for not only sharing our workspace but also engaging in both life and mathematical conversations. A heartfelt note of appreciation goes to my teachers, relatives and friends in Vietnam, especially those who provided strong support during the preparations for my master's study in France. Thanks to close friends for their care during my days in France. I also want to extend my thanks to friends in and around Crous Mirabeau, especially the "Mathematics team". Your shared thoughts, life stories, and motivations have been invaluable. Thanks for the valuable advice gained from your experiences. Though some have come and gone, I consider each one a person in my second family in France.

Last but not least, I would like to express my deepest gratitude to my parents. Their unwavering support, encouragement, and sacrifices have been the foundation upon which my academic pursuits stand. Additionally, I want to extend my thanks to my love, Ngoc Ngan, your belief in me has been a constant motivator, thank my love!

France, 14th Dec 2023

Tran Thu Le

Table of Contents

NOTATIONS

Notations with font style	
$\mathscr{C}, \mathscr{M}, \mathscr{H}$	General vector spaces
T, B, H	Sets
$\mathbf{x}, \boldsymbol{\theta}, \mathbf{0}, \mathbf{1}$	Vectors
τ, λ, α	Scalars
$f, g, p, d, \kappa, \iota$	Functions
$\mathbf{A}, \mathbf{K}$	Matrices and operators

Standard notations in convex optimization	
$\mathbb{R}^m_+$	Space of non-negative vectors
$\mathscr{V}^*$	Topological dual space of normed space $\mathscr{V}$
$\mathbf{A}^*$	(Pre-)Adjoint operator of operator $\mathbf{A}$
$\mathbf{A}^{\mathrm{T}}$	Transpose of matrix $\mathbf{A}$
h^*	Conjugate of convex function h
κ°	Polar function of gauge function κ
∇f	Gradient of f (in the sense of Fréchet)
$\operatorname{dom} h$	Domain of function h
∂h	Subdifferential of convex function h
$\mathbf{x}^\star$	An optimal vector solution

Non-standard notations	
$\mathbf{a_t} \in \mathscr{H}$	The atom function evaluated at some $\mathbf{t}$
$\mathbf{a}_i \in \mathbb{R}^m$	The ith column of matrix $\mathbf{A}$
$\mathbf{x}(i) \in \mathbb{R}$	The ith coordinate of vector $\mathbf{x}$

Table 1 – Notations.

SUMMARY

Summary in French

Cette thèse concerne une large classe de problèmes d'optimisation convexe (éventuellement non lisse), pénalisés, qui peuvent être exprimés comme suit :

$$\min_{\mathbf{x}\in\mathscr{M}} \quad f(\mathbf{A}\mathbf{x}) + g(\mathbf{x}),$$

où $f : \mathscr{H} \to \mathbb{R} \cup +\infty$, $g : \mathscr{M} \to \mathbb{R} \cup +\infty$ sont des fonctions convexes et $\mathbf{A} : \mathscr{M} \to \mathscr{H}$ est un opérateur linéaire. Ici, $\mathscr{M}$ est un espace de Banach (éventuellement non réflexif) et $\mathscr{H}$ est un espace de Hilbert.

La fonction objectif comprend deux termes : une fonction lisse f appelée terme d'ajustement des données, et une fonction non lisse g appelée terme de pénalisation qui impose une structure aux solutions optimales. Ce problème revêt une importance dans divers domaines, notamment l'apprentissage automatique, la statistique et le traitement du signal/de l'image.

Dans l'ère du big data, les problèmes d'optimisation en dimensions finies impliquent fréquemment des variables de haute dimension, ce qui pose des défis pour les procédures de résolution numérique. Un défi majeur concerne la complexité. Les algorithmes d'optimisation traditionnels tels que les méthodes basées sur le gradient, les méthodes proximales, les méthodes de points intérieurs et la méthode de Newton présentent souvent des complexités computationnelles par itération qui croissent (au moins) linéairement avec la dimension du problème. Un autre défi notable concerne les contraintes de mémoire, car stocker ou manipuler de grandes matrices peut devenir impraticable, en particulier lorsqu'il s'agit de traiter des ensembles de données massifs.

Au cours de la dernière décennie, les méthodes de *safe screening* ont émergé comme des techniques efficaces pour réduire la dimension des problèmes pénalisés par la norme ℓ_1, c'est-à-dire $g = \lambda \|\cdot\|_1$ pour un paramètre de contrôle $\lambda > 0$. Un problème important de cette classe est le célèbre problème LASSO (également connu sous le nom de problème de débruitage de poursuite de base). Récemment, les techniques de safe screening ont été

étendues à divers problèmes en dimensions finies présentant différents termes de régularisation. Au cœur des méthodes de safe screening et de leurs extensions se trouve le concept d'une *safe region*, qui est un ensemble englobant la solution optimale duale (unique). Une safe region efficace devrait avoir une géométrie simple tout en contenir étroitement la solution optimale duale. La conception d'une safe region efficace est devenue un point central de la recherche active dans ce domaine.

Cette thèse apporte deux contributions majeures : Premièrement, elle introduit une nouvelle famille de safe regions ainsi que des cadres généraux qui unifient les safe regions existantes ; Deuxièmement, elle étend la méthodologie de safe screening à des paramètres infinis définis dans l'espace des mesures, avec des applications pour réduire la complexité d'une procédure numérique.

Nouvelles safe regions et cadres unificateurs. Nous introduisons trois nouvelles safe regions : la boule FBI, le demi-espace Hölder et la boule géométrique.

Notre première safe region, appelée *boule FBI*, découle d'une inégalité novatrice appelée *l'Inégalité de Fenchel Bregman (FBI)*. Cette inégalité implique la décomposition de l'écart dual en deux quantités non négatives : la divergence de Fenchel (associée à g) et la divergence de Bregman (associée à f). Cette décomposition nous permet d'obtenir une estimation précise de l'emplacement de la solution optimale duale, en supposant la condition modérée de continuité Lipschitz du gradient de f. En particulier, nous démontrons que toutes les safe regions en boule proposées au cours de la dernière décennie, selon notre connaissance, sont soit des cas particuliers, soit des ensembles contenant la boule FBI.

La deuxième safe region est le *demi-espace Hölder*, qui contient l'ensemble dual réalisable lorsque g est une fonction jauge. Lorsqu'il est combiné avec la boule FBI, cela donne naissance à une nouvelle région bornée appelée le *dôme FBI*. Notamment, le demi-espace Hölder sert également de cadre unificateur pour les demi-espaces existants.

Enfin, mais de manière significative, nous fournissons une formule générale en forme fermée pour la plus petite boule en termes de rayon, centrée arbitrairement, englobant un certain dôme donné. Bien que cette approche ait été utilisée par plusieurs chercheurs dans des contextes de dimension finie dans la littérature, elle a souvent été appliquée dans des configurations spécifiques sans spécifier explicitement la formule générale pour la construction. Ce résultat comble cette lacune. Notez que notre construction est valable dans n'importe quel espace de Hilbert.

En résumé, ces contributions n'introduisent pas seulement de nouvelles safe regions, mais offrent également une perspective complète pour élucider les relations complexes

entre les safe regions existantes. Nous pensons que cette compréhension servira de base à d'éventuelles avancées dans l'étude des safe regions à l'avenir.

Safe screening sur l'espace des mesures. La deuxième contribution étend le principe de safe screening aux problèmes régularisés par la norme de variation totale (TV), c'est-à-dire que nous considérons $g = \lambda \|\cdot\|_{TV}$ pour un certain $\lambda > 0$. Ces problèmes sont de dimension infinie et sont définis dans l'espace des mesures de Radon supportées par un ensemble de paramètres compact T.

Tout d'abord, nous établissons une règle de safe screening analogue pour le problème pénalisé par la norme TV en exploitant la condition d'optimalité dans la théorie de dualité Fenchel-Rockafellar. Cette règle de sélection permet d'identifier les éléments dans T pour lesquels la solution optimale primale a une masse nulle. Plus précisément, elle facilite l'identification des éléments dans T qui n'appartiennent pas au support des mesures optimales primales.

Cependant, cette règle de safe screening rencontre deux limitations pratiques : *i)* elle dépend de la connaissance de la solution optimale duale ; *ii)* elle ne sélectionne qu'un seul élément dans T, alors que l'ensemble de paramètres T comprend un nombre infini non dénombrable de paramètres. Pour résoudre le premier problème, nous pouvons utiliser une safe region. En ce qui concerne le deuxième problème, plutôt que de sélectionner un seul élément dans T, nous pouvons suivre la technique dite de *safe screening conjointe* qui sélectionne un sous-ensemble de T.

Par la suite, nous explorons l'application de la méthode de safe screening proposée pour accélérer une technique de résolution des problèmes régularisés par la norme de variation totale (TV). En particulier, nous nous concentrons sur une procédure récente de résolution pour le problème régularisé par la norme TV connue sous le nom de *Refinement Grid Based (RGB).*

Le concept fondamental de la méthode RGB consiste à discrétiser de manière itérative l'ensemble de paramètres T en cellules (segments en 1D, carrés en 2D et cubes en 3D) et à résoudre la version de dimension finie du problème régularisé par la norme TV sur les sommets de la grille. Cela transforme efficacement le problème en problèmes LASSO. À chaque itération de la méthode RGB, un problème LASSO est résolu sur une grille nouvellement raffinée de sommets pour améliorer la précision de la méthode.

Cependant, la méthode RGB fait face à un défi important lié aux goulots d'étranglement computationnels résultant de la partition de la grille. Bien que les auteurs aient démontré théoriquement que la croissance de la taille de la grille (nombre de cellules) peut être

contrôlée, en pratique, elle a tendance à augmenter de manière significative même lorsque T appartient à des espaces de basse dimension.

Pour résoudre ce problème, nous intégrons l'approche de safe screening avec la méthode RGB. À chaque itération, nous utilisons la safe screening pour identifier et exclure un certain nombre de cellules de la grille RGB, réduisant ainsi efficacement la taille des problèmes LASSO à résoudre.

Notamment, nous prouvons que l'intégration de la safe screening dans RGB réduit non seulement la complexité de la méthode RGB, mais préserve également les propriétés de convergence de la méthode originale. Nous appelons cette propriété souhaitable la *consistance* entre la safe screening et la méthode RGB.

En résumé, notre deuxième contribution étend l'application de la méthodologie de safe screening des problèmes de dimension finie impliquant une pénalisation par la norme ℓ_1 à des problèmes de dimension infinie incorporant une pénalisation par la norme TV. De plus, nous explorons l'efficacité de la safe screening pour atténuer la complexité computationnelle de la méthode de résolution RGB tout en garantissant la consistance. Cette contribution souligne le potentiel de la safe screening pour accélérer la résolution de problèmes de dimension infinie.

Summary in English

This thesis concerns a broad class of (possibly non-smooth) penalized convex optimization problems, which can be expressed as:

$$\min_{\mathbf{x}\in\mathscr{M}} \quad f(\mathbf{A}\mathbf{x}) + g(\mathbf{x}),$$

where $f : \mathscr{H} \to \mathbb{R}\cup\{+\infty\}$, $g : \mathscr{M} \to \mathbb{R}\cup\{+\infty\}$ are convex functions and $\mathbf{A} : \mathscr{M} \to \mathscr{H}$ is a linear operator. Here $\mathscr{M}$ is a (possibly non-reflexive) Banach space and $\mathscr{H}$ is a Hilbert space.

The objective function comprises two terms: a smooth function f called the data fitting term, and a non-smooth function g called penalization term that imposes structure on the optimal solutions. This problem holds significance in various fields, including machine learning, statistics, and signal/image processing.

In the era of big data, optimization problems in finite-dimensions frequently involve high-dimensional variables, posing challenges for numerical solving procedures. A primary challenge involving complexity issue. Traditional optimization algorithms, such as gradient-based methods, proximal-based methods, interior-point methods, and Newton's method, often exhibit computational complexities per iteration that grow (at least) linearly with the dimension of the problem. Another notable challenge pertains to memory constraints, as storing or manipulating large matrices can become impractical, especially when dealing with massive datasets.

In the past decade, *safe screening* methods have emerged as efficient techniques for reducing the dimension of ℓ_1-norm penalized problems, *i.e.*, $g = \lambda\|\cdot\|_1$ for some control parameter $\lambda > 0$. One important problem in this class is the well-known LASSO problem (*a.k.a.* Basis Pursuit Denoising problem). Recently, the safe screening techniques have been extended to various finite-dimensional problems featuring different regularization terms. Central to the safe screening methods and their extensions is the concept of a *safe region*, which is a set encompassing the (unique) dual optimal solution. An effective safe region should have a simple geometry while tightly contain the dual optimal solution. The design of an effective safe region has become a focal point of active research in this field.

This thesis makes two primary contributions: First, it introduces a novel family of safe regions along with general frameworks that unifies existing safe regions; Second, it extends the safe screening methodology to infinite-dimensional settings defined on the space of measures with applications in reducing the complexity of a numerical procedure.

New safe regions and unifying frameworks. We introduce three novel safe regions: FBI ball, Hölder half-space and geometric ball.

Our first safe region, named *FBI ball*, originates from a novel inequality termed the *Fenchel Bregman Inequality (FBI)*. This inequality involves the decomposition of the dual gap into two non-negative quantities: the Fenchel divergence (associated with g) and the Bregman divergence (associated with f). This decomposition enables us to obtain a tight estimation for the location of the dual optimal solution, assuming the mild condition regrading the gradient Lipschitz continuity of f. Specifically, we prove that all safe ball regions proposed in the last decade, according to the best of our knowledge, are either special cases or supersets of the FBI ball.

The second safe region is the *Hölder half-space*, which contains the dual feasible set when g is a gauge function. When combined with the FBI ball, it gives rise to a new bounded region referred to as the *FBI dome*. Notably, the Hölder half-space also serves as a unifying framework for existing safe half-spaces.

Lastly, yet significantly, we provide a general closed-form formula for the smallest ball in terms of radius, centered arbitrarily, that encompasses some given dome. While this approach has been employed by several researchers in finite-dimensional settings in the literature, it has often been applied in specific setups without explicitly specifying the general formula for the construction. This result bridges this gap. Note that our construction holds in any Hilbert space.

In summary, these contributions not only introduce new safe regions but also offer a comprehensive perspective for elucidating the intricate relationships among existing safe regions. We believe that this understanding will serve as a foundation for potential advancements in the study of safe regions in the future.

Safe screening on space of measures. The second contribution extends the safe screening principle to total variation (TV) norm regularized problems, *i.e.*, we consider $g = \lambda \|\cdot\|_{TV}$ for some $\lambda > 0$. These problems are of infinite-dimension and are defined on the space of Radon measures supported on a compact parameter set T.

First, we establish an analogous safe screening rule for the TV-norm penalized problem by leveraging the optimality condition in Fenchel-Rockafellar duality theory. This screening rule enables the identification of elements in T for which the primal optimal solution has zero mass. To be more precise, it facilitates the identification of elements in T that do not belong to the support of the primal optimal measures.

Nevertheless, this safe screening rule faces two practical limitations: *i)* it relies on

knowledge of the dual optimal solution; *ii)* it screens only a single element in T, whereas the parameter set T comprises an infinite uncountable number of parameters. To address the first issue, we can employ a safe region. Regarding the second issue, rather than screening a single element in T, we may follow the so-called *joint safe screening* technique which screens a subset of T.

Subsequently, we explore the application of the proposed safe screening method to expedite a solving technique for TV-norm penalized problems. In particular, we focus on a recent solving procedure for TV-norm penalized problem known as the *Refinement Grid Based (RGB)* method.

The fundamental concept of the RGB method involves iteratively discretizing the parameter set T into cells (segments in 1D, squares in 2D, and cubes in 3D) and solving the finite-dimensional version of the TV-norm penalized problem over the grid vertices. This effectively transforms the problem into LASSO problems. In each iteration of the RGB method, a LASSO problem is addressed over a newly refined grid of vertices to improve the method's precision.

Nevertheless, the RGB method faces a significant challenge related to computational bottlenecks arising from grid partitioning. While the authors have theoretically demonstrated that the growth in grid size (number of cells) can be controlled, in practice, it tends to expand dramatically even when T belongs to low-dimensional spaces.

To address this issue, we integrate the safe screening approach with the RGB method. In each iteration, we utilize safe screening to identify and exclude a number of cells from the RGB grid, effectively reducing the size of the LASSO problems that need to be solved.

Notably, we prove that the integration of safe screening into RGB not only reduces the complexity of the RGB method but also preserves the convergence properties of the original method. We term this desirable property as *consistency* between the safe screening and RGB method.

In summary, our second contribution extends the application of the safe screening methodology from finite-dimensional problems involving ℓ_1-norm penalization to infinite-dimensional problems incorporating TV-norm penalization. Additionally, we explore the effectiveness of safe screening in mitigating the computational complexity of the RGB solving method while achieving a consistency guarantee. This contribution underscores the potential of safe screening in accelerating the resolution of infinite-dimensional problems.

Chapter 1

Introduction

Abstract. *Regularization plays a pivotal role in convex optimization problems appearing in various fields, including statistics, machine learning, signal and image processing. These optimization problems often yield solutions with specific structures, such as sparsity. Recently, innovative methods have emerged that leverage these structural characteristics to develop dimensionality reduction techniques, such as screening rules. At the core of these state-of-the-art methods lies the concept of safe region, which is a set containing optimal solutions of the dual problem.*

This thesis makes a twofold contribution. Firstly, we introduce a family of safe regions with ball and dome geometries, referred to as FBI regions. These regions are rooted in what we term the Fenchel Bregman Inequality (FBI), and our results reveal that all existing safe regions, up to our knowledge, can be seen as special cases within this family. Secondly, we extend the safe screening principle to address regularization problems involving the total variation norm, defined within the space of Radon measures. We also seamlessly integrate this screening approach into a novel algorithm, the Refinement Grid Based method. Remarkably, our approach preserves the iterative solutions, thereby maintaining convergence speed, while significantly reducing computational complexity.

The goal of this chapter is to provide a quick overview of the context and the contributions of the thesis. It is organized as follows. In Section 1.1, we introduce the concepts pivotal to our study, namely "safe screening" and "safe region". Following this, Section 1.2 provides a brief outline of the main contributions of the thesis. Lastly, in Section 1.3, we elaborate on the manuscript's structure.

1.1 Context

General convex optimization problem. In this thesis, our focus is on a broad class of (possibly non-smooth) convex optimization problems, which can be expressed as:

$$\min_{\mathbf{x}\in\mathscr{M}} \quad f(\mathbf{A}\mathbf{x}) + g(\mathbf{x}), \tag{1.1-p_g^f}$$

where $f : \mathscr{H} \to \mathbb{R} \cup \{+\infty\}$, $g : \mathscr{M} \to \mathbb{R} \cup \{+\infty\}$ are convex functions and $\mathbf{A} : \mathscr{M} \to \mathscr{H}$ is a linear operator. Here $\mathscr{M}$ is a (possibly non-reflexive) Banach space and $\mathscr{H}$ is a Hilbert space. This model includes finite-dimensional problems if $\mathscr{M}$ and $\mathscr{H}$ are of finite-dimension.

This type of problem is ubiquitous in machine learning, statistics or signal/image processing, see *e.g.*, [16]. By decomposing the objective function p_g^f into two parts, we often assume that f is a well-behaved function [1] while g encodes all the technical complexities such as non-smoothness. Therefore, we emphasize that problem (1.1-p_g^f) is not a restrictive model but rather a general model with refined structure.

The challenge of solving high-dimensional optimization problems. In the era of big data, optimization problems frequently involve high-dimensional variables. This presents challenges for numerical procedures [97].

One of the main challenges is the complexity of the numerical procedures addressing these problems. Traditional optimization algorithms, such as gradient-based methods, proximal-based methods, interior-point methods and Newton's method, often have computational complexities per iteration growing (at least) linearly with the dimension of the problem. Another challenge is about memory constraints since storing or manipulating large matrices can be infeasible, particularly when dealing with massive datasets.

To address these challenges, a promising approach is to reduce the dimension of the problem before or during the solving process. This reduction of the problem dimension

1. In this thesis, we will assume that f is gradient Lipschitz.

can significantly improve computational efficiency and alleviate memory constraints.

Dimension reduction for structured problems. A widely advocated way to reduce the dimension of some optimization problem is to exploit some known structure of its solutions. One notable example of procedure following this strategy is the so-called *"safe screening"* method proposed in the seminal work [52]. The terminology and idea of this dimensionality reduction technique will be concisely outlined below.

Safe region. A pivotal concept in the construction of dimensionality-reduction techniques (such as safe screening mentioned above) is the notion of *"safe region"*. Letting [2]

$$\mathbf{u}^\star \in \arg\max_{\mathbf{u}\in\mathscr{H}} \quad -f^*(-\mathbf{u}) - g^*(\mathbf{A}^*\mathbf{u}) \tag{1.2-d_g^f}$$

be the pre-dual problem of (1.1-p_g^f), we say that some subset $S \subset \mathscr{H}$ is a safe region if

$$\mathbf{u}^\star \in S. \tag{1.3}$$

In other word, a safe region is a subset of the dual space provably containing a maximizer of the pre-dual problem. The construction of "good" safe regions is one of the central theme of this thesis. We demonstrate below the crucial role of these regions in the construction of effective safe screening methods.

Dimension reduction by identification of the zeros. Consider the following ℓ_1-norm penalized problem:

$$\min_{\mathbf{x}\in\mathbb{R}^n} \quad f(\mathbf{A}\mathbf{x}) + \lambda \|\mathbf{x}\|_1 , \tag{1.4-$p^f_{\lambda\|\cdot\|_1}$}$$

where $f : \mathbb{R}^m \longrightarrow \mathbb{R} \cup \{+\infty\}$ is some proper, closed, convex function, $\mathbf{A} \in \mathbb{R}^{m\times n}$ and $\lambda > 0$. We note that (1.4-$p^f_{\lambda\|\cdot\|_1}$) is a particular instance of (1.1-p_g^f) with $g = \lambda\|\cdot\|_1$.

In the sequel, to simplify our exposition we will assume that the problem (1.4-$p^f_{\lambda\|\cdot\|_1}$) admits a unique optimal solution, denoted by $\mathbf{x}^\star$.

It is important to note that using the ℓ_1-norm as a penalization function induces a sparsity structure in $\mathbf{x}^\star$, meaning that most of the coordinates of $\mathbf{x}^\star$ are zeros. For instance, in the case of the LASSO problem (where $f = \|\mathbf{b} - \cdot\|_2^2/2$ for some $\mathbf{b} \in \mathbb{R}^m$), it is known that $\mathbf{x}^\star$ will have at least $n-m$ zero entries [49, Theorem 6.1]. This observation highlights the prevalence of sparsity in the optimal solution, particularly when $m \ll n$.

2. Here f^* and g^* denote the convex conjugate of f and g, respectively, $\mathbf{A}^*$ is the pre-adjoint operator of $\mathbf{A}$. We note that if $\mathbf{A} \in \mathbb{R}^{m\times n}$, then $\mathbf{A}^* = \mathbf{A}^{\mathrm{T}}$.

We now illustrate how the knowledge of the position of zero/non-zero entries in $\mathbf{x}^\star$ can help reducing the problem dimension. Let

$$L \supseteq \{i \in \{1, \dots, n\} : \mathbf{x}^\star(i) \neq 0\} \tag{1.5}$$

be some set provably containing the indices of the non-zero elements of $\mathbf{x}^\star$. Then, problem (1.4-$p^f_{\lambda\|\cdot\|_1}$) can be equivalently rewritten as

$$\min_{\mathbf{x}_L \in \mathbb{R}^{|L|}} \quad f(\mathbf{A}_L \mathbf{x}_L) + \lambda \|\mathbf{x}_L\|_1 , \tag{1.6}$$

where $\mathbf{x}_L$ and $\mathbf{A}_L$ denote the restriction of $\mathbf{x}$ and $\mathbf{A}$ to their coordinates and column indices in L, respectively. We note that, depending on the cardinality of L, problem (1.6) can be of much lower dimension than (1.4-$p^f_{\lambda\|\cdot\|_1}$). In particular, if equality holds in (1.5) and the minimizer $\mathbf{x}^\star$ is very sparse, we typically have $|L| \ll n$. In this case, addressing problem (1.6) rather than (1.4-$p^f_{\lambda\|\cdot\|_1}$) leads to significant advantages, as enhanced computational efficiency and reduced memory storage.

Safe screening. Screening (also sometimes called *"feature elimination"*) refers to a technique to construct some superset L verifying (1.5). These names stem from the observation that estimating L is equivalent to recognizing the zero entries in the optimal solutions $\mathbf{x}^\star$, which in turn implies the elimination of non-contributing columns in the matrix $\mathbf{A}$.

Screening methods have been extensively studied in the literature and can be classified into two categories: *safe* and *unsafe* approaches. The exploration of unsafe screening methods predates that of the safe approaches. Two of them are *e.g.*, *strong screening* [86] and *sure screening* [44] with a short overview presented in [72]. The significant drawback of the unsafe approaches is their potential to mistakenly eliminate relevant features, resulting in the removal of non-zero entries in the optimal solution $\mathbf{x}^\star$. On the other hand, safe screening, which is one of the main focuses of this thesis, provably removes entries that are guaranteed to be zero in $\mathbf{x}^\star$.

Considering problem (1.4-$p^f_{\lambda\|\cdot\|_1}$), the basic idea of most safe screening methods of the literature is as follows. Let

$$\begin{aligned} \mathbf{u}^\star \in \arg\max_{\mathbf{u} \in \mathbb{R}^m} \quad & -f^*(-\mathbf{u}) \\ \text{s.t.} \quad & |\langle \mathbf{a}_i, \mathbf{u} \rangle| \leq \lambda, \forall i = 1, ..., n \end{aligned} \tag{1.7-$d^f_{\lambda\|\cdot\|_1}$}$$

be the dual problem of (1.4-$p^f_{\lambda\|\cdot\|_1}$), where $\mathbf{a}_i$ is the ith column of matrix $\mathbf{A}$. Assuming that $\mathbf{u}^\star$ is unique, standard optimality conditions lead to [3]

$$|\langle \mathbf{a}_i, \mathbf{u}^\star \rangle| < \lambda \Longrightarrow \mathbf{x}^\star(i) = 0. \tag{1.8}$$

In other words, detecting that some dual constraints are not saturated by the dual optimal solution $\mathbf{u}^\star$ lead to the conclusion that some elements of the primal solution are zeros.

Unfortunately, solving the dual problem is usually as complex as solving the target primal problem. Nevertheless, as first suggested by El Ghaoui et al in [52], the left-hand side of (1.8) can be relaxed if some "safe region" for $\mathbf{u}^\star$ is known. More specifically, assuming that one knows some set S verifying (1.3), we have

$$\sup_{\mathbf{u}\in S} |\langle \mathbf{a}_i, \mathbf{u} \rangle| < \lambda \Longrightarrow \mathbf{x}^\star(i) = 0. \tag{1.9}$$

It is clear from the above expression that depending on the choice of S: *i)* evaluating the left-hand side of (1.9) may or not be tractable; *ii)* the left-hand side of (1.9) may or not be a good proxy for (1.8). In the following, we will briefly describe the basic principles on which practioners rely to choose a "good" safe region with respect to these criteria.

Constructing "good" safe regions. Roughly speaking, a good safe region should possess "simplicity" and "tightness", that is to say, should ensure that the evaluation of the supremum in (1.9) is straightforward and that $\sup_{\mathbf{u}\in S} |\langle \mathbf{a}_i, \mathbf{u} \rangle|$ closely approximates the value of $|\langle \mathbf{a}_i, \mathbf{u}^\star \rangle|$.

The "simplicity" criterion is usually addressed by enforcing S to have (by construction) some desirable geometry. For example, letting $S = B(\mathbf{c}, r)$ be a ball with center $\mathbf{c}$ and radius r, we have

$$\sup_{\mathbf{u}\in S} |\langle \mathbf{a}_i, \mathbf{u} \rangle| = |\langle \mathbf{a}_i, \mathbf{c} \rangle| + r\|\mathbf{a}_i\|_2, \tag{1.10}$$

that is the complexity required to compute the supremum is dominated by the evaluation of one inner product. On top of balls, several other "simple" geometric shapes have been explored in the literature: dome (intersection of ball and half-space) [96], refined dome (intersection of ball and two half-spaces) [97, Section 4.5] or ellipsoid [23]. Among these options, the simplest (and the most popular) geometries are balls and domes, which have

3. This is known as the *complementary slackness* in the Karush–Kuhn–Tucker (KKT) optimality conditions.

garnered substantial attention in the research literature and will be the main focus of this thesis.

The design of "tight" safe regions with a given geometry is a challenging task that has sparked the interest of many researchers in the recent years. We refer the reader to Table 1.1 and Chapter 2 for a review of the existing safe ball/dome constructions of the literature. Hereafter we make a small focus on one of the most influential result proposed during the last decade, namely the "GAP" ball [45]. The GAP ball is proven to be safe for any problem (1.1-p_g^f) with f is α^{-1}-gradient-Lipschitz and g is a norm. It is defined as

$$B_{\texttt{GAP}}(\mathbf{x}, \mathbf{u}) \triangleq B\left(\mathbf{u}, \sqrt{\frac{2\,\mathrm{GAP}(\mathbf{x}, \mathbf{u})}{\alpha}}\right), \tag{1.11}$$

where $(\mathbf{x}, \mathbf{u})$ denotes some primal-dual couple and $\mathrm{GAP}(\mathbf{x}, \mathbf{u})$ is the duality gap defined as the difference between the primal value (1.4-$p^f_{\lambda\|\cdot\|_1}$) and dual value (1.7-$d^f_{\lambda\|\cdot\|_1}$). We note (for the sake of comparison with one of the results derived in this thesis) that the GAP ball is a consequence of the following inequality, valid for any primal-dual feasible couple $(\mathbf{x}, \mathbf{u})$:

$$\frac{\alpha}{2}\,\|\mathbf{u}^\star - \mathbf{u}\|_2^2 \leq \mathrm{GAP}(\mathbf{x}, \mathbf{u}). \tag{1.12}$$

We also emphasize that, provided that strong duality and the continuity of dual gap, the radius of the GAP ball can be made arbitrarily small by choosing proper instances of primal-dual couples. Because of this nice feature, the GAP ball has played a dominant role in this field of safe regions with several improvements proposed in [72, 25, 27] and many applications [72, 28, 24, 26, 40, 65, 43, 54, 53].

Year	Safe region	Relation	Safeness inequality
2010	SAFE ball [52]	$\supset B_{\texttt{FBI}}(\mathbf{0}, \mathbf{u})$	$B \leq C,\ D = 0$
2014	SLORES ball [93]	$\supset B_{\texttt{FBI}}\left(\mathbf{x}^\star_{\lambda_0}, \frac{\lambda}{\lambda_0}\mathbf{u}^\star_{\lambda_0}\right)$	$B \leq C,\ D = 0$
2014	SASVI ball [66]	$= B_{\texttt{FBI}}(\mathbf{0}, \mathbf{u})$	$A + B \leq C,\ D = 0$
2015	DPP ball [92]	$\supset B_{\texttt{FBI}}\left(\frac{\lambda}{\lambda_0}\mathbf{x}^\star_{\lambda_0}, \frac{\lambda}{\lambda_0}\mathbf{u}^\star_{\lambda_0}\right)$	$A \leq C,\ D = 0$
2015	EDPP ball [92]	$= B_{\texttt{FBI}}\left(\tau\mathbf{x}^\star_{\lambda_0}, \frac{\lambda}{\lambda_0}\mathbf{u}^\star_{\lambda_0}\right)$	$A + B \leq C,\ D = 0$
2015	GAP ball [45, 72]	$\supset B_{\texttt{FBI}}(\mathbf{x}, \mathbf{u})$	$A \leq C + D$
2016	FNE ball [67]	$= B_{\texttt{FBI}}(\mathbf{x}, \mathbf{u})$	$A + B \leq C,\ D = 0$
2021	DEDPP ball [99]	$= B_{\texttt{FBI}}(2\gamma\mathbf{x}, \mathbf{u})$	$A + B \leq C + D$
2022	SFER ball [75]	$= B_{\texttt{FBI}}\left(\mathbf{x}^\star_{\lambda_0}, \frac{\lambda}{\lambda_0}\mathbf{u}^\star_{\lambda_0}\right)$	$A + B \leq C,\ D = 0$
2022	$\mathbf{x}$-GAP ball [59]	$\supset B_{\texttt{FBI}}(\mathbf{x}, \mathbf{u})$	$B \leq C + D$
2023	FBI ball (this work)	$= B_{\texttt{FBI}}(\mathbf{x}, \mathbf{u})$	$A + B \leq C + D$
2012	ST half-space [96]	$= H_{\texttt{Hö}}(\mathbf{e}_{i_0})$	
2014	SASVI half-space [66]	$= H_{\texttt{Hö}}(\mathbf{x}^\star_{\lambda_0})$	
2015	GAP excluding ball [45]	$\supset H_{\texttt{Hö}}(\mathbf{x})$	
2023	Hölder half-space (this work)	$= H_{\texttt{Hö}}(\mathbf{x})$	
2012	ST dome [96]	$= D_{\texttt{FBI}}(\mathbf{e}_{i_0}, \mathbf{0}, \mathbf{u})$	
2014	SASVI dome [66]	$= D_{\texttt{FBI}}\left(\mathbf{x}^\star_{\lambda_0}, \mathbf{0}, \frac{\lambda}{\lambda_0}\mathbf{u}^\star_{\lambda_0}\right)$	
2015	GAP dome, moon [45]	$\supset D_{\texttt{FBI}}(\mathbf{x}, \mathbf{0}, \mathbf{u})$	
2022	DSASVI dome [99, 87]	$= D_{\texttt{FBI}}(\mathbf{x}, \mathbf{0}, \mathbf{u})$	
2022	SFER dome [75]	$= D_{\texttt{FBI}}\left(\mathbf{e}_{i_0}, \mathbf{x}^\star_{\lambda_0}, \frac{\lambda}{\lambda_0}\mathbf{u}^\star_{\lambda_0}\right)$	
2023	FBI dome (this work)	$= D_{\texttt{FBI}}(\mathbf{x}', \mathbf{x}, \mathbf{u})$	
2011	ST2 ball [95]	is a geo. ball	
2011	ST3 ball [95]	is a geo. ball	
2023	geo. ball (this work)		

Table 1.1 – The proposed safe regions unify existing safe regions. The third column compares the existing safe regions with the proposed regions based the thos choice of $\mathbf{x}$ and $\mathbf{u}$. The fourth column presents the safeness inequality of existing safe ball regions using (1.13-FBI) as a reference. We refer the readers to Section 2.2.3 for the notations and overview of safe regions and to Chapter 3 for the proofs of comparisons.

1.2 Contributions

The contributions of this thesis can be split into two main groups including the introduction of new safe regions (see Section A below) and an extension of safe screening methods to space of measures (see Section B below). Section C contains the description

of some additional side results which have been derived during the thesis.

A. New safe regions. Our three main results are summarized below and correspond to the material presented in Chapter 3.

A1. FBI ball. Our first result is called the *"Fenchel Bregman Inequality"* (FBI). This inequality implies two main outcomes. First, its immediate consequence establishes the safeness of a new ball region, named *"FBI ball"*. Second, it offers a comprehensive framework that characterizes existing safe ball regions as special cases.

The result regarding the FBI is detailed in Lemma 3.1.2, which proves that if strong duality holds between (1.1-p_g^f) and (1.2-d_g^f) and the loss function f is α^{-1}-strongly smooth (*i.e.*, its gradient ∇f is α^{-1}-Lipschitz continuous), then the following inequality holds true for any pair of primal-dual feasible vector $(\mathbf{x}, \mathbf{u})$:

$$\underbrace{\frac{\alpha}{2}\left\|\mathbf{u}^\star - \mathbf{u}\right\|_{\mathscr{H}}^2}_{A} + \underbrace{\frac{\alpha}{2}\left\|\mathbf{u}^\star - \mathbf{r}_\mathbf{x}\right\|_{\mathscr{H}}^2}_{B} \leq \overbrace{\underbrace{\mathrm{Breg}_{f^{*-},-\mathbf{A}\mathbf{x}}(\mathbf{u}, \mathbf{r}_\mathbf{x})}_{C} + \underbrace{\mathrm{Fen}_g(\mathbf{x}, \mathbf{A}^*\mathbf{u})}_{D}}^{\mathrm{GAP}(\mathbf{x},\mathbf{u})}. \tag{1.13-FBI}$$

where $\mathbf{r}_\mathbf{x} = -\nabla f(\mathbf{A}\mathbf{x})$ and $f^{*-}(\cdot) = f^*(-\cdot)$. For the precise definitions of Fenchel divergence Fen and Bregman divergence Breg please refer to equations (B.3) and (B.4), respectively. This inequality provides an upper bound estimation on the (weighted squared) distance between optimal dual solution $\mathbf{u}^\star$ and $\mathbf{u}/\mathbf{r}_\mathbf{x}$ as a function of the dual gap. We also show that the latter can be expressed as a sum of non-negative quantities involving Fenchel and Bregman divergences.

The first implication of FBI is the derivation of a new safe region, namely the *"FBI ball"*. Indeed, by rearranging the terms of (1.13-FBI), one can easily verify that the following ball region is safe:

$$B_{\texttt{FBI}}(\mathbf{x}, \mathbf{u}) \triangleq B\left(\frac{\mathbf{u} + \mathbf{r}_\mathbf{x}}{2}, \sqrt{\frac{\mathrm{GAP}\,(\mathbf{x}, \mathbf{u})}{\alpha} - \frac{\left\|\mathbf{u} - \mathbf{r}_\mathbf{x}\right\|_{\mathscr{H}}^2}{4}}\right).$$

The formal statement of this result can be found in Theorem 3.1.3.

When compared to the GAP safe ball region defined in (1.11) (by choosing $\mathscr{H} = \mathbb{R}^m$ in (1.2) and considering g as a gauge function), the following remarks can be raised. First, the squared radius of the FBI ball is (at most) half the size of that of the GAP ball. Second, it can be seen from (1.13-FBI) and (1.12) that the FBI ball is a strict subset of the GAP ball. Consequently, the FBI ball provides (in some sense) a more precise estimation

of the value of $\mathbf{u}^\star$ than the GAP ball.

It is important to emphasize that the FBI goes beyond merely representing the safeness condition of the newly-proposed safe region: it also enriches our comprehension of other existing safe ball regions. In essence, the FBI serves as a general inequality, providing a unifying framework which, to the best of our knowledge, encompasses the safeness inequalities for all known safe ball regions. A sequence of results, from Corollaries 3.1.8 to 3.1.16, substantiates this assertion and is summarized in the first part of Table 1.1. This table presents a two-tiered comparison, with the third column indicating the choice of $(\mathbf{x}, \mathbf{u})$ for which an existing safe ball region and the FBI ball can be compared. The last column elucidates their relationship using safeness inequality, employing the (1.13-FBI) as a referenced inequality. Therefore, the third and fourth column thus serve as the "blueprint" for distinguishing between the existing safe ball regions.

From a theoretical perspective, the generality of FBI ball provides an explanation for the intricate relationships among the existing safe regions. This understanding sheds light on the underlying structure and connections between different safe regions, offering insights into their properties and potential improvements in the future.

A2. Hölder half-space and FBI dome. Our next result pertains to a safe region characterized by a half-space geometry structure, referred to as *"Hölder half-space"*. In the context of the LASSO problem, this result was previously published in our conference paper [87]. In this thesis, we prove that the Hölder half-space is also safe for a more general class of problems. When combined with the FBI ball, it yields a new bounded region, dubbed *"FBI dome"*. Interestingly, the FBI dome encompasses existing safe dome regions as particular cases.

Here, we assume that regularization function in (1.1-p_g^f) corresponds to a scaled version of some gauge function κ,[4] *i.e.*, $g = \lambda\kappa$ for some tuning parameter $\lambda > 0$. In this case, the pre-dual problem (1.2-d_g^f) takes the form:

$$\max_{\mathbf{u} \in U_{\lambda\kappa}} \quad -f^*(-\mathbf{u})$$

where

$$U_{\lambda\kappa} = \{\mathbf{u} \in \mathscr{H} : \kappa^\circ(\mathbf{A}^*\mathbf{u}) \leq \lambda\}$$

and $\kappa^\circ(\mathbf{z}) \triangleq \sup\{\langle \mathbf{z}, \mathbf{x} \rangle : \kappa(\mathbf{x}) \leq 1, \mathbf{x} \in \mathscr{M}\}$ denotes the polar of κ. In particular, we ob-

4. For the definition of gauge function and its polar, please refer to Definitions B.1.11 and B.1.17.

serve that the dual feasible set $U_{\lambda\kappa}$ satisfies the following relation:

$$U_{\lambda\kappa} \subset \bigcap_{\mathbf{x}\in\mathscr{M}} H(\mathbf{A}\mathbf{x}, \lambda\kappa(\mathbf{x})),$$

see the proof of Theorem 3.2.1. From this observation, we define the "*Hölder half-space*" associated with a primal point $\mathbf{x}$ as:

$$H_{\texttt{Hö}}(\mathbf{x}) \triangleq H(\mathbf{A}\mathbf{x}, \lambda\kappa(\mathbf{x})). \tag{1.14}$$

We note that the safeness of $H_{\texttt{Hö}}(\mathbf{x})$ can be written as

$$\langle \mathbf{A}\mathbf{x}, \mathbf{u}^\star \rangle \leq \kappa^\circ(\mathbf{A}^*\mathbf{u})\kappa(\mathbf{x}) \leq \lambda\kappa(\mathbf{x}),$$

where the first inequality is a generalization of Hölder inequality. This motivates the name "Hölder" given to the safe region (1.14).

Since a dome region is defined as the intersection of a ball and a half-space, one can exploit the new half-space (1.14) to construct new safe dome regions. In particular, if the safe ball region is an instance of FBI ball, we call the resulting region *"FBI dome"*:

$$D_{\texttt{FBI}}(\mathbf{x}', \mathbf{x}, \mathbf{u}) \triangleq H_{\texttt{Hö}}(\mathbf{x}') \cap B_{\texttt{FBI}}(\mathbf{x}, \mathbf{u}).$$

In the thesis, we emphasize that this new dome generalizes previous results of the literature. In particular, by specifying a particular choice for $\mathbf{x}$, we obtain the cutting half-space employed in the ST dome [95] and SASVI domes [66, 99]. Furthermore, it can be proven to be a subset of GAP dome [45]. These comparison results are stated in Corollaries 3.2.8 to 3.2.11 and summarized in Table 1.1.

A3. Geometric ball. In the literature, a common method for constructing a safe region involves creating a ball (with the smallest possible radius) that contains a given safe dome region. However, it is important to note that in the literature, such balls are typically constructed under a specific condition: the center lies on the hyperplane of the half-space used to define the dome, see ST2 and ST3 balls in [95].

In this thesis, we present a general closed-form formula for the minimum-volume ball with an arbitrary center encompassing a given dome. More specifically, let $D = B(\mathbf{c}, r) \cap H(\mathbf{g}, s)$ be a dome and let $B(\mathbf{v}, r_\mathbf{v})$ be the *smallest* ball centered at $\mathbf{v} \in \mathscr{H}$ containing

D.[5] We show in Proposition A.3.5 that

$$r_{\mathbf{v}} = \begin{cases} \|\mathbf{v}-\mathbf{c}\|_{\mathscr{H}} + r, & \text{if } \cos(\mathbf{g}, \mathbf{v}-\mathbf{c}) \geq -\psi_D, \\ \sqrt{\|\mathbf{v}-\mathbf{v}_P\|_{\mathscr{H}}^2 + \left(\|\mathbf{v}_P - \mathbf{c}_P\|_{\mathscr{H}} + r\sqrt{1-\psi_D^2}\right)^2}, & \text{otherwise.} \end{cases} \tag{1.15}$$

where $\mathbf{v}_P$ denotes the projection of $\mathbf{v}$ onto the hyperplane P associated with half-space H and $\psi_D \triangleq \dfrac{s - \langle \mathbf{g}, \mathbf{c} \rangle}{r \|\mathbf{g}\|_{\mathscr{H}}}$ denotes the intersection index of dome region D, see (A.8). We name this region *"geometric ball"* since its construction only relies on geometric arguments.

Regarding the generality of geometric ball, one can see that the safe ball region ST2 and ST3 [95] are instances of geometric ball. This observation is also summarized in Table 1.1. Furthermore, under a specific setup, one can show that our new FBI ball can be seen as a particular instance of geometric ball, see Theorem 3.3.2.

B. Safe screening on a space of measures. The second main contribution of this thesis is the extension of the safe screening principle to TV-norm regularized problems, which are infinite-dimensional problems defined on the space of Radon measures (see Section B.1). We demonstrate that within this context, safe screening can be effectively applied to enhance the performance of a recent method, namely Refinement Grid Based solver [48] (see Section B.2).

B1. Extending safe screening principle. Let $T \subset \mathbb{R}^d$ be a compact set and $\mathscr{M} = \mathscr{M}(T, \mathbb{R})$ be a space of real-valued Radon measures with support on T. Here $\mathscr{M}$ is a non-reflexive Banach space endowed with the so-called *total variation* norm $\|\cdot\|_{TV}$. Let $\mathbf{A} : \mathscr{M} \to \mathscr{H}$ be a linear operator, which is defined by $\mathbf{A}\mathbf{x} = \int_{\mathbf{t}\in T} \mathbf{a}_{\mathbf{t}} \, \mathrm{d}\mathbf{x}(\mathbf{t})$,[6] for some atom function $\mathbf{a} : \mathbf{t} \in T \mapsto \mathbf{a}_{\mathbf{t}} \in \mathscr{H}$. Here the problem we consider is[7]

$$\min_{\mathbf{x}\in\mathscr{M}} \quad f(\mathbf{A}\mathbf{x}) + \lambda \|\mathbf{x}\|_{TV}, \tag{1.16}$$

where $f : \mathscr{M} \to \mathbb{R} \cup \{+\infty\}$ is convex. This problem is a specific instance of (1.1-p_g^f) with $g = \lambda \|\cdot\|_{TV}$ for some $\lambda > 0$.

Under certain conditions, the optimal solution of (1.16) exhibits a sparse structure,

5. Here, we use the notation $r_{\mathbf{v}}$ to insist on the fact that this radius depends on $\mathbf{v}$.

6. Here, the integral takes value in a Hilbert space $\mathscr{H}$ rather than $\mathbb{R}$, therefore, it should be understood in the sense of Bochner integral, see [22, Appendix E].

7. A more comprehensive description of our target problem (1.16) (with further assumptions on f and $\mathbf{A}$) can be found in Section 4.1.

i.e., $\mathbf{x}^\star = \sum_{i=1}^n w_i \delta_{\mathbf{t}_i}$, where $(w_i, \mathbf{t}_i) \in \mathbb{R} \times T$ for $i = 1, \ldots, n$, see [32]. Here $\delta_{\mathbf{t}}$ denotes the Dirac mass (spike) at location $\mathbf{t} \in T$. Here for simplicity, we assume that $\mathbf{x}^\star$ is unique.

To solve (1.16), various methods have been developed in the literature, as reviewed in [64]. In these approaches, one often involves the task of tuning the weights of a huge number of Dirac masses resulting high-dimensional problems. Efforts to reduce the parameter set T - the locations of Dirac masses of the optimal solution - can substantially enhance computational efficiency and resolution speed. This idea draws parallels to the idea of safe screening. However, current safe screening principles are only applicable for finite-dimensional optimization problems.

One contribution of Chapter 4 is to demonstrate that an analogous safe screening rule can be applied to our infinite-dimensional problem (1.16). More specifically, we have for any $\mathbf{t} \in T$:

$$|\langle \mathbf{a}_\mathbf{t}, \mathbf{u}^\star \rangle| < \lambda \Longrightarrow \mathbf{t} \notin \operatorname{supp} \mathbf{x}^\star. \tag{1.17}$$

where $\mathbf{u}^\star$ is an optimal dual solution (will be assumed to be unique) and supp denotes the support of measure. This result is formally stated in Theorem 4.2.1. Note that (1.17) holds without any assumption on the structure of the solution $\mathbf{x}^\star$. In particular, our safe screening principle also applies when (1.16) admits some solution which are continuous measures (*i.e.*, the measure with density function).

Unsurprisingly, the screening rule (1.17) also presents practical challenges since: *i)* it relies on the knowledge of $\mathbf{u}^\star$; *ii)* it only screens one single parameter, while the parameter set T contains an infinite uncountable number of parameters.

To address the first issue, as previously discussed, we can employ a safe region S, for instance, the FBI safe ball region. Note that our FBI regions remain safe for general vector spaces. For the second issue, instead of screening a single parameter $\mathbf{t}$, we may screen a subset Θ of T. This approach is known as the *joint safe screening* [58]. The resulting screening rule becomes:

$$\sup_{(\boldsymbol{\theta}, \mathbf{u}) \in \Theta \times S} |\langle \mathbf{a}_{\boldsymbol{\theta}}, \mathbf{u} \rangle| < \lambda \Longrightarrow \Theta \cap \operatorname{supp} \mathbf{x}^\star = \emptyset. \tag{1.18}$$

We also refer to (1.18) as a joint safe screening rule in the space of measures with formal statement given in Theorem 4.2.2.

B2. Accelerating "Refinement Grid Based" method with safe screening. A recent solving procedure for (1.16) known as *Refinement Grid Based (RGB)* method was

proposed in [48]. The basic idea of RGB method is to iteratively discretize the parameter set T into cells (segments in 1D, squares in 2D and cubes in 3D) and solve the finite-dimensional version of (1.16) over the grid vertices, effectively transforming it into LASSO problems. In other words, in each iteration of RGB method, we need to solve a LASSO problem over a newly refined grid vertices. A convergence analysis for this method is also established.

However, the RGB method encounters a notable issue related to computational bottlenecks due to the dyadic partition of the grid. Although the authors have theoretically shown that the growth in grid size (number of cells) can be controlled, it tends to expand dramatically in practice, even when T belongs to a low dimensional space.

As a first investigation of application of safe screening in the context of measures, we study the application of safe screening in conjunction with RGB method. Specifically, at each iteration, we employ safe screening (1.18) to identify and exclude some useless cells from the grid, see Algorithm 1 in Section 4.3.2. Remarkably, we demonstrate that the integration of safe screening into RGB yields two crucial properties: 1) It does not affect the splitting cell process, 2) It does not alter the k-iteration solution $\mathbf{x}^{(k)}$, for all $k \geq 0$. We refer to this as a *consistency* result, see Theorem 4.3.2. Consequently, we assert that the inclusion of joint safe screening preserves the convergence results established in the RGB method with potentially significant savings (and no major additional computational cost).

C. Side results. In Appendix A, we study the properties of geometric regions such as balls, half-spaces and domes regions in the general Hilbert spaces. In Appendix B, we revisit some basic notions in convex optimization and discuss the Fenchel-Rockafellar duality under various sufficient equivalent conditions.

D. Publications

1. Tran, T.L., Elvira, C., Dang, H.P. and Herzet, C., 2022. Beyond GAP screening for Lasso by exploiting new dual cutting half-spaces. **In 2022 30th European Signal Processing Conference (EUSIPCO)** (pp. 2056-2060) [87, 88].

2. _, 2022. Une nouvelle méthode d'accélération pour LASSO par élimination sûre de variables. **In CAP 2022-Conférence sur l'Apprentissage automatique** [89].

3. _, 2023, Dimensionality reduction for convex optimization based on safe regions: A unified approach, **In Vietnam Mathematical Congress** (Abstract submission).

1.3 Organization

In this section, we summarize the results obtained in each chapter of the thesis.

Chapter 2. This chapter introduces dimensionality reduction methods for convex optimization problems of the form (1.1-p_g^f), encompassing safe screening, safe squeezing techniques and beyond. Additionally, we outline the criteria that an "effective" safe region should fulfill and provide a concise literature overview of all existing safe regions to the best of our knowledge.

Chapter 3. In this chapter, we introduce several novel safe regions and conduct a comprehensive comparison with existing safe regions, the summary of which can be found in Table 1.1.

In Section 3.1, we define a safe region known as the *FBI ball* (see Theorem 3.1.3). Remarkably, this ball encompasses all existing safe ball regions as special cases or supersets, as detailed in Corollaries 3.1.8 to 3.1.16.

In Section 3.2, we introduce two safe regions: the *Hölder half-space* (Theorem 3.2.1) and the *FBI dome* (Theorem 3.2.4). These results also generalize the existing safe regions with half-space and dome geometry, as demonstrated in Corollaries 3.2.8, 3.2.9 and 3.2.11.

In Section 3.3, we present an explicit construction for the so-called *geometric ball* with an arbitrary center and smallest radius containing a given dome region, which is outlined in Proposition A.3.5. We show in Theorem 3.3.2 that under a suitable setup, FBI ball can be considered as an geometric ball associated with a certain FBI dome.

Chapter 4. This chapter studies the application of safe screening principle to the total variation norm regularization problem (1.16), examining its integration with the newly introduced Refinement Grid Based solver.

In Section 4.1, we provide the preliminaries for (1.16) including the space of Radon measures, dictionary operator, inverse problem on the space of measures and a brief overview of solving methods.

In Section 4.2, we extend safe screening principle to total variation norm regularization problem (1.16) including the ideal rule (1.17) and the practical rule (1.18), see Theorem 4.2.1 and Theorem 4.2.2, respectively.

In Section 4.3, we propose a modification of Refinement Grid Based solver by integrating joint safe screening method (1.18) into it, see Algorithm 1. Additionally, we provide consistency guarantee for this modified solver in Theorem 4.3.2.

Appendix A. In this appendix, we provide closed-form expressions of geometric regions including balls, half-spaces and domes in general Hilbert spaces.

Appendix B. In this appendix, we revisit the basic notions in convex optimization and study the various sufficient conditions of the Fenchel-Rockafellar duality.

Chapter 2

An overview of safe screening and safe regions

Abstract. *In this chapter, we provide a concise introduction to various dimensionality reduction methods tailored for convex optimization problems. These encompass safe screening, safe squeezing, and their variants. Central to these approaches is the concept of safe region. Consequently, we delve into the essential criteria that define an effective safe region and proceed to present a thorough overview of all existing safe regions in the literature to the best of our knowledge.*

2.1 Safe screening and extensions

In this section, we revisit the fundamental ideas behind some dimensionality reduction techniques for convex optimization problems, such as safe screening, safe squeezing, and their variations. Our primary goal is to explain why the concept of "safe region" emerges in these methods and why it is essential in practical implementations. However, the formal definition of "safe region" in general setups is postponed until the next section. At the end of this section, we will also briefly discuss the complexity trade-off when integrating these methods within numerical solving procedures.

2.1.1 Screening

Consider the following ℓ_1-norm penalized problem:

$$\min_{\mathbf{x}\in\mathbb{R}^n} \quad f(\mathbf{A}\mathbf{x}) + \lambda \|\mathbf{x}\|_1 , \tag{2.1}$$

where $f\colon \mathbb{R}^m \to \mathbb{R}\cup\{+\infty\}$ is a closed proper convex function, $\mathbf{A}\in\mathbb{R}^{m\times n}$ and $\lambda > 0$. This problem is a particular case of (1.1-p_g^f) with $g = \lambda\|\cdot\|_1$, $\mathscr{H} = \mathbb{R}^m$ and $\mathscr{M} = \mathbb{R}^n$. Here, we also impose the technical assumption that f is differentiable on $\mathrm{dom}(f) = \mathbb{R}^m$. Furthermore, we suppose that (2.1) admits a unique minimizer, denoted $\mathbf{x}^\star$. We note however that the latter assumption is not essential but rather made to simplify our exposition.

The parameter λ controls the penalization norm. In particular, if λ exceeds the threshold $\lambda_{\max} = \left\|\mathbf{A}^{\mathrm{T}}\nabla f(\mathbf{0}_{\mathbb{R}^m})\right\|_\infty$, the origin will be a (somewhat trivial) optimal solution of (2.1), see [72, Proposition 4]. We therefore assume that $\lambda < \lambda_{\max}$ in the sequel.

A well-known special case of (2.1) arises when the data fitting term f takes the form of a least squares function, specifically $f(\cdot) = \frac{1}{2}\|\mathbf{b} - \cdot\|_2^2$ for some $\mathbf{b}\in\mathbb{R}^m$. This problem is known as the *Least Absolute Shrinkage and Selection Operator (LASSO)* [85] in statistics or *Basis Pursuit Denoising* [19] in signal processing.

It is known that the solution of (2.1) exhibits some "sparse" structure, that is most of its coordinates are zeros. The intuition is because the optimal solutions are often located at the extreme points (the vertices) of the (scaled) polytope defined by ℓ_1-norm unit ball, see Figure 2.1. [1] For a more rigorous statement regarding sparsity in the case of LASSO

1. Taking LASSO as an example, one can show that if $\mathbf{x}^\star$ is an optimal solution to $\min\{f(\mathbf{A}\mathbf{x}) : \|\mathbf{x}\|_1 \le \tau\}$ for some $\tau > 0$, then there exists some λ such that $\mathbf{x}^\star$ is also optimal to (2.1),

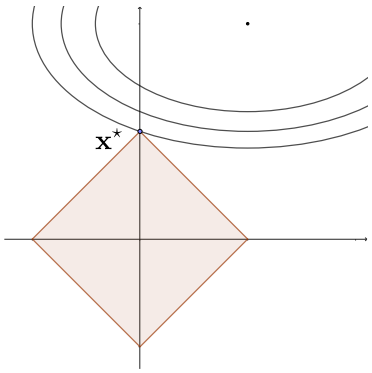

Figure 2.1 – A 2D visualization of sparse solution $\mathbf{x}^\star$ of (2.1). The square is the ℓ_1-norm unit ball and the curves are level sets of $\mathbf{x} \mapsto f(\mathbf{A}\mathbf{x})$.

problem, please refer to [49, Theorem 6.1], which shows that (under uniqueness assumption) the LASSO solution has at least $n - m$ zero entries. For a broader understanding of the structure of the solution induced by general convex penalization functions, please refer to [12, Theorem 1].

We now describe how to leverage the sparsity of $\mathbf{x}^\star$ to define a problem equivalent to (2.1) but with reduced dimension. Let L be some superset of the coordinates corresponding to nonzero elements of $\mathbf{x}^\star$, *i.e.*,

$$L \supseteq \{i \in \{1, \dots, n\} : \mathbf{x}^\star(i) \neq 0\}. \tag{2.2}$$

Then, problem (2.1) is equivalent to

$$\min_{\mathbf{x}_L \in \mathbb{R}^{|L|}} \quad f(\mathbf{A}_L \mathbf{x}_L) + \lambda \left\|\mathbf{x}_L\right\|_1, \tag{2.3}$$

where $\mathbf{x}_L$ and $\mathbf{A}_L$ denote the restriction of $\mathbf{x}$ and $\mathbf{A}$ to their coordinate indices and column indices in L, respectively. We note that if one can identify many zero entries of $\mathbf{x}^\star$, then the problem (2.3) is of much smaller dimension than (2.1). In practice, solving (2.3) instead of (2.1) may thus offer significant advantages in terms of complexity and memory storage. Specifically, since the solution $\mathbf{x}^\star$ contains at most m non-zero elements, the gain in complexity (per iteration) or storage is at least $\frac{n}{m}$ if all the zeros are identified.

At this stage, the problem is to estimate L. To do so, one can leverage the problem's optimality conditions. In particular, $\mathbf{x}^\star$ must verify Fermat's rule [5, Proposition 2.61],

see [50, Proposition 3.2 (c)]. This explains the interpretation of Figure 2.1.

i.e.,

$$\mathbf{0}_{\mathbb{R}^n} \in \mathbf{A}^{\mathrm{T}} \nabla f(\mathbf{A}\mathbf{x}^\star) + \partial\lambda \left\|\mathbf{x}^\star\right\|_1 . \tag{2.4}$$

Here, notice that ∇f is well-defined due to our differentiability assumption on f. Moreover, the subdifferential of the ℓ_1-norm is given by (see [6, Example 3.41]):

$$\begin{aligned}\partial\lambda \left\|\mathbf{x}\right\|_1 &= \{\mathbf{z} \in \mathbb{R}^n : \left\|\mathbf{z}\right\|_\infty \leq \lambda, \langle \mathbf{z}, \mathbf{x}\rangle = \lambda \left\|\mathbf{x}\right\|_1\} \\ &= \{\mathbf{z} \in \mathbb{R}^n : \mathbf{z}(i) = \lambda \mathrm{sign}(\mathbf{x}(i)) \text{ if } \mathbf{x}(i) \neq 0,\ \mathbf{z}(i) \in [-\lambda, \lambda] \text{ if } \mathbf{x}(i) = 0\}.\end{aligned}$$

Letting

$$\mathbf{u}^\star \triangleq -\nabla f(\mathbf{A}\mathbf{x}^\star), \tag{2.5}$$

the optimality condition (2.4) can thus be equivalently expressed as:

$$\langle \mathbf{a}_i, \mathbf{u}^\star \rangle = \begin{cases} \lambda, & \text{if } \mathbf{x}^\star(i) > 0, \\ s \in [-\lambda, \lambda], & \text{if } \mathbf{x}^\star(i) = 0, \\ -\lambda, & \text{if } \mathbf{x}^\star(i) < 0. \end{cases} \tag{2.6}$$

Taking the duality point of view, one can prove that $\mathbf{u}^\star$ is actually the unique optimal solution of the Fenchel-Rockafellar dual problem of (2.1), [2] *i.e.*,

$$\mathbf{u}^\star = \underset{\mathbf{u} \in U_{\lambda\|\cdot\|_1}}{\arg\max} \ -f^*(-\mathbf{u}), \tag{2.7}$$

where

$$U_{\lambda\|\cdot\|_1} = \{\mathbf{u} \in \mathbb{R}^m : |\langle \mathbf{a}_i, \mathbf{u}\rangle| \leq \lambda, \forall i = 1, \ldots, n\} \tag{2.8}$$

is a polytope referred to as *dual feasible set*. Here $\mathbf{a}_i$ denotes the ith-column of $\mathbf{A}$. In this context, the optimality conditions (2.5) and (2.6) are known as the *Karush–Kuhn–Tucker* conditions, with (2.6) being equivalent to the so-called *complementary slackness* condition.

Assuming that $\mathbf{u}^\star$ is known, we can use (2.6) to identify some zero entries in $\mathbf{x}^\star$ as follows: if the absolute value of the inner product between the ith column of $\mathbf{A}$ and the dual optimal solution $\mathbf{u}^\star$ is strictly less than λ, then the corresponding entry in the optimal solution $\mathbf{x}^\star$ is guaranteed to be zero. This observation forms the main principle underlying most *"safe screening"* methods of the literature and is summarized in the

2. Here, the uniqueness of $\mathbf{u}^\star$ follows from the uniqueness of $\mathbf{x}^\star$ and their relation (2.5).

following implication:

$$|\langle \mathbf{a}_i, \mathbf{u}^\star \rangle| < \lambda \Longrightarrow \mathbf{x}^\star(i) = 0. \tag{2.9}$$

In practice, solving the dual problem (2.7) to find $\mathbf{u}^\star$ is unfortunately equally challenging as solving the primal problem (2.1). Hence, (2.9) is of poor practical interest to identify the zeros of $\mathbf{x}^\star$. One approach to address this issue is to replace the inequality in (2.9) with a more practical test. This is where the concept of a "safe region" comes into play. A set $S \subset \mathbb{R}^m$ is called a *safe region* if it verifies:

$$\mathbf{u}^\star \in S. \tag{2.10}$$

Assuming that a safe region S is known, (2.9) can then be relaxed as follows:

$$\sup_{\mathbf{u} \in S} |\langle \mathbf{a}_i, \mathbf{u} \rangle| < \lambda \Longrightarrow \mathbf{x}^\star(i) = 0. \tag{2.11}$$

Safe regions thus play a critical role in the design of practical safe-screening tests. In the following, we present a simple example illustrating how a safe region can be constructed for the LASSO problem. Further discussion on more advanced constructions of safe regions will be presented in the next section.

Example 2.1.1 (Concrete example of safe screening method for LASSO)**.** *Consider LASSO and its dual problem:*

$$\min_{\mathbf{x} \in \mathbb{R}^n} \quad \frac{1}{2} \|\mathbf{b} - \mathbf{A}\mathbf{x}\|_2^2 + \lambda \|\mathbf{x}\|_1 = \max_{\mathbf{u} \in U_{\lambda\|\cdot\|_1}} \quad \frac{1}{2} \|\mathbf{b}\|_2^2 - \frac{1}{2} \|\mathbf{b} - \mathbf{u}\|_2^2 \tag{2.12}$$

where $\mathbf{b} \in \mathbb{R}^m$, $\lambda > 0$ *and* $U_{\lambda\|\cdot\|_1}$ *is defined in* (2.8)*. The dual problem is actually a closest point projection problem of* $\mathbf{b}$ *onto* $U_{\lambda\|\cdot\|_1}$*, therefore,* $\|\mathbf{u}^\star - \mathbf{b}\|_2 \leq \|\mathbf{u} - \mathbf{b}\|_2$ *for all* $\mathbf{u} \in U_{\lambda\|\cdot\|_1}$*. Thus, the ball with center at* $\mathbf{b}$ *and radius* $\|\mathbf{b} - \mathbf{u}\|_2$ *is a safe region. In this case, the screening rule* (2.11) *takes the form:*

$$|\langle \mathbf{a}_i, \mathbf{u} \rangle| + \|\mathbf{b} - \mathbf{u}\|_2 \|\mathbf{a}_i\|_2 < \lambda \Longrightarrow \mathbf{x}^\star(i) = 0.$$

In particular, if $\mathbf{u} \triangleq \frac{\lambda}{\|\mathbf{A}^\mathrm{T}\mathbf{b}\|_\infty}\mathbf{b}$ *then* $\mathbf{u} \in U_{\lambda\|\cdot\|_1}$ *and we recover the so-called called SAfe Feature Elimination (SAFE) rule proposed in [52].*

2.1.2 Squeezing

In the previous section, we have seen how safe screening methods can reduce the problem size by exploiting the sparsity structure of the optimal solution induced by ℓ_1-regularization. In this section, our goal is to illustrate that the rationale of safe screening can be extended to ℓ_∞-penalized problems and to clarify why the concept of safe region still plays an essential role in this framework.

Consider the following ℓ_∞-norm penalized optimization problem:

$$\min_{\mathbf{x}\in\mathbb{R}^n} \quad f(\mathbf{A}\mathbf{x}) + \lambda \left\|\mathbf{x}\right\|_\infty . \tag{2.13}$$

Similar to the framework of safe screening, we assume the differentiability of f on $\mathbb{R}^m$. Furthermore, we assume the uniqueness of the optimal solution $\mathbf{x}^\star$ of (2.13). As mentioned previously, this uniqueness assumption is considered for the sake of simplicity but can be easily generalized to the non-uniqueness case. Additionally, we assume that $\lambda < \lambda_{\max} \triangleq \left\|\mathbf{A}^{\mathrm{T}}\nabla f(\mathbf{0}_{\mathbb{R}^m})\right\|_1$ so that $\mathbf{x}^\star$ is nonzero [72, Proposition 4].

It is known that the minimizer of (2.13) exhibits some "anti-sparse" structure. More specifically, in [42] the authors showed that if $f(\cdot) = \frac{1}{2}\left\|\mathbf{b} - \cdot\right\|_2^2$ for some $\mathbf{b} \in \mathbb{R}^m$, and the *Kruskal* rank of $\mathbf{A}$ is m, then $\mathbf{x}^\star$ has at least $n - m + 1$ "saturated" entries, *i.e.*, indices $i \in \{1, \ldots, n\}$ for which $\mathbf{x}^\star(i) = \pm \left\|\mathbf{x}^\star\right\|_\infty$. This characteristic may be seen as the opposite of sparsity and thus explains why it is usually referred to as "anti-sparsity".

The anti-sparse structure of $\mathbf{x}^\star$ can be leveraged to develop a dimensionality reduction technique reminiscent to safe screening. Instead of screening the zero entries as in the sparsity case, the basic idea is here to "squeeze" the saturated entries of $\mathbf{x}^\star$. More specifically, assuming the knowledge of some sets L_+, L_- and L such that:

$$\begin{aligned} L_+ &\subset \{i : \mathbf{x}^\star(i) = +\left\|\mathbf{x}^\star\right\|_\infty, i = 1, \ldots, n\}, \\ L_- &\subset \{i : \mathbf{x}^\star(i) = -\left\|\mathbf{x}^\star\right\|_\infty, i = 1, \ldots, n\}, \\ L &= \{1, \ldots, n\} \setminus (L_- \cup L_+), \end{aligned}$$

one can derive a problem equivalent to (2.13) by "squeezing" the columns of $\mathbf{A}$ with

indices in $L_\pm$ into a single vector $\mathbf{v} = \sum_{i\in L_+} \mathbf{a}_i - \sum_{i\in L_-} \mathbf{a}_i$, *i.e.*,

$$\begin{aligned} \min_{(\mathbf{x}_L, w)\in\mathbb{R}^k\times\mathbb{R}_+} \quad & f(\mathbf{A}_L\mathbf{x}_L + w\mathbf{v}) + \lambda w \\ \text{s.t.} \quad & \|\mathbf{x}_L\|_\infty \le w \end{aligned} \tag{2.14}$$

where $k = |L| = n - |L_- \cup L_+|$. Notice that the total dimension of primal variable $(\mathbf{x}_L, w)$ is much smaller than that of $\mathbf{x}$ provided that a large number of saturated coordinates have been identified. Therefore, solving (2.14) can be much more efficient than solving (2.13) directly.

We now discuss how proper sets L_- and L_+ can be estimated by using the knowledge of some safe region S. Similar to safe screening, Fermat's rule implies the following optimality criterion:

$$\mathbf{A}^{\mathrm{T}}\mathbf{u}^\star \in \partial\lambda \|\mathbf{x}^\star\|_\infty , \tag{2.15}$$

where $\mathbf{u}^\star = -\nabla f(\mathbf{A}\mathbf{x}^\star)$ is the unique dual optimal solution. Since $\mathbf{x}^\star$ is guaranteed to be nonzero by assumption, one has

$$\partial\lambda \|\mathbf{x}^\star\|_\infty = \{\mathbf{z}\in\mathbb{R}^n : \|\mathbf{z}\|_1 \le \lambda, \langle \mathbf{z}, \mathbf{x}^\star\rangle = \lambda \|\mathbf{x}^\star\|_\infty\},$$

see [6, Example 3.52]. Therefore, for $\mathbf{z} \in \partial\lambda \|\mathbf{x}^\star\|_\infty$, if $\mathbf{z}(i) \neq 0$, it is necessary that $\mathbf{x}^\star(i)$ saturates with the same sign as $\mathbf{z}(i)$. Combining this observation with (2.15), one can deduce the following implication:

$$|\langle \mathbf{a}_i, \mathbf{u}^\star\rangle| > 0 \Longrightarrow i \in L_{\mathrm{sign}(\langle \mathbf{a}_i, \mathbf{u}^\star\rangle)}. \tag{2.16}$$

Here again, solving the dual problem (2.14) to find $\mathbf{u}^\star$ turns out to a complicated task. Nevertheless, a more practical rule can be derived if some safe region S (*i.e.*, $\mathbf{u}^\star \in S$) is known:

$$\inf_{\mathbf{u}\in S} \langle \mathbf{a}_i, \mathbf{u}\rangle > 0 \Longrightarrow i \in L_+ \tag{2.17}$$

$$\sup_{\mathbf{u}\in S} \langle \mathbf{a}_i, \mathbf{u}\rangle < 0 \Longrightarrow i \in L_-. \tag{2.18}$$

These results highlight the essential role of safe region in practical safe squeezing rules.

Problem	$L(z,b)$	$g(\mathbf{x})$	**Screening**
LASSO	$\frac{1}{2}(z-b)^2$	$\lambda \left\|\mathbf{x}\right\|_1$	*e.g.*, [45]
Non-neg. LASSO	$\frac{1}{2}(z-b)^2$	$\lambda \left\|\mathbf{x}\right\|_1 + \iota(\mathbf{x} \geq 0)$	*e.g.*, [99]
Sparse Group LASSO	$\frac{1}{2}(z-b)^2$	—	[71]
Fused LASSO	$\frac{1}{2}(z-b)^2$	—	[91]
Anti-sparse coding	$\frac{1}{2}(z-b)^2$	$\lambda \left\|\mathbf{x}\right\|_\infty$	[42]
Least squares & SLOPE norm	$\frac{1}{2}(z-b)^2$	—	[41, 3]
Least squares & atomic norm	$\frac{1}{2}(z-b)^2$	—	[84]
Least squares & squared ℓ_1-norm	$\frac{1}{2}(z-b)^2$	$\lambda \left\|\mathbf{x}\right\|_1^2$	[81]
Elastic-Net	$\frac{1}{2}(z-b)^2$	$\lambda \left\|\mathbf{x}\right\|_1 + \lambda' \left\|\mathbf{x}\right\|_2^2$	[54, 98]
Soft SVM	$\max(0, 1-bz)$	$\lambda \left\|\mathbf{x}\right\|_2$	*e.g.*, [74]
Sparse soft SVM	$\max(0, 1-bz)$	$\lambda \left\|\mathbf{x}\right\|_1$	*e.g.*, [59]
Sparse logistic regression	$-bz + \log(1+e^z)$	$\lambda \left\|\mathbf{x}\right\|_1$	[75]
Sparse KL regression	$z\log(z/b) - z + b$	$\lambda \left\|\mathbf{x}\right\|_1$	*e.g.*, [26]
Sparse Huber regression	—	$\lambda \left\|\mathbf{x}\right\|_1$	[18]
Sparse quantile regression	—	$\lambda \left\|\mathbf{x}\right\|_1$	[82]

Table 2.1 – Some convex optimization problems and their corresponding safe screening methods. Where L function satisfies $f(\mathbf{Ax}) = \sum_i^m L((\mathbf{Ax})(i), \mathbf{b}(i))$.

2.1.3 Beyond

In the preceding two sections, we demonstrated that safe regions play an essential role in designing screening/squeezing tests for convex optimization problems with ℓ_1-norm or ℓ_∞-norm penalization functions. In this section, we illustrate how safe regions are equally vital in deriving dimensionality reduction techniques for convex optimization problems with various penalization functions.

Several instances of (1.1-p_g^f) (where f is not necessarily assumed to be differentiable) that have associated dimensionality reduction methods are collected in Table 2.1. It is important to note that when the regularization function is "separable", a more general form of the safe screening rule, referred to as "active set identification" is thoroughly discussed in [70, Section 2.1]. For example, ℓ_1-norm regularized problem, Elastic-Net problem and sparse group LASSO are instances of this framework.

We described some examples in greater details below.

Screening and Relaxing rule for Elastic-Net problem. Elastic-Net problem is an ℓ_1-ℓ_2-norm

regularized least squares problem:

$$\min_{\mathbf{x}\in\mathbb{R}^n_+} \quad \frac{1}{2}\|\mathbf{b}-\mathbf{A}\mathbf{x}\|_2^2 + \langle \boldsymbol{\lambda}, \mathbf{x}\rangle + \frac{\varepsilon}{2}\|\mathbf{x}\|_2^2, \tag{2.19}$$

where $\boldsymbol{\lambda} \in \mathbb{R}^n_+$ and $\varepsilon > 0$ are tuning parameters. Safe screening rules for Elastic-Net was considered in several papers [45, 98, 54]. Note that the optimal solution of this problem $\mathbf{x}^\star$ is unique since the problem (2.19) is strongly convex. For this problem, one can determine the zero entries in $\mathbf{x}^\star$ using the following safe screening rule [54, Equation (12)]:

$$\sup_{\mathbf{u}\in S} \langle \mathbf{a}_i, \mathbf{u}\rangle \leq \boldsymbol{\lambda}(i) \Longrightarrow \mathbf{x}^\star(i) = 0,$$

where S is some safe region and $\mathbf{a}_i$ denotes the ith column of matrix $\mathbf{A}$. In addition, the authors of [54] also introduced the so-called *safe relaxing rule*, which is able to identify non-zero entries of $\mathbf{x}^\star$ [54, Equation (21)]:

$$\inf_{\mathbf{u}\in S} \langle \mathbf{a}_i, \mathbf{u}\rangle > \boldsymbol{\lambda}(i) \Longrightarrow \mathbf{x}^\star(i) > 0.$$

Screening rules for least squares regression with squared ℓ_1-norm penalization. This problem is considered in [81]:

$$\min_{\mathbf{x}\in\mathbb{R}^n} \quad \frac{1}{2}\|\mathbf{b}-\mathbf{A}\mathbf{x}\|_2^2 + \lambda\|\mathbf{x}\|_1^2, \tag{2.20}$$

The corresponding safe screening rule *w.r.t.* to safe region S reads as follows:

$$\sup_{\mathbf{u}\in S} |\langle \mathbf{a}_i, \mathbf{u}\rangle| - \left\|\mathbf{A}^{\mathrm{T}}\mathbf{u}\right\|_\infty < 0 \Longrightarrow \mathbf{x}^\star(i) = 0.$$

This implication follows directly from [81, Equation 3.15]. The authors then exploit this fact and the framework of GAP safe ball [72] to derive a specific screening rule for (2.20) as detailed in [81, Theorem 3.6].

Screening rules for sparse group LASSO problem. Sparse Group LASSO is a least squares optimization problem with a penalization defined as a convex combination of ℓ_1-norm and "separable norm" [72, Section 5.2]:

$$\min_{\mathbf{x}\in\mathbb{R}^n} \quad \frac{1}{2}\|\mathbf{b}-\mathbf{A}\mathbf{x}\|_2^2 + \tau\|\mathbf{x}\|_1 + (1-\tau)\sum_{G\in G}\lambda_G\|\mathbf{x}_G\|_2, \tag{2.21}$$

where G is a partition of the index set $\{1,\ldots,n\}$ and $\mathbf{x}_G$ denotes the restriction of $\mathbf{x}$ to

its elements with indices in group $G \in \mathcal{G}$. Here $\tau > 0$ and $\lambda_G > 0$ for $G \in \mathcal{G}$ are control parameters.

Ndiaye *et al.* [72] proposed two safe screening methods for this problem. The first one corresponds to the screening on the "group level", which identifies the groups G so that all entries of $\mathbf{x}^\star$ associated with that group equal to zero:

$$\sup_{\mathbf{u} \in S} \left\| \mathbf{A}^{\mathrm{T}} \mathbf{u} \right\|_{\epsilon_G} < \tau + (1-\tau)\lambda_G \Longrightarrow \mathbf{x}^\star_G = \mathbf{0}_{\mathbb{R}^{|G|}},$$

where $\epsilon_G \triangleq \dfrac{(1-\tau)\lambda_G}{\tau + (1-\tau)\lambda_G}$ and the definition of $\|\cdot\|_{\epsilon_G}$ is given by [72, Section 5.3]. The second screening rule regarding the "feature level" is:

$$|\langle \mathbf{a}_i, \mathbf{u} \rangle| < \tau \Longrightarrow \mathbf{x}^\star(i) = 0,$$

for all $i \in \{1, \ldots, n\}$.

Screening rule for SLOPE problem. Consider the *Sorted L-One Penalized Estimation (SLOPE)* problem,

$$\min_{\mathbf{x} \in \mathbb{R}^n} \quad \frac{1}{2} \|\mathbf{b} - \mathbf{A}\mathbf{x}\|_2^2 + \lambda \|\mathbf{x}\|_{\texttt{SLOPE}}, \tag{2.22}$$

where the SLOPE norm $\|\cdot\|_{\texttt{SLOPE}}$, associated with a non-increasing sequence of parameters $\gamma_1 \geq \cdots \geq \gamma_n \geq 0$ with $\gamma_1 > 0$, is defined as:

$$\|\mathbf{x}\|_{\texttt{SLOPE}} = \sum_{i=1}^{n} \gamma_i \, |\mathbf{x}|_{[i]},$$

with $|\mathbf{x}|_{[i]}$ representing the ith largest element among the entries of $\mathbf{x}$, *i.e.*, $|\mathbf{x}|_{[1]} \geq \cdots \geq |\mathbf{x}|_{[n]}$.

The SLOPE norm can be seen as a generalization of several regularizations previously proposed in the literature. For example, if $\gamma_i = 1$ for $i = 1, \ldots, n$, then $\|\cdot\|_{\texttt{SLOPE}}$ reduces to the ℓ_1-norm. If $\gamma_1 = 1$ and all other γ_i's' are zero, then it corresponds to the ℓ_∞-norm. Finally, if $\gamma_i - \gamma_{i+1} = c > 0$ for all $i \in \{1, \ldots, n-1\}$, then the SLOPE norm corresponds to the so-called *Octagonal Shrinkage and Clustering Algorithm for Regression (OSCAR)* regularizer, as considered in [3, 9, 39].

The safe screening in this context reads as follows [40]: [3]

$$\left(\forall q \in \{1, ..., n\} : \sup_{\mathbf{u}\in S} |\langle \mathbf{a}_i, \mathbf{u}\rangle| + \sum_{k=1}^{q-1} \left|\mathbf{A}_{\setminus i}^{\mathrm{T}}\mathbf{u}\right|_{[k]} < \lambda \sum_{k=1}^{q} \gamma_k\right) \Longrightarrow \mathbf{x}^\star(i) = 0. \tag{2.23}$$

where $\mathbf{A}_{\setminus i}$ denotes matrix $\mathbf{A}$ deprived of its ith column.

2.1.4 Implementation into numerical solvers

The dimensionality reduction techniques discussed in the previous section can be integrated into numerical solvers in three different ways: static, sequential, and dynamic.

Static Approach. The static safe screening approach predates other methods and was first proposed in [52]. In this approach, we reduce the problem size before actually solving it. The primary advantage of this approach is that it effectively decouples the task of reducing the problem size from the task of solving the problem.

Sequential approach. In the sequential approach, the objective is to solve a sequence of problems parameterized by $\lambda > 0$, $\lambda \in \{\lambda_0, \lambda_1, ..., \lambda_k\}$,

$$\min_{\mathbf{x}\in\mathscr{M}} \quad f(\mathbf{A}\mathbf{x}) + \lambda g(\mathbf{x}) = \max_{\mathbf{u}\in\mathscr{H}} \quad -f^*(-\mathbf{u}) - \lambda g^*\left(\frac{\mathbf{A}^*\mathbf{u}}{\lambda}\right), \tag{2.24}$$

This is a common task in machine learning known as *hyperparameter tuning*, in which we need to select the most suitable λ for the problem model in order to optimize subsequent tasks, see *e.g.*, [70]. In this approach, to reduce the dimension of ith problem where $i \geq 1$, we exploit the knowledge from the $(i-1)$th problem (precisely, the optimal solution $(\mathbf{x}^\star_{\lambda_{i-1}}, \mathbf{u}^\star_{\lambda_{i-1}})$). The earliest discussions on these sequential approaches includes [93, 66].

Dynamic approach. In the dynamic approach, the dimensionality reduction technique is integrated within the iterations of numerical solvers. This dynamic methodology was initially proposed in [10] and subsequently enhanced by [45, 72, 25], demonstrating its applicability on various problems.

It is worth mentioning that the approach taken to implement dimensionality reduction techniques significantly influences the construction of safe regions, as discussed in detail in the next section.

3. Precisely, Equation (2.23) is actually a relaxation of [40, Equation (4.6)] using safe region.

2.2 Safe region

In the previous section, we elucidated the pivotal role of safe regions in various dimensionality reduction techniques in the context of convex optimization. In this section, we will formally define a safe region within a general framework over potentially infinite-dimensional vector spaces as well as the fundamental properties that a safe region should possess to lead to efficient and effective dimensionality reduction techniques. Lastly, we will provide an overview of existing safe regions of the literature.

2.2.1 Definition of safe region

In this section, we consider the general problem (1.1-p_g^f) where $\mathscr{M}$ and $\mathscr{H}$ can be arbitrary Banach and Hilbert spaces (possibly of infinite-dimension). In the following, we assume that strong duality holds between the primal problem (1.1-p_g^f) and its pre-dual problem (1.2-d_g^f), *i.e.*,

$$\min_{\mathbf{x}\in\mathscr{M}} \quad f(\mathbf{A}\mathbf{x}) + g(\mathbf{x}) = \max_{\mathbf{u}\in\mathscr{H}} \quad -f^*(-\mathbf{u}) - g^*(\mathbf{A}^*\mathbf{u}). \tag{2.25-SD}$$

We moreover suppose that the primal problem and the pre-dual problem in (2.25-SD) have unique minimizer $\mathbf{x}^\star$ and unique maximizer $\mathbf{u}^\star$, respectively. We acknowledge that assuming the uniqueness of $\mathbf{x}^\star$ is for the purpose of simplifying our exposition. The assumption regarding the uniqueness of $\mathbf{u}^\star$ is a consequence of another assumption on f, which will be specified later in Chapter 3.

We now properly define the conception of "safe region":

Definition 2.2.1 (Safe region)**.** *We say that a region $S \subset \mathscr{H}$ is* safe *if it contains the unique dual optimal solution $\mathbf{u}^\star$,*[4] *i.e.,*

$$\mathbf{u}^\star \in S.$$

2.2.2 On the design of effective safe regions

On two desirable properties of safe regions. As discussed in the previous section, the dimensionality reduction methods often rely on the evaluation of $\langle \mathbf{v}, \mathbf{u}^\star \rangle$ for some

4. When the dual optimal solution is not unique, a safe region S should contain at least one of them. However, in this thesis, we confine our focus to the case where $\mathbf{u}^\star$ is unique. This setup is still general enough to cover a wide range of applications.

known vector $\mathbf{v} \in \mathscr{H}$, see *e.g.*, (2.9). Practical implementations relax this quantity to a supremum or infimum of $\langle \mathbf{v}, \mathbf{u} \rangle$ for $\mathbf{u} \in S$ where S is a safe region, see for example (2.11). It is worth noting that such quantities can be represented using the so-called *support function* $\varphi_S(\cdot)$ associated with S. Here $\varphi_S(\cdot) : \mathscr{H} \to \mathbb{R} \cup \{+\infty\}$ is given by:

$$\varphi_S(\mathbf{v}) = \sup_{\mathbf{u} \in S} \langle \mathbf{v}, \mathbf{u} \rangle. \tag{2.26}$$

Note that when the safe region S has a small radius (where the radius is defined as $\mathrm{rad}(S) \triangleq \frac{1}{2} \sup_{\mathbf{u},\mathbf{u}' \in S} \|\mathbf{u} - \mathbf{u}'\|_{\mathscr{H}}$), the corresponding support function provides a good approximation of $\langle \mathbf{v}, \mathbf{u}^\star \rangle$ since

$$|\varphi_S(\mathbf{v}) - \langle \mathbf{v}, \mathbf{u}^\star \rangle| \leq \sup_{\mathbf{u} \in S} \; |\langle \mathbf{v}, \mathbf{u} - \mathbf{u}^\star \rangle| \leq 2\,\mathrm{rad}(S)\, \|\mathbf{v}\|_{\mathscr{H}}\,, \tag{2.27}$$

where the last upper bound follows from the Cauchy-Schwarz inequality and the definition of the radius of S.

Building upon this observation, to obtain an estimation for $\langle \mathbf{v}, \mathbf{u}^\star \rangle$, the evaluation $\varphi_S(\mathbf{v})$ needs to meet two crucial criteria: 1) it should be easy to compute, and 2) it should closely approximate the target value $\langle \mathbf{v}, \mathbf{u}^\star \rangle$. Consequently, a well-designed safe region is expected to inherit these two essential properties including:

1. *Simplicity.* The safe region should have a simple geometry so that the evaluation of (2.26) has low-computational cost.
2. *Tightness.* The safe region should be as small as possible in the sense of inclusion (or at least in the sense of the radius size) since the support function with a smaller safe region provides a more accurate estimation of $\langle \mathbf{v}, \mathbf{u}^\star \rangle$.

On the construction of simple safe regions. Among the popular choices of "simple" regions, ball and dome have empirically proven to be promising candidates. Let us formally define the notion of "ball", "half-space" and "dome":

$$B(\mathbf{c}, r) = \{\mathbf{u} \in \mathscr{H} : \|\mathbf{u} - \mathbf{c}\|_{\mathscr{H}} \leq r\}, \tag{2.28}$$

$$H(\mathbf{g}, s) = \{\mathbf{u} \in \mathscr{H} : \langle \mathbf{g}, \mathbf{u} \rangle \leq s\}, \tag{2.29}$$

$$D(\mathbf{c}, r, \mathbf{g}, s) = B(\mathbf{c}, r) \cap H(\mathbf{g}, s). \tag{2.30}$$

Here, $\mathbf{c}, \mathbf{g} \in \mathscr{H}$ and $r, s \in \mathbb{R}$. In this notational setup, $\mathbf{c}$ and r denote the center and radius of the ball, $\mathbf{g}$ and s denote the normal vector and intercept of the half-space, while

the dome is defined as the intersection of a ball and a half-space.

We should note that the half-space (2.29) is unbounded, while the ball (2.28) and the dome (2.30) are closed and bounded. It is important to highlight that the ball and the dome are typically not compact in infinite-dimensional Hilbert space $\mathscr{H}$, except when the space has finite-dimension. Despite the non-compactness of balls and domes, their support functions - considered as an optimization problem over a non-compact region - admit the following simple closed-form expressions:

Ball region. If $S = B(\mathbf{c}, r)$ is a ball, then

$$\varphi_S(\mathbf{v}) = \langle \mathbf{v}, \mathbf{c} \rangle + r \left\| \mathbf{v} \right\|_{\mathscr{H}}. \tag{2.31}$$

Dome region. If $S = D(\mathbf{c}, r, \mathbf{g}, s) = B(\mathbf{c}, r) \cap H(\mathbf{g}, s)$ is a non-empty dome with $r > 0$ and $\mathbf{g} \neq \mathbf{0}_{\mathscr{H}}$, then

$$\varphi_S(\mathbf{v}) = \langle \mathbf{v}, \mathbf{c} \rangle + r \left\| \mathbf{v} \right\|_{\mathscr{H}} \cos([\theta_D - \theta_{\mathbf{v}}]_+), \tag{2.32}$$

where

$$\theta_{\mathbf{v}} = \arccos \frac{\langle \mathbf{v}, \mathbf{g} \rangle}{\left\| \mathbf{v} \right\|_{\mathscr{H}} \left\| \mathbf{g} \right\|_{\mathscr{H}}}, \quad \theta_D = \arccos \left[\frac{s - \langle \mathbf{g}, \mathbf{c} \rangle}{r \left\| \mathbf{g} \right\|_{\mathscr{H}}} \right]_{[-1,1]}.$$

Here we used the notations $[\cdot]_+ = \max(\cdot, 0)$ and $[\cdot]_{[-1,1]} = \max(\min(\cdot, 1), -1)$. The support function over a ball (2.31) can be derived easily while the support function over a dome (2.32) is a reformulation of [97, Lemma 3]. These two results and, in particular, the meaning of θ_D are also thoroughly discussed in the propositions A.1.1 and A.3.2.

As the above formulas demonstrate, computing the support function over ball or dome regions is computationally tractable, involving mainly the evaluation of inner products and norms. Note that in practice most of these quantities are often pre-computed by solvers, which can further enhance computational efficiency.

On the construction of tight safe region. To construct a tight safe region, there are three main approaches which align with the three modus operandi discussed in the previous section. It is important to note that a safe region S is constructed by leveraging some primal-dual feasible pair $(\mathbf{x}, \mathbf{u})$ with respect to (2.25-SD). To emphasize this dependency, we denote the safe region as $S(\mathbf{x}, \mathbf{u})$.

The first approach amounts to construct a safe region $S(\mathbf{x}_0, \mathbf{u}_0)$ based on a chosen fixed feasible and easily to obtain pair $(\mathbf{x}_0, \mathbf{u}_0)$. However, safe regions constructed using

this approach typically exhibit poor performance for the corresponding dimensionality reduction technique in practical applications.

The second approach involves a sequence of parametric problems (2.24), where the safe region $S(\mathbf{x}^\star_{\lambda_0}, \mathbf{u}^\star_{\lambda_0})$ is built using an optimal pair $(\mathbf{x}^\star_{\lambda_0}, \mathbf{u}^\star_{\lambda_0})$ with respect to a specific parameter λ_0. However, a significant drawback is the heavy reliance on the optimality of $(\mathbf{x}^\star_{\lambda_0}, \mathbf{u}^\star_{\lambda_0})$ to ensure the safeness of $S(\mathbf{x}^\star_{\lambda_0}, \mathbf{u}^\star_{\lambda_0})$. Achieving exact knowledge of $(\mathbf{x}^\star_{\lambda_0}, \mathbf{u}^\star_{\lambda_0})$ is practically impossible. In a numerical experiment [70, Figure 2.7, Section 2.4], Ndiaye demonstrated that using incorrect optimal pairs $(\mathbf{x}^\star_{\lambda_0}, \mathbf{u}^\star_{\lambda_0})$ may wrongly discard non-zero entries in the optimal solution.

The third approach entails constructing the safe region $S(\mathbf{x}, \mathbf{u})$ based on any feasible pair $(\mathbf{x}, \mathbf{u})$. This safe region is commonly used in *e.g.*, dynamic safe screening method [10], where it is iteratively updated along the solver's iterations to yield new safe regions with reduced radii. This approach effectively addresses the limitations of the first two approaches. As it does not impose specific constraints on $(\mathbf{x}, \mathbf{u})$ other than feasibility, the safe region has the potential to progressively reduce its radius toward zero while remaining practically safe.

2.2.3 A comprehensive overview of existing safe regions

The objective of this section is to present a comprehensive overview of all existing safe regions in the literature (to the best of our knowledge). The primary emphasis here is on elucidating their definitions. Additionally, we will briefly touch on their construction methods, avoiding excessive technical details, and also discuss known results regarding their interrelationships whenever it is appropriate.

Existing safe regions have been defined in various setups, all of which are particular cases of our general setup (2.25-SD). From the perspective of (2.25-SD), the following information needs to be specified for each particular setup: the spaces $\mathscr{M}$ and $\mathscr{H}$, the functions f and g, and the primal and dual vectors $\mathbf{x}$ and $\mathbf{u}$ used to define the safe region.

In the existing literature, safe regions have typically been defined in finite-dimensional settings. Therefore, throughout this section, we confine our discussion to the finite-dimensional case:

$$\mathscr{M} = \mathbb{R}^n \text{ and } \mathscr{H} = \mathbb{R}^m.$$

However, it is important to note that all the construction methodologies discussed here can be readily extended to general Banach space $\mathscr{M}$ and Hilbert space $\mathscr{H}$.

Before delving into details, it is noteworthy that all the safe regions discussed in the following were originally proposed in the context of safe screening methods. While many authors provided names for their safe screening methods, they did not explicitly name the corresponding safe regions. To redirect the focus on the safe region itself, we will therefore refer to the safe region by the name of the corresponding safe screening method.

Safe balls

SAFE and SASVI ball.

Here we consider LASSO problem for which strong duality reads as follows:

$$\min_{\mathbf{x}\in\mathbb{R}^n} \quad \frac{1}{2}\left\|\mathbf{b}-\mathbf{A}\mathbf{x}\right\|_2^2+\lambda\left\|\mathbf{x}\right\|_1=\max_{\mathbf{u}\in U_{\lambda\|\cdot\|_1}} \quad \frac{1}{2}\left\|\mathbf{b}\right\|_2^2-\frac{1}{2}\left\|\mathbf{b}-\mathbf{u}\right\|_2^2, \tag{2.33}$$

for some $\mathbf{b}\in\mathbb{R}^m$, $\mathbf{A}=[\mathbf{a}_1,\ldots,\mathbf{a}_n]\in\mathbb{R}^{m\times n}$, $\lambda>0$ and $U_{\lambda\|\cdot\|_1}$ is defined by

$$U_{\lambda\|\cdot\|_1}=\{\mathbf{u}\in\mathbb{R}^m:|\langle\mathbf{a}_i,\mathbf{u}\rangle|\leq\lambda,\,\forall i=1,...,n\}. \tag{2.34}$$

Let $\mathbf{x}_\lambda^\star$ and $\mathbf{u}_\lambda^\star$ denote minimizer and maximizer corresponding to the primal and dual problem defined in (2.33). Notice that $\mathbf{u}_\lambda^\star$ is unique since the dual problem can be interpreted as the closest point projection problems (*w.r.t.* ℓ_2-norm) from $\mathbf{b}$ onto the closed convex set $U_{\lambda\|\cdot\|_1}$. Therefore, $\mathbf{u}_\lambda^\star$ verifies:

$$\left\|\mathbf{b}-\mathbf{u}_\lambda^\star\right\|_2\leq\left\|\mathbf{b}-\mathbf{u}\right\|_2,$$

for all $\mathbf{u}\in U_{\lambda\|\cdot\|_1}$. This inequality yields the following safe region:

$$\mathbf{u}_\lambda^\star\in B_{\texttt{SAFE}}(\mathbf{u})\triangleq B(\mathbf{b},\left\|\mathbf{b}-\mathbf{u}\right\|_2). \tag{2.35-SAFE-b}$$

This result was first obtained in [52] in which the authors consider $\mathbf{u}=\frac{\lambda}{\|\mathbf{A}^{\mathrm{T}}\mathbf{b}\|_\infty}\mathbf{b}$, *i.e.*, a scaled version of $\mathbf{b}$. Here the scaling is chosen so that $\mathbf{u}$ belongs to $U_{\lambda\|\cdot\|_1}$. They refer to their method as *SAfe Feature Elimination (SAFE)* technique. We therefore name this region as *SAFE ball*.

Another approach for building a safe region for LASSO is to leverage the first-order

optimality condition [5] relative to the dual problem in (2.33), which reads as

$$\langle \mathbf{b} - \mathbf{u}^\star_\lambda, \mathbf{u} - \mathbf{u}^\star_\lambda \rangle \leq 0, \tag{2.36}$$

for all $\mathbf{u} \in U_{\lambda\|\cdot\|_1}$. This observation directly leads to the safeness of the following ball:

$$\mathbf{u}^\star_\lambda \in B_{\texttt{SASVI}}(\mathbf{u}) \triangleq B\left(\frac{\mathbf{b}+\mathbf{u}}{2}, \frac{\|\mathbf{b}-\mathbf{u}\|_2}{2}\right). \tag{2.37-SASVI-b}$$

This safeness is proved in sequential screening method [66, Equation (14)] where the authors consider $\mathbf{u} = \frac{\lambda}{\lambda_0}\mathbf{u}^\star_{\lambda_0} \in U_{\lambda\|\cdot\|_1}$ for some other parameter $\lambda_0 > 0$. Since the screening method associated with this safe region is called *SAfe Screening with Variational Inequalities (SASVI)*, we refer to this ball as *SASVI ball*. It is not hard to verify that $B_{\texttt{SASVI}}(\mathbf{u}) \subset B_{\texttt{SAFE}}(\mathbf{u})$ for any $\mathbf{u} \in U_{\lambda\|\cdot\|_1}$.

DPP and EDPP ball.

We now consider the same setup (2.33). Recall that $\mathbf{u}^\star_\lambda$ is the closest projection of $\mathbf{b}$ onto the dual polytope $U_{\lambda\|\cdot\|_1}$, *i.e.*,

$$\mathbf{u}^\star_\lambda = \operatorname*{arg\,min}_{\mathbf{u} \in U_{\lambda\|\cdot\|_1}} \|\mathbf{b} - \mathbf{u}\|_2 . \tag{2.38}$$

Now, by substituting $\lambda = \lambda_0$ for some other parameter $\lambda_0 > 0$ into (2.38), we see that $\frac{\lambda}{\lambda_0}\mathbf{u}^\star_{\lambda_0}$ is also the closest point projection of $\frac{\lambda}{\lambda_0}\mathbf{b}$ onto $U_{\lambda\|\cdot\|_1}$, since

$$\frac{\lambda}{\lambda_0}\mathbf{u}^\star_{\lambda_0} = \operatorname*{arg\,min}_{\frac{\lambda}{\lambda_0}\mathbf{u} \in \frac{\lambda}{\lambda_0} U_{\lambda_0\|\cdot\|_1}} \left\| \frac{\lambda}{\lambda_0}\mathbf{b} - \frac{\lambda}{\lambda_0}\mathbf{u} \right\|_2 = \operatorname*{arg\,min}_{\mathbf{u}' \in U_{\lambda\|\cdot\|_1}} \left\| \frac{\lambda}{\lambda_0}\mathbf{b} - \mathbf{u}' \right\|_2 . \tag{2.39}$$

Here, we let $\mathbf{u}' = \frac{\lambda}{\lambda_0}\mathbf{u}$ and notice that $\frac{\lambda}{\lambda_0} U_{\lambda_0\|\cdot\|_1} = U_{\lambda\|\cdot\|_1}$.

Combining (2.38) and (2.39) together with the so-called *non-expansiveness* property of projection operator [5, Definition 4.1 and Proposition 4.16], one deduces:

$$\left\| \mathbf{u}^\star_\lambda - \frac{\lambda}{\lambda_0}\mathbf{u}^\star_{\lambda_0} \right\|_2 \leq \left\| \mathbf{b} - \frac{\lambda}{\lambda_0}\mathbf{b} \right\|_2 .$$

5. It is known as the *Variational inequality*, see *e.g.*, [2, Theorem 9.5.5].

Exploiting this observation, Wang *et al.* [92] proposed the following safe ball region:

$$\mathbf{u}^\star_\lambda \in B_{\texttt{DPP}}(\mathbf{u}^\star_{\lambda_0}) \triangleq B\left(\frac{\lambda}{\lambda_0}\mathbf{u}^\star_{\lambda_0}, \left\|\mathbf{b} - \frac{\lambda}{\lambda_0}\mathbf{b}\right\|_2\right). \tag{2.40-DPP-b}$$

They name their corresponding safe screening using this ball as the *Dual Polytope Projection* approach. We therefore, call this region *DPP ball*.

The authors also propose three improvements [92, Theorem 10, 16 and 18] of DPP ball. The smallest ball (in the sense of inclusion), which is referred to as the *Enhanced DPP (EDPP) ball*,[6] is defined as a safe ball region associated with $\mathbf{u}^\star_{\lambda_0}$ for some parameter $\lambda_0 \geq \lambda$ [92, Theorem 18]:

$$\mathbf{u}^\star_\lambda \in B_{\texttt{EDPP}}(\mathbf{u}^\star_{\lambda_0}) \triangleq B\left(\frac{\lambda}{\lambda_0}\mathbf{u}^\star_{\lambda_0} + \frac{1}{2}\mathbf{v}_2^\perp, \frac{1}{2}\left\|\mathbf{v}_2^\perp\right\|_2\right), \tag{2.41-EDPP-b}$$

where

$$\begin{aligned}
\mathbf{v}_2^\perp &\triangleq \mathbf{v}_2 - \frac{\langle \mathbf{v}_1, \mathbf{v}_2\rangle}{\|\mathbf{v}_1\|_2^2}\mathbf{v}_1,\\
\mathbf{v}_1 &\triangleq \mathbf{b} - \mathbf{u}^\star_{\lambda_0} = \mathbf{A}\mathbf{x}^\star_{\lambda_0},\\
\mathbf{v}_2 &\triangleq \mathbf{b} - \frac{\lambda}{\lambda_0}\mathbf{u}^\star_{\lambda_0}.
\end{aligned}$$

The construction of EDPP ball is quite complex, but the authors (via the comparisons with an intermediate safe ball region) assert that $B_{\texttt{EDPP}}(\mathbf{u}^\star_{\lambda_0}) \subset B_{\texttt{DPP}}(\mathbf{u}^\star_{\lambda_0})$. Note that the EDPP ball can also be applied for other problems than LASSO, see [98] for an application in solving Elastic-Net problem.

GAP and $\mathbf{x}$-GAP ball.

Here, we consider the ℓ_1-norm penalization problem with the associated strong duality:

$$\min_{\mathbf{x}\in\mathbb{R}^n} \quad f(\mathbf{A}\mathbf{x}) + \lambda\|\mathbf{x}\|_1 = \max_{\mathbf{u}\in U_{\lambda\|\cdot\|_1}} \quad -f^*(-\mathbf{A}\mathbf{u}), \tag{2.42}$$

where $f : \mathbb{R}^m \to \mathbb{R}\cup\{+\infty\}$ is a closed proper convex function, $\mathbf{A} \in \mathbb{R}^{m\times n}$ and $\lambda > 0$. We further assume that f has gradient being α^{-1}-Lipschitz continuous on the whole space

6. In fact, they use the term "Enhanced DPP" to name their the sequential safe screening rather than the safe ball region.

$\mathbb{R}^m$. [7]

Under this, setting, Ndiaye *et al.* [72, Theorem 6] proved that the following assertion holds true, [8]

$$\mathbf{u}^\star_\lambda \in B_{\texttt{GAP}}(\mathbf{x}, \mathbf{u}) \triangleq B\left(\mathbf{u}, \sqrt{\frac{2\,\mathrm{GAP}(\mathbf{x}, \mathbf{u})}{\alpha}}\right), \tag{2.43-GAP-b}$$

for any feasible primal-dual couple $(\mathbf{x}, \mathbf{u})$. Here the dual gap $\mathrm{GAP}(\mathbf{x}, \mathbf{u})$ is defined as the difference between the primal and dual functions in (2.42). We refer to this region as *GAP ball*. This region was first proposed in the context of LASSO [45] and later extended to general convex function f in [72, 25] and general convex function g in [73].

GAP ball exhibits two crucial characteristics. Firstly, assuming that the mapping $(\mathbf{x}, \mathbf{u}) \mapsto \mathrm{GAP}(\mathbf{x}, \mathbf{u})$ is continuous and vanishes at some optimal pairs $(\mathbf{x}^\star, \mathbf{u}^\star)$, [9] the radius of $B_{\texttt{GAP}}(\mathbf{x}, \mathbf{u})$ can be arbitrarily small when $(\mathbf{x}, \mathbf{u})$ is sufficiently close to $(\mathbf{x}^\star, \mathbf{u}^\star)$. However, not all dynamic safe regions possess this property, *e.g.*, the SAFE ball (2.35-SAFE-b). Secondly, the construction of the GAP ball does not rely on any specific assumptions about $(\mathbf{x}, \mathbf{u})$ except the feasibility of $\mathbf{u}$. This is different from the cases of DPP and EDPP ball where $(\mathbf{x}, \mathbf{u})$ is assumed to be optimal (*w.r.t.* to some parameter λ_0). These two fundamental properties make the GAP ball the most preferred result in both theoretical analysis and practical applications. Moreover, these two key properties set the standard that newly devised safe ball regions should meet.

Many later works sought to extend/apply/improve the GAP ball in various ways. Firstly, Dantas *et al.* [25] proved the safeness of GAP ball under weaker assumptions. Secondly, several studies showcased that the GAP ball can be applied for dimensionality reduction in various convex optimization problems [72, 24, 26, 41, 65, 79], and even beyond convex optimization problems [54, 53]. These demonstrated the GAP ball's influence, spanning a wide range of applications.

Recently, a safe region analogous to the GAP ball has been introduced in [59]. This safe region is obtained as a particularization of the general framework known as the "region-free safe screening method", applied to the strong duality setup (2.42). Interestingly, this safe ball has center located at $-\nabla f(\mathbf{A}\mathbf{x})$ instead of $\mathbf{u}$ as in GAP ball. In other words, the center of this ball exploits the primal information $\mathbf{x}$ not the dual information $\mathbf{u}$ as in case

7. This means $\|\nabla f(\mathbf{v}_1) - \nabla f(\mathbf{v}_2)\|_2 \leq \alpha^{-1} \|\mathbf{v}_1 - \mathbf{v}_2\|_2$ for all $\mathbf{v}_1, \mathbf{v}_2 \in \mathbb{R}^m$. Note that in the original result [72, Theorem 6], the authors consider a slightly general setup where ℓ_1-norm penalization function is replaced by any general norm.

8. Actually, the result presented in [72, Theorem 6] holds for general norm penalization problem.

9. The vanishing of dual gap $\mathrm{GAP}(\mathbf{x}^\star_\lambda, \mathbf{u}^\star_\lambda) = 0$ is equivalent to the strong duality assumed in (2.42).

of (2.43-GAP-b). To emphasize this dependency, in this thesis, we refer to this safe ball as $\mathbf{x}$-*GAP ball*. Its definition is provided below,

$$\mathbf{u}_\lambda^\star \in B_{\texttt{xGAP}}(\mathbf{x},\mathbf{u}) \triangleq B\left(-\nabla f(\mathbf{A}\mathbf{x}), \sqrt{\frac{2\,\mathrm{GAP}(\mathbf{x},\mathbf{u})}{\alpha}}\right). \tag{2.44-$\mathbf{x}$-GAP-b}$$

FNE and DEDPP ball.

Let us consider again the LASSO problem with its strong duality (2.33). In [67], the authors showed that if $(\mathbf{x},\mathbf{u})$ satisfies the following condition

$$\langle \mathbf{u}, \mathbf{A}\mathbf{x}\rangle = \lambda \left\|\mathbf{x}\right\|_1, \tag{2.45}$$

then $\mathbf{u}$ is the closest point projection of $\mathbf{b}' \triangleq \mathbf{A}\mathbf{x}+\mathbf{u}$ onto $U_{\lambda\|\cdot\|_1}$. Recall that $\mathbf{u}_\lambda^\star$ is also the closest point projection of $\mathbf{b}$ onto $U_{\lambda\|\cdot\|_1}$, then the *Firmly Non-Expansiveness (FNE)* property of projection operator yields

$$\|\mathbf{u}_\lambda^\star - \mathbf{u}\|_2^2 \leq \langle \mathbf{u}^\star - \mathbf{u}, \mathbf{b}-\mathbf{b}'\rangle.$$

It can be equivalently rewritten as:

$$\left\|\mathbf{u}_\lambda^\star - \left(\mathbf{u}+\frac{1}{2}(\mathbf{b}-\mathbf{b}')\right)\right\|_2 \leq \frac{1}{2}\left\|\mathbf{b}-\mathbf{b}'\right\|_2.$$

This inequality results in a safe ball region called *FNE ball* defined as:

$$\mathbf{u}_\lambda^\star \in B_{\texttt{FNE}}(\mathbf{x},\mathbf{u}) \triangleq B\left(\mathbf{u}+\frac{1}{2}(\mathbf{b}-\mathbf{A}\mathbf{x}-\mathbf{u}), \frac{1}{2}\left\|\mathbf{b}-\mathbf{A}\mathbf{x}-\mathbf{u}\right\|_2\right). \tag{2.46-FNE-b}$$

Under certain conditions, the authors showed that FNE ball is a subset of GAP ball [67, Lemma 1]. Note that constructing a pair $(\mathbf{x},\mathbf{u})$ which satisfies the relation (2.45) while obtaining a small-radius ball is not practically easy. A relaxation for FNE ball is therefore proposed in [67, Theorem 2].

Another safe region introduced recently, is the so-called *Dynamic EDPP (DEDPP)* ball [99]. This is an extension of EDDP ball (2.41-EDPP-b) which is safe for any primal-dual feasible couples $(\mathbf{x},\mathbf{u})$. The construction of this ball is quite intricate so will be

skipped here. Its definition is provided below:

$$\mathbf{u}^\star_\lambda \in B_{\texttt{DEDPP}}(\mathbf{x}, \mathbf{u}) \triangleq B\left(\frac{1}{2}(\mathbf{b}+\mathbf{u}) - \gamma\mathbf{A}\mathbf{x}, \sqrt{\frac{1}{4}\left\|\mathbf{b}-\mathbf{u}\right\|_2^2 - \gamma^2\left\|\mathbf{A}\mathbf{x}\right\|_2^2}\right), \quad \text{(2.47-DEDPP-b)}$$

where

$$\gamma \triangleq \max\left(0, \frac{1}{2}\frac{\langle \mathbf{A}\mathbf{x}, \mathbf{b}+\mathbf{u}\rangle - 2\lambda\left\|\mathbf{x}\right\|_1}{\left\|\mathbf{A}\mathbf{x}\right\|_2^2}\right).$$

By the construction of DEDPP, the authors assert that its radius is guaranteed to be less than or equal to radius of GAP ball if the same pair $(\mathbf{x}, \mathbf{u})$ is used.

SLORES and SFER ball.

We now consider the ℓ_1-norm penalization of logistic regression, with the strong duality defined as an instance of (2.42) with f defined as a logistic loss function:

$$f(\mathbf{v}) = \frac{1}{m}\sum_{i=1}^{m} -\mathbf{b}(i)\mathbf{v}(i) + \log(1+\exp(\mathbf{v}(i))), \tag{2.48}$$

for any $\mathbf{v} \in \mathbb{R}^m$. In this case ∇f is $\frac{m}{4}$-Lipschitz continuous. In [75], the authors showed that the following ball is safe,

$$\mathbf{u}^\star_\lambda \in B_{\texttt{SFER}}\left(\mathbf{u}^\star_{\lambda_0}\right) \triangleq B\left(\frac{1}{2}\left(\mathbf{u}^\star_{\lambda_0} + \frac{\lambda}{\lambda_0}\mathbf{u}^\star_{\lambda_0}\right), \sqrt{\frac{\xi}{\alpha} - \frac{1}{4}\left\|\mathbf{u}^\star_{\lambda_0} - \frac{\lambda}{\lambda_0}\mathbf{u}^\star_{\lambda_0}\right\|_2^2}\right), \quad \text{(2.49-SFER-b)}$$

where

$$\xi = \mathrm{Breg}_{f^{*-}, -\mathbf{A}\mathbf{x}^\star_{\lambda_0}}\left(\frac{\lambda}{\lambda_0}\mathbf{u}^\star_{\lambda_0}, \mathbf{u}^\star_{\lambda_0}\right). \tag{2.50}$$

Here Breg denotes the Bregman divergence. [10] The authors exploit this safe ball region to derive the so-called *Safe Feature Elimination Rule (SFER)*. Thus, we name this safe region as *SFER ball*.

Note that the safeness of SFER ball can be written as follows:

$$\frac{\alpha}{2}\left\|\mathbf{u}^\star_\lambda - \frac{\lambda}{\lambda_0}\mathbf{u}^\star_{\lambda_0}\right\|_2^2 + \frac{\alpha}{2}\left\|\mathbf{u}^\star_\lambda - \mathbf{u}^\star_{\lambda_0}\right\|_2^2 \leq \xi, \tag{2.51}$$

10. Bregman divergence is a non-negative quantity defined in (B.4).

By relaxing the first term in LHS of (2.51), one directly obtains a weaker inequality,

$$\frac{\alpha}{2}\left\|\mathbf{u}_{\lambda}^{\star}-\mathbf{u}_{\lambda_0}^{\star}\right\|_2^2 \leq \xi, \tag{2.52}$$

This corresponds to the following safe ball region:

$$\mathbf{u}_{\lambda}^{\star} \in B_{\texttt{SLORES}}(\mathbf{u}_{\lambda_0}^{\star}) \triangleq B\left(\mathbf{u}_{\lambda_0}^{\star}, \sqrt{\frac{2}{\alpha}\xi}\right). \tag{2.53-SLORES-b}$$

The corresponding safe screening method associated with this safe region is called *Sparse LOgistic REgression Screening (SLORES)* rule [93, Theorem 2]. Consequently, we name this safe ball region as *SLORES ball*.

Safe half-spaces

In the following, we examine the LASSO problem and its strong duality as represented by (2.33). Our objective is to review three approaches for creating a safe half-space, namely ST, SASVI and Hölder half-spaces, as discussed in the literature. It is important to note that the discussion regarding the GAP half-space [45] will be deferred to the next section due to its distinct construction technique.

ST half-space. The first straightforward approach for constructing a safe half-space involves the following observation:

$$\langle \mathbf{a}_i, \mathbf{u}\rangle \leq \lambda, \quad \forall \mathbf{u} \in U_{\lambda\|\cdot\|_1}, \forall i \in 1,\ldots,n.$$

This signifies that the dual feasible set $U_{\lambda\|\cdot\|_1}$ is, in fact, a subset of the half-spaces $H(\mathbf{a}_i, \lambda)$ for any $i = 1,\ldots,n$. By combining this insight with the knowledge that $\mathbf{u}_{\lambda}^{\star} \in U_{\lambda\|\cdot\|_1}$, it becomes evident that all these half-spaces are safe. Choosing an arbitrary index $i_0 \in \{1,\ldots,n\}$, we have a safe half-space denoted as $H_{\texttt{ST}}(i_0)$:

$$\mathbf{u}_{\lambda}^{\star} \in H_{\texttt{ST}}(i_0) \triangleq H(\mathbf{a}_{i_0}, \lambda). \tag{2.54-ST-h}$$

In [95], the authors exploited this half-space to derive the so-called *Sphere Tests (ST)* in the context of safe screening. We therefore refer to this region as *ST half-space*.

SASVI half-space. The second approach to build a safe half-space is to apply the first

order optimality condition (2.36) for parameter λ_0, we obtain

$$\left\langle \mathbf{b} - \mathbf{u}^\star_{\lambda_0}, \mathbf{u}' - \mathbf{u}^\star_{\lambda_0} \right\rangle \leq 0, \tag{2.55}$$

for all $\mathbf{u}' \in U_{\lambda_0 \|\cdot\|_1}$. Substituting $\mathbf{u}' = \frac{\lambda_0}{\lambda}\mathbf{u}^\star_\lambda \in U_{\lambda_0\|\cdot\|_1}$ to (2.55), one derives

$$\frac{\lambda}{\lambda_0}\left\langle \mathbf{b} - \mathbf{u}^\star_{\lambda_0}, \mathbf{u}^\star_\lambda - \frac{\lambda}{\lambda_0}\mathbf{u}^\star_{\lambda_0} \right\rangle \leq 0. \tag{2.56}$$

This inequality defines a safe half-space region for $\mathbf{u}^\star_\lambda$:

$$\mathbf{u}^\star_\lambda \in H_{\texttt{SASVI}}(\mathbf{u}^\star_{\lambda_0}) \triangleq H\left(\mathbf{b} - \mathbf{u}^\star_{\lambda_0}, \left\langle \mathbf{b} - \mathbf{u}^\star_{\lambda_0}, \frac{\lambda}{\lambda_0}\mathbf{u}^\star_{\lambda_0} \right\rangle\right). \tag{2.57-SASVI-h}$$

We refer to this region as *SASVI half-space* since it was observed in the safe screening approach called SASVI, see [66, Equation (13)].

Hölder half-space. In [87], we proved that: [11]

$$\langle \mathbf{A}\mathbf{x}, \mathbf{u}^\star_\lambda \rangle \leq \left\| \mathbf{A}^{\mathrm{T}}\mathbf{u}^\star_\lambda \right\|_\infty \|\mathbf{x}\|_1 \leq \lambda \|\mathbf{x}\|_1,$$

for any $\mathbf{x} \in \mathbb{R}^n$. Here the first inequality follows the Hölder inequality and the second one is a consequence of the feasibility of $\mathbf{u}^\star_\lambda$. We therefore call this region *Hölder half-space*.

$$\mathbf{u}^\star_\lambda \in H_{\texttt{Hö}}(\mathbf{x}) \triangleq H(\mathbf{A}\mathbf{x}, \lambda \|\mathbf{x}\|_1). \tag{2.58-Hölder-h}$$

This half-space was also introduced simultaneously in [99]. In particular, the authors also notice that Hölder half-space is a generalization of SASVI half-space.

Safe domes

To construct a safe dome region, it is sufficient to take the intersection of a safe ball and a safe half-space. We list in the following four historical ways of choosing safe ball and half-spaces in the context of LASSO problem with strong duality (2.33).

ST dome. This safe region was proposed in [96], by cutting the SAFE ball using ST half-space (2.54-ST-h), in which the author proposed the choice for index i_0 so that it

11. Note that the result remains valid if $\|\cdot\|_1$ is replaced by a general gauge function.

maximizes the absolute correlation of atom $\mathbf{a}_i$ and $\mathbf{b}$, *i.e.*,

$$i_0 \in \underset{i=1,\dots,n}{\arg\max} \left|\langle \mathbf{a}_i, \mathbf{b}\rangle\right|.$$

The ST half-space with this index i_0 is then used to cut the SAFE ball (2.35-SAFE-b) to obtain a safe dome region, say *ST dome* [96, Equation (7)]:

$$\mathbf{u}^\star_\lambda \in D_{\texttt{ST}}(i_0, \mathbf{u}) \triangleq H_{\texttt{ST}}(i_0) \cap B_{\texttt{SAFE}}(\mathbf{u}), \tag{2.59-ST-d}$$

for any $\mathbf{u} \in U_{\lambda\|\cdot\|_1}$.

SFER dome. Given the acknowledgment of the dual optimal solution $\mathbf{u}^\star_{\lambda_0}$ *w.r.t.* a parameter λ_0, another approach for selecting i_0 [75] is to choose it as an index that maximizes the absolute correlation of atoms $\mathbf{a}_i$ and $\mathbf{u}^\star_{\lambda_0}$,

$$i_0 \in \underset{i=1,\dots,n}{\arg\max} \left|\left\langle \mathbf{a}_i, \mathbf{u}^\star_{\lambda_0}\right\rangle\right| = \{i \in \{1,\dots,n\} : \left|\left\langle \mathbf{a}_i, \mathbf{u}^\star_{\lambda_0}\right\rangle\right| = \lambda_0\}.$$

The authors then consider the safe dome region obtained by taking the intersection of $H_{\texttt{ST}}(i_0)$ and the SFER ball $B_{\texttt{SFER}}(\mathbf{u}^\star_{\lambda_0})$:

$$\mathbf{u}^\star_\lambda \in D_{\texttt{SFER}}(i_0, \mathbf{u}^\star_{\lambda_0}) \triangleq H_{\texttt{ST}}(i_0) \cap B_{\texttt{SFER}}(\mathbf{u}^\star_{\lambda_0}). \tag{2.60-SFER-d}$$

We refer to this safe region as *SFER dome*.

SASVI dome. By taking the intersection of SASVI half-space $H_{\texttt{SASVI}}$ (2.57-SASVI-h) and SASVI ball (2.37-SASVI-b), we can obtain a safe dome region [66, Equation (15)], namely *SASVI dome*:

$$\mathbf{u}^\star_\lambda \in D_{\texttt{SASVI}}(\mathbf{u}^\star_{\lambda_0}) \triangleq H_{\texttt{SASVI}}(\mathbf{u}^\star_{\lambda_0}) \cap B_{\texttt{SASVI}}(\mathbf{u}^\star_{\lambda_0}). \tag{SASVI-d}$$

DSASVI dome. By taking the intersection of Hölder half-space $H_{\texttt{Hö}}(\mathbf{x})$ (2.58-Hölder-h) and SASVI ball (2.37-SASVI-b), we can obtain a safe dome region

$$\mathbf{u}^\star_\lambda \in D_{\texttt{SASVI}}(\mathbf{x}, \mathbf{u}) \triangleq H_{\texttt{Hö}}(\mathbf{x}) \cap B_{\texttt{SASVI}}(\mathbf{u}), \tag{2.61-DSASVI-d}$$

for all $(\mathbf{x}, \mathbf{u}) \in \mathbb{R}^n \times U_{\lambda\|\cdot\|_1}$. This region is referred to as *Dynamic SASVI (DSASVI) dome* in [99, Theorem 8] and *Hölder dome* [87, Theorem 1]. In this thesis, we call it DSASVI ball.

GAP moon, half-space and dome. Considering the LASSO's strong duality (2.33), Fercoq

et al. [45] introduced a sequence of safe regions with different shapes including excluding ball, moon, half-space and dome, which serve intermediate steps in constructing the GAP ball region (2.43-GAP-b).

We now briefly review the idea of constructing these safe regions. Notice that the strong duality (2.33) implies that, for any $(\mathbf{x}, \mathbf{u}) \in \mathbb{R}^n \times U_{\lambda\|\cdot\|_1}$,

$$\frac{1}{2}\|\mathbf{b}-\mathbf{A}\mathbf{x}\|_2^2 + \lambda\|\mathbf{x}\|_1 \geq \frac{1}{2}\|\mathbf{b}\|_2^2 - \frac{1}{2}\|\mathbf{b}-\mathbf{u}\|_2^2 .$$

Re-aranging terms in this inequality, we obtain

$$\frac{1}{2}\|\mathbf{b}-\mathbf{u}\|_2^2 \geq \frac{1}{2}\|\mathbf{b}\|_2^2 - \frac{1}{2}\|\mathbf{b}-\mathbf{A}\mathbf{x}\|_2^2 - \lambda\|\mathbf{x}\|_1 .$$

Let us define the *GAP excluding ball* $E_{\texttt{GAP}}$ as follows,

$$E_{\texttt{GAP}}(\mathbf{x}) = \left\{\mathbf{u} \in \mathbb{R}^m : \|\mathbf{b}-\mathbf{u}\|_2 \geq \sqrt{[\|\mathbf{b}\|_2^2 - \|\mathbf{b}-\mathbf{A}\mathbf{x}\|_2^2 - 2\lambda\|\mathbf{x}\|_1]_+}\right\}. \tag{2.62-GAP-e}$$

Then, it is clear that $\mathbf{u}_\lambda^\star \in U_{\lambda\|\cdot\|_1} \subset E_{\texttt{GAP}}(\mathbf{x})$, *i.e.*, $E_{\texttt{GAP}}(\mathbf{x})$ is safe. Now, we define the *GAP moon* region [12] as the intersection of GAP excluding ball and SASVI ball,

$$M_{\texttt{GAP}}(\mathbf{x}, \mathbf{u}) \triangleq B_{\texttt{SASVI}}(\mathbf{u}) \cap E_{\texttt{GAP}}(\mathbf{x}). \tag{2.63-GAP-m}$$

Now, the *GAP half-space* $H_{\texttt{GAP}}(\mathbf{x}, \mathbf{u})$ is defined (indirectly) as a half-space such that the *GAP dome* $D_{\texttt{GAP}}(\mathbf{x}, \mathbf{u})$ is the convex hull of $M_{\texttt{GAP}}(\mathbf{x}, \mathbf{u})$, where

$$D_{\texttt{GAP}}(\mathbf{x}, \mathbf{u}) \triangleq B_{\texttt{SASVI}}(\mathbf{u}) \cap H_{\texttt{GAP}}(\mathbf{x}, \mathbf{u}). \tag{2.64-GAP-d}$$

Then, the authors defined the GAP ball $B_{\texttt{GAP}}(\mathbf{x}, \mathbf{u})$ as a ball with center at $\mathbf{u}$ and the smallest radius containing $D_{\texttt{GAP}}(\mathbf{x}, \mathbf{u})$. The GAP ball then has a closed form expression as given by (2.43-GAP-b).

Although $H_{\texttt{GAP}}(\mathbf{x}, \mathbf{u})$ has a descriptive definition, it also possesses a closed-form expression [87, Equation (20-21)]:

$$H_{\texttt{GAP}}(\mathbf{x}, \mathbf{u}) = H\Big(\mathbf{b}-\mathbf{c}, \mathrm{GAP}\,(\mathbf{x}, \mathbf{u}) + \langle \mathbf{b}-\mathbf{c}, \mathbf{c}\rangle - r^2\Big), \tag{2.65-GAP-h}$$

where $\mathbf{c} = \frac{\mathbf{b}-\mathbf{u}}{2}$ and $r = \frac{\|\mathbf{b}-\mathbf{u}\|_2}{2}$ denote the center and radius of the SASVI ball $B_{\texttt{SASVI}}(\mathbf{u})$,

12. Here, the term "moon" was used in [99].

respectively.

Other safe regions

In [95], the authors introduced *ST2 and ST3 ball* as the balls with specific centers and smallest radii containing ST dome (2.59-ST-d).

Note that in addition to the ball and dome shapes, there are other safe regions with different shapes, such as the refined dome (intersection of a ball and two half-spaces) [97, Section 4.5] and ellipsoid [23]. However, due to the complexity of constructing and implementing these regions in practical dimensionality reduction methods, and their limited utilization by researchers, they are beyond the scope of this thesis.

Chapter 3

Unifying existing safe regions with FBI regions

Abstract. *This chapter exploits the Bregman and Fenchel divergences to derive a novel inequality called* Fenchel Bregman Inequality (FBI) *for estimating the location of the dual optimal solution in convex optimization problems with a general convex penalization function. The FBI defines a corresponding safe region, termed the* FBI ball*. In particular, if the penalization is a gauge function, we introduce yet another new safe region, termed the* Hölder half-space*. By combining these two safe regions, we further derive the* FBI dome*. We also present the closed-form construction of a ball (with arbitrary center and smallest radius) containing a given dome, called* geometric ball*. Furthermore, we demonstrate that existing safe regions, previously introduced in the context of static, sequential, and dynamic safe screening methods, are either special cases or supersets of our FBI regions, underscoring the generality of our framework.*

3.1 FBI ball

In this section, we present a novel safe ball region termed the "FBI ball". At the core of constructing this secure region lies what we term the "Fenchel Bregman Inequality". We then explore the capability of this region to achieve a zero radius and offer a comprehensive comparison for showing that the FBI ball is in fact a generalization of existing safe ball regions proposed over the last 10+ years.

3.1.1 Definition

This section is dedicated to proving an inequality, namely *Fenchel Bregman Inequality (FBI)*, which provides an estimate for the position of the dual optimal solution by the dual gap in which the dual gap is proven to be the sum of Fenchel and Bregman divergences. Leveraging this inequality, we introduce a novel safe ball region termed the *FBI ball*.

Let us start by providing the description of our working setup. Here, we consider the following general strong duality:

$$\min_{\mathbf{x}\in\mathscr{M}} \underbrace{f(\mathbf{A}\mathbf{x}) + g(\mathbf{x})}_{p(\mathbf{x})} = \max_{\mathbf{u}\in\mathscr{H}} \underbrace{-f^*(-\mathbf{u}) - g^*(\mathbf{A}^*\mathbf{u})}_{d(\mathbf{u})}, \tag{3.1}$$

where $f : \mathscr{H} \to \mathbb{R} \cup \{+\infty\}$ and $g : \mathscr{M} \to \mathbb{R} \cup \{+\infty\}$ are convex functions, and $\mathbf{A} : \mathscr{M} \to \mathscr{H}$ is a linear operator. Here, recall that $\mathscr{M}$ is a (possibly non-reflexive) Banach space and $\mathscr{H}$ is a Hilbert space. Recall that f^*, g^* denote the conjugate of f, g, and $\mathbf{A}^*$ denotes the pre-adjoint operator of $\mathbf{A}$. Please prefer to Appendix B.2 for a more detailed discussion on the duality (3.1) in infinite-dimensional settings.

To ensure the well-defined nature of (3.1), we assume that the following hypotheses (H1) and (H2) hold true. Furthermore, we also incorporate hypothesis (H3) as a central technical assumption in deriving subsequent results.

Hypothesis 3.1.1. *We impose the following hypotheses for* (3.1)*:*

(H1) There exist $\mathbf{x}^\star \in \mathscr{M}$ *minimizing the LHS and* $\mathbf{u}^\star \in \mathscr{H}$ *minimizing the RHS of* (3.1)*.*

(H2) The strong duality holds, i.e., $p(\mathbf{x}^\star) = d(\mathbf{u}^\star)$ *for any optimal pair* $(\mathbf{x}^\star, \mathbf{u}^\star)$*.*

(H3) f *has* α^{-1}*-Lipschitz continuous gradient for some* $\alpha > 0$ *on the whole space* $\mathscr{H}$*.* [1]

1. That is $\|\nabla f(\mathbf{v}_1) - \nabla f(\mathbf{v}_2)\|_{\mathscr{H}} \leq \alpha^{-1} \|\mathbf{v}_1 - \mathbf{v}_2\|$, for all $\mathbf{v}_1, \mathbf{v}_2 \in \mathscr{H}$, where the gradient ∇f is defined in the sense of Fréchet derivative [5, Definition 2.56].

Here, we remark that (H1) and (H2) hold under mild assumptions on f, g, and $\mathbf{A}$, see Theorem B.2.1, and are usually met in our problems of interest. A function f that satisfies (H3) is said to be α^{-1}-*strongly smooth* and this property is equivalent to the fact that f^* is α-*strongly convex* on its domain dom f^* (but not necessary on the whole space $\mathscr{H}$), see Theorem B.1.7. Therefore, $-d(\cdot)$ is strongly convex, which then implies the existence and uniqueness of $\mathbf{u}^\star$ [6, Theorem 5.25]. We refer the readers to Proposition B.2.5 and Proposition B.2.6 for the practical sufficient conditions for hypotheses (H1), (H2) and (H3).

Now we are ready for deriving FBI, which provides an estimation for $\mathbf{u}^\star$ based on the primal information $\mathbf{x} \in \mathscr{M}$ and dual information $\mathbf{u} \in \mathscr{H}$.

To estimate $\mathbf{u}^\star$, one may use any dual vector $\mathbf{u}$ sufficiently close to its. However, one cannot use directly primal variable $\mathbf{x}$ to estimate $\mathbf{u}^\star$. To get an idea of how to obtain a quantity that depends on $\mathbf{x}$ and close to $\mathbf{u}^\star$, one can notice the optimality condition that $\mathbf{u}^\star = -\nabla f(\mathbf{A}\mathbf{x}^\star)$. This inspires the idea of using $-\nabla f(\mathbf{A}\mathbf{x})$ as a good candidate close to $\mathbf{u}^\star$ if $\mathbf{x}$ is closed to $\mathbf{x}^\star$. To facilitate frequent use of this important quantity, we give it a shorthand notation:

$$\mathbf{r}_\mathbf{x} \triangleq -\nabla f(\mathbf{A}\mathbf{x}). \tag{3.2}$$

The following result shows that the total (weighted squared) distance from $\mathbf{u}^\star$ to $\mathbf{u}$ and to $\mathbf{r}_\mathbf{x}$ is upper-bounded by the dual gap. Recall that the definition of dual gap $\mathrm{GAP}(\mathbf{x}, \mathbf{u}) = p(\mathbf{x}) - d(\mathbf{u}) \geq 0$ for any primal-dual feasible pair $(\mathbf{x}, \mathbf{u})$, with p and d defined in (3.1). Furthermore, in this result, we show that the dual gap can be decomposed into two non-negative quantities involving Fenchel and Bregman divergences, which leads to the term "Fenchel Bregman Inequality". For the definitions of Fenchel and Bregman divergences, please refer to (B.3) and (B.4).

Lemma 3.1.2 (Fenchel Bregman Inequality (FBI))**.** *Let $(\mathbf{x}, \mathbf{u}) \in \mathscr{M} \times \mathscr{H}$. Under the hypotheses (H1), (H2) and (H3), $\mathbf{u}^\star$ satisfies the following inequality:*

$$\frac{\alpha}{2}\left\|\mathbf{u}^\star - \mathbf{u}\right\|_\mathscr{H}^2 + \frac{\alpha}{2}\left\|\mathbf{u}^\star - \mathbf{r}_\mathbf{x}\right\|_\mathscr{H}^2 \leq \mathrm{GAP}(\mathbf{x}, \mathbf{u}) = \mathrm{Breg}_{f^{*-}, -\mathbf{A}\mathbf{x}}(\mathbf{u}, \mathbf{r}_\mathbf{x}) + \mathrm{Fen}_g(\mathbf{x}, \mathbf{A}^*\mathbf{u}), \tag{3.3}$$

where $f^{*-} = f^*(-\cdot)$ and $\mathbf{r}_\mathbf{x}$ is defined in (3.2).

Proof. Here, we split the proof into two steps corresponding to the equality and inequality in (3.3).

Step 1. Proving equality in (3.3). Notice that one can decompose the dual gap as

a function of the Fenchel divergences of f and g as follows:

$$\begin{aligned}\mathrm{GAP}(\mathbf{x},\mathbf{u}) &= p(\mathbf{x}) - d(\mathbf{u}) \\ &= f(\mathbf{A}\mathbf{x}) + f^*(-\mathbf{u}) + g(\mathbf{x}) + g(\mathbf{A}^*\mathbf{u}) \\ &= f(\mathbf{A}\mathbf{x}) + f^*(-\mathbf{u}) + \langle \mathbf{A}\mathbf{x}, \mathbf{u}\rangle + g(\mathbf{x}) + g^*(\mathbf{A}^*\mathbf{u}) - \langle \mathbf{x}, \mathbf{A}^*\mathbf{u}\rangle \\ &= \mathrm{Fen}_f(\mathbf{A}\mathbf{x}, -\mathbf{u}) + \mathrm{Fen}_g(\mathbf{x}, \mathbf{A}^*\mathbf{u}). \end{aligned} \tag{3.4}$$

To prove the equality in (3.3), it is sufficient to show that

$$\mathrm{Fen}_f(\mathbf{A}\mathbf{x}, -\mathbf{u}) = \mathrm{Breg}_{f^{*-},-\mathbf{A}\mathbf{x}}(\mathbf{u}, \mathbf{r}_\mathbf{x}). \tag{3.5}$$

We now prove (3.5) by showing that the two quantities are actually equal via the intermediate value $\mathrm{Fen}_{f^{*-}}(\mathbf{u}, -\mathbf{A}\mathbf{x})$. First, notice that it is not hard to show that $(f^{*-})^* = f^{**-} = f^- = f(-\cdot)$.[2] This yields

$$\begin{aligned}\mathrm{Fen}_{f^{*-}}(\mathbf{u}, -\mathbf{A}\mathbf{x}) &= f^{*-}(\mathbf{u}) + (f^{*-})^*(-\mathbf{A}\mathbf{x}) - \langle \mathbf{u}, -\mathbf{A}\mathbf{x}\rangle \\ &= f^*(-\mathbf{u}) + f(\mathbf{A}\mathbf{x}) - \langle -\mathbf{u}, \mathbf{A}\mathbf{x}\rangle \\ &= \mathrm{Fen}_f(\mathbf{A}\mathbf{x}, -\mathbf{u}). \end{aligned} \tag{3.6}$$

Second, by the definition of $\mathbf{r}_\mathbf{x}$ (3.2), we have

$$\{\mathbf{r}_\mathbf{x}\} = \{-\nabla f(\mathbf{A}\mathbf{x})\} = \{\nabla f^-(-\mathbf{A}\mathbf{x})\} = \partial(f^{*-})^*(-\mathbf{A}\mathbf{x}).$$

This observation verifies the condition for establishing the relation of $\mathrm{Breg}_{f^{*-}}$ and $\mathrm{Fen}_{f^{*-}}$ (B.5), hence,

$$\mathrm{Breg}_{f^{*-},-\mathbf{A}\mathbf{x}}(\mathbf{u}, \mathbf{r}_\mathbf{x}) = \mathrm{Fen}_{f^{*-}}(\mathbf{u}, -\mathbf{A}\mathbf{x}). \tag{3.7}$$

Combining (3.6) and (3.7), we derive (3.5) and, thus, the equality in (3.3).

Step 2. Proving inequality in (3.3). We now focus on proving the inequality in (3.3). By (H3), one notices that f^{*-} is also α-strongly convex. This strong convexity implies that $\mathrm{Breg}_{f^{*-},-\mathbf{A}\mathbf{x}}(\mathbf{u}, \mathbf{r}_\mathbf{x}) \geq \frac{\alpha}{2}\|\mathbf{u} - \mathbf{r}_\mathbf{x}\|^2_\mathscr{H}$. As we have previously demonstrated, the dual

2. The main ingredient to prove this claim is to use the biconjugate theorem (see Theorem B.1.3), which asserts that $f^{**} = f$ when f is closed proper convex.

gap is the sum of non-negative quantities $\mathrm{Breg}_{f^*-,-\mathbf{Ax}}(\mathbf{u}, \mathbf{r}_\mathbf{x})$ and $\mathrm{Fen}_g(\mathbf{x}, \mathbf{A}^*\mathbf{u})$, therefore,

$$\mathrm{GAP}(\mathbf{x}, \mathbf{u}) \geq \frac{\alpha}{2} \|\mathbf{u} - \mathbf{r}_\mathbf{x}\|_\mathscr{H}^2 . \tag{3.8}$$

By (H1), there exists at least a primal-dual optimal pair $(\mathbf{x}^\star, \mathbf{u}^\star)$ for (3.1). Substituting $(\mathbf{x}, \mathbf{u}) = (\mathbf{x}^\star, \mathbf{u})$ and $(\mathbf{x}, \mathbf{u}) = (\mathbf{x}, \mathbf{u}^\star)$ into (3.8) and adding them together, we derive

$$\begin{aligned}
\frac{\alpha}{2} \|\mathbf{u} - \mathbf{u}^\star\|_\mathscr{H}^2 + \frac{\alpha}{2} \|\mathbf{u}^\star - \mathbf{r}_\mathbf{x}\|_\mathscr{H}^2 = \frac{\alpha}{2} \|\mathbf{u} - \mathbf{r}_{\mathbf{x}^\star}\|_\mathscr{H}^2 + \frac{\alpha}{2} \|\mathbf{u}^\star - \mathbf{r}_\mathbf{x}\|_\mathscr{H}^2 \\
&\leq \mathrm{GAP}(\mathbf{x}^\star, \mathbf{u}) + \mathrm{GAP}(\mathbf{x}, \mathbf{u}^\star) \\
&= p(\mathbf{x}^\star) - d(\mathbf{u}) + p(\mathbf{x}) - d(\mathbf{u}^\star) \\
&= p(\mathbf{x}) - d(\mathbf{u}) \\
&= \mathrm{GAP}(\mathbf{x}, \mathbf{u}).
\end{aligned}$$

Here we exploited the facts that $\mathbf{r}_{\mathbf{x}^\star} = \mathbf{u}^\star$ in the first equality and $p(\mathbf{x}^\star) = d(\mathbf{u}^\star)$ due to (H2) in the third equality.

Hence, the theorem is proven. □

By rearranging (3.3), one can show that $\mathbf{u}^\star$ belongs to a ball region, namely FBI ball. This result is formalized by the following theorem.

Theorem 3.1.3 (FBI ball)**.** *Let* $(\mathbf{x}, \mathbf{u}) \in \mathscr{M} \times \mathscr{H}$*. Under the hypotheses (H1), (H2) and (H3), we have*

$$\mathbf{u}^\star \in B_{\mathtt{FBI}}(\mathbf{x}, \mathbf{u}) \triangleq B\left(\frac{\mathbf{u} + \mathbf{r}_\mathbf{x}}{2}, \sqrt{\frac{\mathrm{GAP}(\mathbf{x}, \mathbf{u})}{\alpha} - \frac{\|\mathbf{u} - \mathbf{r}_\mathbf{x}\|_\mathscr{H}^2}{4}}\right) \tag{3.9-FBI-b}$$

with $\mathbf{r}_\mathbf{x}$ *defined in* (3.2)*. We call this safe region the* FBI ball*. In particular, if* $\mathbf{x}$ *and* $\mathbf{u}$ *are all feasible, i.e.,* $\mathrm{GAP}\,(\mathbf{x}, \mathbf{u}) < +\infty$*, then the radius of* $B_{\mathtt{FBI}}(\mathbf{x}, \mathbf{u})$ *is finite.*

Proof. The proof mainly relies on Lemma 3.1.2 and the Apollonius's identity in Hilbert space,[3] see *e.g.*, [5, Item (iv) of Lemma 2.12], which states that for any pair of vectors $\mathbf{v}, \mathbf{w}$ from a Hilbert space $\mathscr{H}$, $\|\mathbf{v} + \mathbf{w}\|_\mathscr{H}^2 + \|\mathbf{v} - \mathbf{w}\|_\mathscr{H}^2 = 2\big(\|\mathbf{v}\|_\mathscr{H}^2 + \|\mathbf{w}\|_\mathscr{H}^2\big)$. Particularizing the latter identity to $\mathbf{v} = \mathbf{u}^\star - \mathbf{u}$ and $\mathbf{w} = \mathbf{u}^\star - \mathbf{r}_\mathbf{x}$, one obtains

$$\left\|\mathbf{u}^\star - \frac{\mathbf{u} + \mathbf{r}_\mathbf{x}}{2}\right\|_\mathscr{H}^2 + \frac{\|\mathbf{u} - \mathbf{r}_\mathbf{x}\|_\mathscr{H}^2}{4} = \frac{\|\mathbf{u}^\star - \mathbf{u}\|_\mathscr{H}^2}{2} + \frac{\|\mathbf{u}^\star - \mathbf{r}_\mathbf{x}\|_\mathscr{H}^2}{2}.$$

3. *a.k.a.* law of parallelogram.

Substituting this in to (3.3), one sees that $\mathbf{u}^\star$ satisfies

$$\left\|\mathbf{u}^\star - \frac{\mathbf{u}+\mathbf{r}_\mathbf{x}}{2}\right\|_{\mathscr{H}} \leq \sqrt{\frac{\mathrm{GAP}(\mathbf{x},\mathbf{u})}{\alpha} - \frac{\|\mathbf{u}-\mathbf{r}_\mathbf{x}\|^2_{\mathscr{H}}}{4}}.$$

We therefore conclude that $\mathbf{u}^\star \in B_{\mathtt{FBI}}(\mathbf{x},\mathbf{u})$.

Finally, feasibility of $\mathbf{x}$ and $\mathbf{u}$ implies that $\mathrm{GAP}(\mathbf{x},\mathbf{u}) < +\infty$ and therefore finiteness of the radius. This completes the proof. □

3.1.2 Zero-radius property

Our next result demonstrates that FBI balls associated with the primal-dual optimal pair $(\mathbf{x},\mathbf{u})$ will contain $\mathbf{u}^\star$ as a unique point. This fact confirms the "tightness" property of FBI balls, which is a desirable characteristic of effective safe regions.

Proposition 3.1.4 (Zero-radius of FBI ball)**.** *Under the hypotheses (H1), (H2) and (H3), the FBI ball evaluated at any optimal pair* $(\mathbf{x}^\star,\mathbf{u}^\star)$ *uniquely contains* $\mathbf{u}^\star$*, i.e.,*

$$\{\mathbf{u}^\star\} = B_{\mathtt{FBI}}(\mathbf{x}^\star,\mathbf{u}^\star).$$

Proof. Optimality of the pair $(\mathbf{x}^\star,\mathbf{u}^\star)$ together with strong duality (H2) imply that $\mathrm{GAP}(\mathbf{x}^\star,\mathbf{u}^\star) = 0$ and $\mathbf{r}_{\mathbf{x}^\star} = \mathbf{u}^\star$. As a consequence, the center and radius of FBI ball $B_{\mathtt{FBI}}(\mathbf{x}^\star,\mathbf{u}^\star)$ reduces to $\mathbf{u}^\star$ and zero, respectively. Hence $B_{\mathtt{FBI}}(\mathbf{x}^\star,\mathbf{u}^\star) = B(\mathbf{u}^\star,0) = \{\mathbf{u}^\star\}$. □

3.1.3 Particularizations

This section presents two instances of FBI ball in which FBI ball has simplified safeness inequality. These particularizations serve as an intermediate step essential to comparison results between FBI ball and existing safe ball regions in the next section.

An FBI ball for parametric problem

We now focus on the following strong duality with primal and pre-dual problem parameterized by $\lambda > 0$:

$$\min_{\mathbf{x}\in\mathscr{M}} \underbrace{f(\mathbf{A}\mathbf{x}) + \lambda g(\mathbf{x})}_{p_\lambda(\mathbf{x})} = \max_{\mathbf{u}\in\mathscr{H}} \underbrace{-f^*(-\mathbf{u}) - \lambda g^*\left(\frac{\mathbf{A}^*\mathbf{u}}{\lambda}\right)}_{d_\lambda(\mathbf{u})}. \tag{3.10}$$

Here, $\mathscr{M}$, $\mathscr{H}$, f, g and $\mathbf{A}$ are defined as in the (non-parametric) strong duality (3.1). Note that (3.1) and (3.10) and are equivalent; each can be derived from the other. [4]

To explicitly mention the dependency on λ, we add λ-subscript to relevant quantities. For example, we denote by $(\mathbf{x}_\lambda, \mathbf{u}_\lambda)$ some feasible pair, and $(\mathbf{x}^\star_\lambda, \mathbf{u}^\star_\lambda)$ some optimal pair.

Let $(\mathbf{x}_{\lambda_0}, \mathbf{u}_{\lambda_0})$ be a feasible pair for a given parameter $\lambda_0 > 0$. We will now use $(\mathbf{x}_{\lambda_0}, \mathbf{u}_{\lambda_0})$ to construct a safe FBI ball containing $\mathbf{u}^\star_\lambda$. Of particular interest in this consideration is the property that, under suitable conditions, the Fenchel divergence in the safeness inequality of the FBI ball will be zero.

Corollary 3.1.5. *For $\tau, \lambda, \lambda_0 > 0$, the FBI ball $B_{\texttt{FBI}}\left(\tau\mathbf{x}_{\lambda_0}, \dfrac{\lambda}{\lambda_0}\mathbf{u}_{\lambda_0}\right)$ contains $\mathbf{u}^\star_\lambda$ with the safeness inequality reads as follows:*

$$\frac{\alpha}{2}\left\|\mathbf{u}^\star_\lambda - \mathbf{r}_{\tau\mathbf{x}_{\lambda_0}}\right\|^2_{\mathscr{H}} + \frac{\alpha}{2}\left\|\mathbf{u}^\star_\lambda - \frac{\lambda}{\lambda_0}\mathbf{u}_{\lambda_0}\right\|^2_{\mathscr{H}} \leq \mathrm{Breg}_{f^{*-}, -\tau\mathbf{A}\mathbf{x}_{\lambda_0}}\left(\frac{\lambda}{\lambda_0}\mathbf{u}_{\lambda_0}, \mathbf{r}_{\tau\mathbf{x}_{\lambda_0}}\right) + \frac{\lambda}{\lambda_0}\,\mathrm{Fen}_{\lambda_0 g}(\tau\mathbf{x}_{\lambda_0}, \mathbf{A}^*\mathbf{u}_{\lambda_0}).$$

In particular, if one of the following condition holds true

1. $(\mathbf{x}_{\lambda_0}, \mathbf{u}_{\lambda_0}) = (\mathbf{x}^\star_{\lambda_0}, \mathbf{u}^\star_{\lambda_0})$ *and* $\tau = 1$,
2. $(\mathbf{x}_{\lambda_0}, \mathbf{u}_{\lambda_0}) = (\mathbf{x}^\star_{\lambda_0}, \mathbf{u}^\star_{\lambda_0})$ *and g is a gauge function,*

where $(\mathbf{x}^\star_{\lambda_0}, \mathbf{u}^\star_{\lambda_0})$ denotes an optimal pair associated with λ_0, then the Fenchel divergence vanishes, i.e.,

$$\mathrm{Fen}_{\lambda_0 g}\left(\tau\mathbf{x}^\star_{\lambda_0}, \mathbf{A}^*\mathbf{u}^\star_{\lambda_0}\right) = 0.$$

Proof. One can notice that the first result corollary 3.1.5 is a consequence of Lemma 3.1.2 with a change of penalization $g := \lambda g$. The only thing one needs to verify is that the two terms involving the Fenchel divergence are equal. Indeed, we have

$$\mathrm{Fen}_{\lambda g}(\mathbf{x}, \mathbf{A}^*\mathbf{u}) = \lambda\left(g(\mathbf{x}) + g\left(\frac{\mathbf{A}^*\mathbf{u}}{\lambda}\right) - \left\langle \mathbf{x}, \frac{\mathbf{A}^*\mathbf{u}}{\lambda}\right\rangle\right).$$

Moreover, the particularization of the latter equation to the pair $(\mathbf{x}, \mathbf{u}) = \left(\tau\mathbf{x}_{\lambda_0}, \dfrac{\lambda}{\lambda_0}\mathbf{u}_{\lambda_0}\right)$, verifies

$$\mathrm{Fen}_{\lambda g}\left(\tau\mathbf{x}_{\lambda_0}, \frac{\lambda}{\lambda_0}\mathbf{A}^*\mathbf{u}_{\lambda_0}\right) = \frac{\lambda}{\lambda_0}\,\mathrm{Fen}_{\lambda_0 g}(\tau\mathbf{x}_{\lambda_0}, \mathbf{A}^*\mathbf{u}_{\lambda_0}).$$

4. Specifically, (3.1) can be obtained from (3.10) by setting $\lambda = 1$, and conversely, (3.10) can be obtained from (3.1) by replacing g by λg.

This proves the desired safeness inequality.

We now focus on the cases of vanishing Fenchel divergence. Let $(\mathbf{x}_{\lambda_0}, \mathbf{u}_{\lambda_0}) = (\mathbf{x}^\star_{\lambda_0}, \mathbf{u}^\star_{\lambda_0})$ and consider two cases.

Case 1. Assume that $\tau = 1$. We then observe that

$$0 \leq \mathrm{Fen}_{\lambda_0 g}\Big(\mathbf{x}^\star_{\lambda_0}, \mathbf{A}^*\mathbf{u}^\star_{\lambda_0}\Big) \leq \mathrm{GAP}_{\lambda_0}(\mathbf{x}^\star_{\lambda_0}, \mathbf{u}^\star_{\lambda_0}) = 0,$$

where the first inequality is a consequence of non-negativity of Fenchel divergence, the second inequality holds due to the dual gap decomposition (3.3) and the equality holds since $(\mathbf{x}^\star_{\lambda_0}, \mathbf{u}^\star_{\lambda_0})$ is assumed to be optimal. This shows that $\mathrm{Fen}_{\lambda_0 g}\Big(\tau\mathbf{x}^\star_{\lambda_0}, \mathbf{A}^*\mathbf{u}^\star_{\lambda_0}\Big) = 0$ since $\tau = 1$.

Case 2. Assume that $g = \kappa$ for some gauge function κ (see Definition B.1.11). In this case, $(\lambda_0\kappa)^*$ is an indicator function, thus, $(\lambda_0\kappa)^*(\mathbf{A}^*\mathbf{u}^\star_{\lambda_0}) = 0$ since optimal solution $\mathbf{u}^\star_{\lambda_0}$ is dual feasible. By definition of Fenchel divergence, we have

$$\begin{aligned}
\mathrm{Fen}_{\lambda_0 g}\Big(\tau\mathbf{x}^\star_{\lambda_0}, \mathbf{A}^*\mathbf{u}^\star_{\lambda_0}\Big) &= \lambda_0\kappa(\tau\mathbf{x}^\star_{\lambda_0}) + (\lambda_0\kappa)^*(\mathbf{A}^*\mathbf{u}^\star_{\lambda_0}) - \Big\langle \tau\mathbf{x}^\star_{\lambda_0}, \mathbf{A}^*\mathbf{u}^\star_{\lambda_0} \Big\rangle \\
&= \tau\Big(\lambda_0\kappa(\mathbf{x}^\star_{\lambda_0}) - \Big\langle \mathbf{A}\mathbf{x}^\star_{\lambda_0}, \mathbf{u}^\star_{\lambda_0} \Big\rangle\Big) \\
&= \tau\,\mathrm{Fen}_{\lambda_0 g}\Big(\mathbf{x}^\star_{\lambda_0}, \mathbf{A}^*\mathbf{u}^\star_{\lambda_0}\Big) \\
&= 0.
\end{aligned}$$

Here, in the second equality, we exploited the observation that $\kappa(\tau\mathbf{x}^\star_{\lambda_0}) = \tau\kappa(\mathbf{x}^\star_{\lambda_0})$ since gauge function κ is positively homogeneous, see Definition B.1.11.

This completes the proof. □

An FBI ball for LASSO-like problem

In the following, we will investigate the FBI ball in the context of "LASSO-like" problem, which is a least squares problem with (convex) gauge penalization κ. [5] The gauge function is a broader category encompassing both norms and seminorms. In a comparison with LASSO in which the sparsity induced by the ℓ_1-norm, in the LASSO-like problem, the gauge function κ can be arbitrary general, for example, it can be ℓ_∞-norm which then implies the anti-sparse structure of the optimal solutions [43].

5. See Definition B.1.11 for definition of gauge function.

In this case, we assume the following strong duality holds:

$$\min_{\mathbf{x}\in\mathscr{M}} \quad \frac{1}{2}\|\mathbf{b}-\mathbf{A}\mathbf{x}\|_{\mathscr{H}}^2+\lambda\kappa(\mathbf{x}) = \max_{\mathbf{u}\in U_{\lambda\kappa}} \quad \frac{1}{2}\|\mathbf{b}\|_{\mathscr{H}}^2-\frac{1}{2}\|\mathbf{b}-\mathbf{u}\|_{\mathscr{H}}^2, \tag{3.11}$$

where $\mathbf{b}\in\mathscr{H}$ is some known vector, κ is a gauge function, $\lambda>0$ and

$$U_{\lambda\kappa}=\{\mathbf{u}\in\mathscr{H}:\kappa^\circ(\mathbf{A}^*\mathbf{u})\leq\lambda\}. \tag{3.12}$$

Here, recall that κ° denotes the polar of gauge function. Particularizing (3.11) to the case that $\mathscr{M}=\mathbb{R}^n$, $\mathscr{H}=\mathbb{R}^m$, $\kappa=\|\cdot\|_1$, one recovers LASSO's strong duality (2.12).

In this setup, one can verify that the Bregman and Fenchel divergence have explicit form:

$$\mathrm{Breg}_{f^*-,-\mathbf{A}\mathbf{x}}(\mathbf{u},\mathbf{r}_\mathbf{x})=\frac{1}{2}\|\mathbf{u}-\mathbf{r}_\mathbf{x}\|_{\mathscr{H}}^2,$$

where $\mathbf{r}_\mathbf{x}=\mathbf{b}-\mathbf{A}\mathbf{x}$ and

$$\mathrm{Fen}_g(\mathbf{x},\mathbf{A}^*\mathbf{u})=\begin{cases}\lambda\kappa(\mathbf{x})-\langle\mathbf{A}\mathbf{x},\mathbf{u}\rangle, & \text{if } \mathbf{u}\in U_{\lambda\kappa},\\ +\infty, & \text{otherwise.}\end{cases}$$

From Lemma 3.1.2, we know that the dual gap can be expressed as the sum of Bregman and Fenchel divergences. Therefore,

$$\mathrm{GAP}(\mathbf{x},\mathbf{u})=\begin{cases}\frac{1}{2}\|\mathbf{u}-\mathbf{r}_\mathbf{x}\|_{\mathscr{H}}^2+\lambda\kappa(\mathbf{x})-\langle\mathbf{A}\mathbf{x},\mathbf{u}\rangle, & \text{if } \mathbf{u}\in U_{\lambda\kappa},\\ +\infty, & \text{otherwise.}\end{cases} \tag{3.13}$$

In this case, if one assumes that $\mathbf{u}\in U_{\lambda\kappa}$, then FBI (3.3) reads as follows:

$$\frac{1}{2}\|\mathbf{u}^\star-\mathbf{u}\|_{\mathscr{H}}^2+\frac{1}{2}\|\mathbf{u}^\star-\mathbf{r}_\mathbf{x}\|_{\mathscr{H}}^2\leq\frac{1}{2}\|\mathbf{u}-\mathbf{r}_\mathbf{x}\|_{\mathscr{H}}^2+\lambda\kappa(\mathbf{x})-\langle\mathbf{A}\mathbf{x},\mathbf{u}\rangle \tag{3.14}$$

Hence, the FBI ball in this setup can be rewritten as follows:

Corollary 3.1.6 (FBI ball for LASSO-like problem)**.** *Consider strong duality for LASSO-like problem* (3.11)*, if* $\mathbf{u}\in U_{\lambda\kappa}$*, then*

$$B_{\texttt{FBI}}(\mathbf{x},\mathbf{u})=B\left(\frac{\mathbf{u}+\mathbf{r}_\mathbf{x}}{2},\sqrt{\frac{\|\mathbf{u}-\mathbf{r}_\mathbf{x}\|_{\mathscr{H}}^2}{4}+\lambda\kappa(\mathbf{x})-\langle\mathbf{A}\mathbf{x},\mathbf{u}\rangle}\right). \tag{3.15}$$

3.1.4 Comparisons

The objective of this section is to demonstrate that existing safe ball regions, up to the best of our knowledge, are either supersets or special cases of the FBI ball. This finding provides a theoretical insight into the fundamental structure of existing safe regions, which may be insightful for future developments. Readers can grasp the key findings without delving into intricate technical proofs within this section.

The existing safe regions are split into five groups based on their similarity in setup:

— SASVI and SAFE

— DPP and EDPP

— GAP and **x**-GAP

— FNE and DEDPP

— SFER and SLORES

In order to compare a safe region S_0 with $B_{\texttt{FBI}}(\mathbf{x}, \mathbf{u})$, we rely on the FBI (3.3) as a reference inequality. For the ease of doing comparison, we label the non-negative quantities in (3.3) by A, B, C and D:

$$\underbrace{\frac{\alpha}{2}\left\|\mathbf{u}^\star - \mathbf{u}\right\|_{\mathscr{H}}^2}_{A} + \underbrace{\frac{\alpha}{2}\left\|\mathbf{u}^\star - \mathbf{r}_{\mathbf{x}}\right\|_{\mathscr{H}}^2}_{B} \leq \underbrace{\mathrm{Breg}_{f^{*-},-\mathbf{A}\mathbf{x}}(\mathbf{u}, \mathbf{r}_{\mathbf{x}})}_{C} + \underbrace{\mathrm{Fen}_g(\mathbf{x}, \mathbf{A}^*\mathbf{u})}_{D} \tag{3.16-ABCD}$$

If one can demonstrate that the safeness inequality of S_0 takes the form $A \leq C + D$ or $B \leq C + D$ then S_0 contains the FBI ball. Furthermore, if the safeness inequality of S_0 can be expressed as $A + B \leq C$ with $D = 0$ then S_0 corresponds to a particular instance of FBI ball.

Before diving into the details, we reiterate that our setting is now confined to finite-dimension, i.e., $\mathscr{M} = \mathbb{R}^n$ and $\mathscr{H} = \mathbb{R}^m$.

SAFE and SASVI ball

We recall the strong duality of LASSO setup:

$$\min_{\mathbf{x}\in\mathbb{R}^n} \underbrace{\frac{1}{2}\left\|\mathbf{b} - \mathbf{A}\mathbf{x}\right\|_2^2}_{f(\mathbf{A}\mathbf{x})} + \underbrace{\lambda\left\|\mathbf{x}\right\|_1}_{g(\mathbf{x})} = \max_{\mathbf{u}\in U_{\lambda\|\cdot\|_1}} \frac{1}{2}\left\|\mathbf{b}\right\|_2^2 - \frac{1}{2}\left\|\mathbf{b} - \mathbf{u}\right\|_2^2, \tag{3.17}$$

where $U_{\lambda\|\cdot\|_1} = \{\mathbf{u} \in \mathbb{R}^m : |\langle \mathbf{a}_i, \mathbf{u}\rangle| \leq \lambda,\ \forall i = 1, \ldots, n\}$. Let $\mathbf{x}_\lambda^\star$ be a primal optimal solution of the primal problem (left-hand side of (3.17)) and $\mathbf{u}_\lambda^\star$ denote the unique dual

optimal solution to the dual problem (right-hand side of (3.17)). In this case, note that the optimality conditions read as follows:

$$\mathbf{u}_\lambda^\star = \mathbf{b} - \mathbf{A}\mathbf{x}_\lambda^\star, \tag{3.18}$$

$$\langle \mathbf{A}\mathbf{x}_\lambda^\star, \mathbf{u}_\lambda^\star \rangle = \lambda \left\| \mathbf{x}_\lambda^\star \right\|_1, \tag{3.19}$$

$$\left\| \mathbf{A}^{\mathrm{T}} \mathbf{u}_\lambda^\star \right\|_\infty \leq \lambda. \tag{3.20}$$

In this setting, the FBI (3.3) associated with $(\mathbf{x}, \mathbf{u}) \in \mathbb{R}^n \times U_{\lambda\|\cdot\|_1}$ can be rewritten as follows (notice that $\alpha = 1$):

$$\underbrace{\tfrac{1}{2}\left\|\mathbf{u}_\lambda^\star - \mathbf{u}\right\|_2^2}_{A} + \underbrace{\tfrac{1}{2}\left\|\mathbf{u}_\lambda^\star - \mathbf{r}_\mathbf{x}\right\|_2^2}_{B} \leq \underbrace{\tfrac{1}{2}\left\|\mathbf{u} - \mathbf{r}_\mathbf{x}\right\|_2^2}_{C} + \underbrace{\lambda\left\|\mathbf{x}\right\|_1 - \langle \mathbf{A}\mathbf{x}, \mathbf{u}\rangle}_{D}, \tag{3.21-ABCD2}$$

where $\mathbf{r}_\mathbf{x} = \mathbf{b} - \mathbf{A}\mathbf{x}$.

Corollary 3.1.7 (SASVI ball is a special case of FBI ball)**.** *Consider LASSO's strong duality* (3.17)*, we have*

$$B_{\texttt{FBI}}(\mathbf{0}, \mathbf{u}) = B_{\texttt{SASVI}}(\mathbf{u}) \overset{\text{def.}}{=} B\left(\frac{\mathbf{b} + \mathbf{u}}{2}, \frac{\left\|\mathbf{b} - \mathbf{u}\right\|_2}{2}\right), \tag{3.22}$$

for any $\mathbf{u} \in U_{\lambda\|\cdot\|_1}$.

Proof of Corollary 3.1.7. The safeness inequality of SASVI ball is expressed as follows,

$$\left\| \mathbf{u}_\lambda^\star - \frac{\mathbf{b} + \mathbf{u}}{2} \right\|_2 \leq \frac{\left\|\mathbf{b} - \mathbf{u}\right\|_2}{2}. \tag{3.23}$$

By taking the square of both sides and rearranging terms, (3.23) can be rewritten as:

$$\underbrace{\frac{1}{2}\left\|\mathbf{u}_\lambda^\star - \mathbf{u}\right\|_2^2}_{A} + \underbrace{\frac{1}{2}\left\|\mathbf{u}_\lambda^\star - \mathbf{b}\right\|_2^2}_{B} \leq \underbrace{\frac{1}{2}\left\|\mathbf{b} - \mathbf{u}\right\|_2^2}_{C}. \tag{3.24-SASVI-b-ineq}$$

For $\mathbf{u} \in U_{\lambda\|\cdot\|_1}$, we note that (3.24-SASVI-b-ineq) is a particular case of (3.21-ABCD2) *w.r.t.* $\mathbf{x} = \mathbf{0}$. Thus, $B_{\texttt{FBI}}(\mathbf{0}, \mathbf{u}) = B_{\texttt{SASVI}}(\mathbf{u})$. □

Corollary 3.1.8 (SAFE ball is a superset of static FBI ball)**.** *Considering the LASSO's strong duality* (3.17) *and* $\mathbf{u} \in U_{\lambda\|\cdot\|_1}$*, we have*

$$B_{\texttt{FBI}}(\mathbf{0}, \mathbf{u}) \subset B_{\texttt{SAFE}}(\mathbf{u}) \overset{\text{def.}}{=} B(\mathbf{b}, \left\|\mathbf{b} - \mathbf{u}\right\|_2). \tag{3.25}$$

Proof of Corollary 3.1.8. The particularization of the definition of a ball with center $\mathbf{b}$ and radius $\|\mathbf{b}-\mathbf{u}\|_2$ writes

$$\underbrace{\frac{1}{2}\|\mathbf{u}_\lambda^\star-\mathbf{b}\|_2^2}_{B} \leq \underbrace{\frac{1}{2}\|\mathbf{b}-\mathbf{u}\|_2^2}_{C}, \tag{3.26-SAFE-b-ineq}$$

which corresponds to the safeness inequality of the SAFE ball. For $\mathbf{u} \in U_{\lambda\|\cdot\|_1}$, it is clear that (3.26-SAFE-b-ineq) is a relaxation of (3.21-ABCD2) by setting $\mathbf{x}=\mathbf{0}$ and ignoring $A \geq 0$. Therefore, $B_{\texttt{FBI}}(\mathbf{0},\mathbf{u}) \subset B_{\texttt{SAFE}}(\mathbf{u})$. □

DPP and EDPP ball

Let $\lambda_0 > 0$ be some parameter and denote by $(\mathbf{x}_{\lambda_0}^\star, \mathbf{u}_{\lambda_0}^\star)$ some optimal pair corresponding to primal and pre-dual problem in (3.17) with parameter λ_0 instead of λ.

Corollary 3.1.9 (EDPP ball is a special case of FBI ball)**.** *Consider the LASSO's strong duality* (3.17)*, we have*

$$B_{\texttt{FBI}}\left(\tau\mathbf{x}_{\lambda_0}^\star, \frac{\lambda}{\lambda_0}\mathbf{u}_{\lambda_0}^\star\right) = B_{\texttt{EDPP}}(\mathbf{u}_{\lambda_0}^\star) \overset{\text{def.}}{=} B\left(\frac{\lambda}{\lambda_0}\mathbf{u}_{\lambda_0}^\star + \frac{1}{2}\mathbf{v}_2^\perp, \frac{1}{2}\left\|\mathbf{v}_2^\perp\right\|_2\right), \tag{3.27}$$

where

$$\begin{aligned}
\mathbf{v}_2^\perp &= \mathbf{v}_2 - \tau\mathbf{v}_1,\\
\mathbf{v}_1 &= \mathbf{b} - \mathbf{u}_{\lambda_0}^\star = \mathbf{A}\mathbf{x}_{\lambda_0}^\star,\\
\mathbf{v}_2 &= \mathbf{b} - \frac{\lambda}{\lambda_0}\mathbf{u}_{\lambda_0}^\star,\\
\tau &= \frac{\langle\mathbf{v}_1,\mathbf{v}_2\rangle}{\|\mathbf{v}_1\|_{\mathscr{H}}^2}.
\end{aligned}$$

Proof of Corollary 3.1.9. Consider $(\mathbf{x},\mathbf{u}) = (\tau\mathbf{x}_{\lambda_0}^\star, \frac{\lambda}{\lambda_0}\mathbf{u}_{\lambda_0}^\star)$ where $\tau = \frac{\langle\mathbf{v}_1,\mathbf{v}_2\rangle}{\|\mathbf{v}_1\|_{\mathscr{H}}^2}$. Note that, in this case, we have $\mathbf{u} \in U_{\lambda\|\cdot\|_1}$, $\tau \geq 0$ [92, Equation (33)] and $\mathbf{r}_\mathbf{x} - \mathbf{u} = \mathbf{v}_2^\perp$. Therefore,

$$B_{\texttt{EDPP}}(\mathbf{u}_{\lambda_0}^\star) = B\left(\frac{\lambda}{\lambda_0}\mathbf{u}_{\lambda_0}^\star + \frac{1}{2}\mathbf{v}_2^\perp, \frac{1}{2}\left\|\mathbf{v}_2^\perp\right\|_2\right) = B\left(\frac{\mathbf{u}+\mathbf{r}_\mathbf{x}}{2}, \frac{\|\mathbf{u}-\mathbf{r}_\mathbf{x}\|_2}{2}\right).$$

The safeness inequality of $B_{\texttt{EDPP}}(\mathbf{u}^\star_{\lambda_0})$ therefore writes:

$$\underbrace{\frac{1}{2}\left\|\mathbf{u}^\star_\lambda - \mathbf{u}\right\|_2^2}_{A} + \underbrace{\frac{1}{2}\left\|\mathbf{u}^\star_\lambda - \mathbf{r}_\mathbf{x}\right\|_2^2}_{B} \leq \underbrace{\frac{1}{2}\left\|\mathbf{u} - \mathbf{r}_\mathbf{x}\right\|_2^2}_{C}, \tag{3.28-EDPP-b-ineq}$$

which is an instance of (3.21-ABCD2) with $D = 0$. Indeed, the optimality (3.19) *w.r.t.* λ_0 yields:

$$D = \lambda\left\|\mathbf{x}\right\|_1 - \left\langle \mathbf{A}\mathbf{x}, \mathbf{u}\right\rangle = \frac{\tau\lambda}{\lambda_0}\Big(\lambda_0\left\|\mathbf{x}^\star_{\lambda_0}\right\|_1 - \left\langle \mathbf{A}\mathbf{x}^\star_{\lambda_0}, \mathbf{u}^\star_{\lambda_0}\right\rangle\Big) = 0. \tag{3.29}$$

□

Corollary 3.1.10 (DPP ball is a superset of FBI ball)**.** *Consider LASSO's strong duality* (3.17)*, we have*

$$B_{\texttt{FBI}}\left(\frac{\lambda}{\lambda_0}\mathbf{x}^\star_{\lambda_0}, \frac{\lambda}{\lambda_0}\mathbf{u}^\star_{\lambda_0}\right) \subset B_{\texttt{DPP}}(\mathbf{u}^\star_{\lambda_0}) \overset{\text{def.}}{=} B\left(\frac{\lambda}{\lambda_0}\mathbf{u}^\star_{\lambda_0}, \left\|\mathbf{b} - \frac{\lambda}{\lambda_0}\mathbf{b}\right\|_2\right).$$

Proof of Corollary 3.1.10. The proof follows the same line as the one of Corollary 3.1.9 but for a different primal dual pair $(\mathbf{x}, \mathbf{u})$. More precisely, let $(\mathbf{x}, \mathbf{u}) = (\frac{\lambda}{\lambda_0}\mathbf{x}^\star_{\lambda_0}, \frac{\lambda}{\lambda_0}\mathbf{u}^\star_{\lambda_0})$. The safeness inequality of $B_{\texttt{FBI}}\left(\frac{\lambda}{\lambda_0}\mathbf{x}^\star_{\lambda_0}, \frac{\lambda}{\lambda_0}\mathbf{u}^\star_{\lambda_0}\right)$ reads as follows with the observation that $D = 0$ (with the same reason as in (3.29)),

$$\underbrace{\frac{1}{2}\left\|\mathbf{u}^\star_\lambda - \mathbf{u}\right\|_2^2}_{A} + \underbrace{\frac{1}{2}\left\|\mathbf{u}^\star_\lambda - \mathbf{r}_\mathbf{x}\right\|_2^2}_{B} \leq \underbrace{\frac{1}{2}\left\|\mathbf{u} - \mathbf{r}_\mathbf{x}\right\|_2^2}_{C}. \tag{3.30}$$

On the other hand, observing that $\mathbf{r}_\mathbf{x} - \mathbf{u} = \mathbf{b} - \frac{\lambda}{\lambda_0}\mathbf{b}$ the safeness inequality of $B_{\texttt{DPP}}(\mathbf{u}^\star_{\lambda_0})$ is

$$\underbrace{\frac{1}{2}\left\|\mathbf{u}^\star_\lambda - \mathbf{u}\right\|_2^2}_{A} \leq \underbrace{\frac{1}{2}\left\|\mathbf{u} - \mathbf{r}_\mathbf{x}\right\|_2^2}_{C}. \tag{3.31-DPP-b-ineq}$$

Note that, we can derive (3.31-DPP-b-ineq) by relaxing $B \geq 0$ from (3.30), thus, FBI ball is a subset of DPP ball. □

GAP and $\mathbf{x}$-GAP ball

We recall the strong duality *w.r.t.* to primal problem defined as a ℓ_1-norm penalization problem:

$$\min_{\mathbf{x}\in\mathbb{R}^n} \quad f(\mathbf{A}\mathbf{x}) + \lambda\left\|\mathbf{x}\right\|_1 = \max_{\mathbf{u}\in U_{\lambda\|\cdot\|_1}} \quad -f^*(-\mathbf{u}), \tag{3.32}$$

For $(\mathbf{x}, \mathbf{u}) \in \mathbb{R}^n \times U_{\lambda\|\cdot\|_1}$ and f had α^{-1}-Lipschitz continuous gradient, FBI in this setting can be rewritten as follows:

$$\underbrace{\tfrac{\alpha}{2}\left\|\mathbf{u}_\lambda^\star - \mathbf{u}\right\|_2^2}_{A} + \underbrace{\tfrac{\alpha}{2}\left\|\mathbf{u}_\lambda^\star - \mathbf{r}_\mathbf{x}\right\|_2^2}_{B} \leq \underbrace{\mathrm{Breg}_{f^*-,-\mathbf{Ax}}(\mathbf{u}, \mathbf{r}_\mathbf{x})}_{C} + \underbrace{\lambda\left\|\mathbf{x}\right\|_1 - \langle \mathbf{Ax}, \mathbf{u}\rangle}_{D}. \quad \text{(3.33-ABCD3)}$$

where $\mathbf{r}_\mathbf{x} = -\nabla f(\mathbf{Ax})$.

Corollary 3.1.11 (GAP ball is a superset of FBI ball)**.** *Under the strong duality* (3.32)*, then FBI ball is a subset of GAP ball, i.e.,*

$$B_{\texttt{FBI}}(\mathbf{x}, \mathbf{u}) \subset B_{\texttt{GAP}}(\mathbf{x}, \mathbf{u}) \overset{\text{def.}}{=} B\left(\mathbf{u}, \sqrt{\frac{2}{\alpha}\,\mathrm{GAP}(\mathbf{x}, \mathbf{u})}\right),$$

for all $(\mathbf{x}, \mathbf{u}) \in \mathbb{R}^n \times U_{\lambda\|\cdot\|_1}$.

Proof. The safeness of GAP ball can be identified with the following safeness inequality:

$$\underbrace{\tfrac{\alpha}{2}\left\|\mathbf{u}_\lambda^\star - \mathbf{u}\right\|_2^2}_{A} \leq \underbrace{\mathrm{GAP}(\mathbf{x}, \mathbf{u})}_{C+D}. \quad \text{(3.34-GAP-b-ineq)}$$

This is clearly a relaxation of (3.33-ABCD3) by discarding $B \geq 0$. Hence FBI ball in this case is a subset of GAP ball. □

Corollary 3.1.12 (**x**-GAP ball is a superset of FBI ball)**.** *Consider the strong duality* (3.32)*, FBI ball is a subset of* **x***-GAP ball, i.e.,*

$$B_{\texttt{FBI}}(\mathbf{x}, \mathbf{u}) \subset B_{\texttt{xGAP}}(\mathbf{x}, \mathbf{u}) \overset{\text{def.}}{=} B\left(\mathbf{r}_\mathbf{x}, \sqrt{\frac{2}{\alpha}\,\mathrm{GAP}(\mathbf{x}, \mathbf{u})}\right),$$

for all $(\mathbf{x}, \mathbf{u}) \in \mathbb{R}^n \times U_{\lambda\|\cdot\|_1}$.

Proof. The safeness inequality of **x**-GAP ball is:

$$\underbrace{\tfrac{\alpha}{2}\left\|\mathbf{u}_\lambda^\star - \mathbf{r}_\mathbf{x}\right\|_2^2}_{B} \leq \underbrace{\mathrm{GAP}(\mathbf{x}, \mathbf{u})}_{C+D}. \quad \text{(3.35-x-GAP-b-ineq)}$$

This is a relaxation of (3.33-ABCD3) by discarding $A \geq 0$. □

FNE and DEDPP ball

Corollary 3.1.13 (Dynamic FNE ball is a special case of FBI ball)**.** *Consider the LASSO's strong duality in* (3.17) *and let* $(\mathbf{x}, \mathbf{u})$ *be a primal-dual feasible pair satisfying*

$$\langle \mathbf{A}\mathbf{x}, \mathbf{u} \rangle = \lambda \|\mathbf{x}\|_1 . \tag{3.36}$$

Then, FBI and FNE ball are identical, i.e.,

$$B_{\texttt{FBI}}(\mathbf{x}, \mathbf{u}) = B_{\texttt{FNE}}(\mathbf{x}, \mathbf{u}) \overset{\text{def.}}{=} B\Big(\mathbf{u} + \frac{1}{2}(\mathbf{b} - \mathbf{A}\mathbf{x} - \mathbf{u}), \frac{1}{2}\|\mathbf{b} - \mathbf{A}\mathbf{x} - \mathbf{u}\|_2\Big). \tag{3.37}$$

Proof of Corollary 3.1.13. Observing that $\mathbf{r}_{\mathbf{x}} = \mathbf{b} - \mathbf{A}\mathbf{x}$, then FNE ball can be rewritten as follows,

$$B\left(\frac{1}{2}(\mathbf{u} + \mathbf{r}_{\mathbf{x}}), \frac{\|\mathbf{r}_{\mathbf{x}} - \mathbf{u}\|_2}{2}\right).$$

Therefore, its safeness inequality reads as follows,

$$\underbrace{\frac{1}{2}\|\mathbf{u}_\lambda^\star - \mathbf{u}\|_2^2}_{A} + \underbrace{\frac{1}{2}\|\mathbf{u}_\lambda^\star - \mathbf{r}_{\mathbf{x}}\|_2^2}_{B} \leq \underbrace{\frac{1}{2}\|\mathbf{u} - \mathbf{r}_{\mathbf{x}}\|_2^2}_{C}. \tag{3.38-FNE-b-ineq}$$

This inequality is indeed an instance of (3.21-ABCD2) since $D = \lambda\|\mathbf{x}\|_1 - \langle \mathbf{A}\mathbf{x}, \mathbf{u}\rangle = 0$ according to (3.36).

□

Corollary 3.1.14 (DEDPP ball is a special case of FBI ball)**.** *Consider the LASSO's strong duality in* (3.17)*. For any* $\mathbf{u} \in U_{\lambda\|\cdot\|_1}$ *and any* $\mathbf{x} \in \mathbb{R}^n$ *such that* $\mathbf{A}\mathbf{x} \neq \mathbf{0}_{\mathbb{R}^m}$*, DEDPP ball equals to FBI ball up to a scaling of* $\mathbf{x}$*. Specifically,*

$$B_{\texttt{FBI}}(2\gamma\mathbf{x}, \mathbf{u}) = B_{\texttt{DEDPP}}(\mathbf{x}, \mathbf{u}) \overset{\text{def.}}{=} B\left(\frac{1}{2}(\mathbf{b} + \mathbf{u}) - \gamma\mathbf{A}\mathbf{x}, \sqrt{\frac{1}{4}\|\mathbf{b} - \mathbf{u}\|_2^2 - \gamma^2\|\mathbf{A}\mathbf{x}\|_2^2}\right). \tag{3.39}$$

Here γ *is defined as*

$$\gamma = \max\left(0, \frac{1}{2}\frac{\langle \mathbf{A}\mathbf{x}, \mathbf{b} + \mathbf{u}\rangle - 2\lambda\|\mathbf{x}\|_1}{\|\mathbf{A}\mathbf{x}\|_2^2}\right). \tag{3.40}$$

Proof. Notice that $\mathbf{r}_{2\gamma\mathbf{x}} = \mathbf{b} - 2\gamma\mathbf{A}\mathbf{x}$ and $\gamma \geq 0$, thus

$$B_{\texttt{DEDPP}}(\mathbf{x}, \mathbf{u}) = B\left(\frac{\mathbf{u} + \mathbf{r}_{2\gamma\mathbf{x}}}{2}, \sqrt{\frac{1}{4}\|\mathbf{b} - \mathbf{u}\|_2^2 - \frac{1}{4}\|\mathbf{b} - \mathbf{r}_{2\gamma\mathbf{x}}\|_2^2}\right). \tag{3.41}$$

The safeness inequality of DEDPP ball is equivalent to

$$\underbrace{\frac{1}{2}\left\|\mathbf{u}_\lambda^\star - \mathbf{u}\right\|_2^2}_{A} + \underbrace{\frac{1}{2}\left\|\mathbf{u}_\lambda^\star - \mathbf{r}_{2\gamma\mathbf{x}}\right\|_2^2}_{B} \leq \underbrace{\frac{1}{4}\left\|\mathbf{b} - \mathbf{u}\right\|_2^2 - \frac{1}{4}\left\|\mathbf{b} - \mathbf{r}_{2\gamma\mathbf{x}}\right\|_2^2 + \frac{1}{4}\left\|\mathbf{u} - \mathbf{r}_{2\gamma\mathbf{x}}\right\|_2^2}_{C+D} \tag{3.42-DEDPP-b-ineq}$$

In a comparison with safeness inequality of $B_{\texttt{FBI}}(2\gamma\mathbf{x}, \mathbf{u})$, the two ball are equal iff

$$\frac{1}{4}\left\|\mathbf{b} - \mathbf{u}\right\|_2^2 - \frac{1}{4}\left\|\mathbf{b} - \mathbf{r}_{2\gamma\mathbf{x}}\right\|_2^2 + \frac{1}{4}\left\|\mathbf{u} - \mathbf{r}_{2\gamma\mathbf{x}}\right\|_2^2 = \frac{1}{2}\left\|\mathbf{u} - \mathbf{r}_{2\gamma\mathbf{x}}\right\|_2^2 + \lambda\left\|2\gamma\mathbf{x}\right\|_1 - 2\gamma\langle\mathbf{A}\mathbf{x}, \mathbf{u}\rangle. \tag{3.43}$$

To this end, we show that definition of γ (3.40) implies (3.43). Indeed, notice that γ satisfies

$$2\lambda\left\|\mathbf{x}\right\|_1 = \langle\mathbf{A}\mathbf{x}, \mathbf{b} + \mathbf{u} - 2\gamma\mathbf{A}\mathbf{x}\rangle = \langle\mathbf{A}\mathbf{x}, \mathbf{u} + \mathbf{r}_{2\gamma\mathbf{x}}\rangle, \tag{3.44}$$

From this observation, we have

$$\begin{aligned}
&\lambda\left\|2\gamma\mathbf{x}\right\|_1 - 2\gamma\langle\mathbf{A}\mathbf{x}, \mathbf{u}\rangle + \frac{1}{4}\left\|\mathbf{u} - \mathbf{r}_{2\gamma\mathbf{x}}\right\|_2 \\
=&\gamma\langle\mathbf{A}\mathbf{x}, \mathbf{r}_{2\gamma\mathbf{x}} + \mathbf{u}\rangle - 2\gamma\langle\mathbf{A}\mathbf{x}, \mathbf{u}\rangle + \frac{1}{4}\left\|\mathbf{u} - \mathbf{r}_{2\gamma\mathbf{x}}\right\|_2^2 \\
=&\gamma\langle\mathbf{A}\mathbf{x}, \mathbf{r}_{2\gamma\mathbf{x}} - \mathbf{u}\rangle + \frac{1}{4}\left\|\mathbf{u} - \mathbf{r}_{2\gamma\mathbf{x}}\right\|_2^2 \\
=&\frac{1}{2}\langle\mathbf{b} - \mathbf{r}_{2\gamma\mathbf{x}}, \mathbf{r}_{2\gamma\mathbf{x}} - \mathbf{u}\rangle + \frac{1}{4}\left\|\mathbf{u} - \mathbf{r}_{2\gamma\mathbf{x}}\right\|_2^2 \\
=&\frac{1}{4}\left\|\mathbf{b} - \mathbf{u}\right\|_2^2 - \frac{1}{4}\left\|\mathbf{b} - \mathbf{r}_{2\gamma\mathbf{x}}\right\|_2^2.
\end{aligned}$$

Hence, (3.43) has been proved, which completes the proof. □

SFER and SLORES ball

Corollary 3.1.15 (SFER ball is a special case of FBI ball)**.** *Consider the strong duality* (3.32)*, if one chooses* $(\mathbf{x}, \mathbf{u}) = \left(\mathbf{x}_{\lambda_0}^\star, \frac{\lambda}{\lambda_0}\mathbf{u}_{\lambda_0}^\star\right)$ *then FBI and SFER ball are the same,*

$$B_{\texttt{FBI}}\left(\mathbf{x}_{\lambda_0}^\star, \frac{\lambda}{\lambda_0}\mathbf{u}_{\lambda_0}^\star\right) = B_{\texttt{SFER}}(\mathbf{u}_{\lambda_0}^\star).$$

Proof of Corollary 3.1.15. Recall that the safeness inequality of SFER ball is:

$$\underbrace{\frac{\alpha}{2}\left\|\mathbf{u}_\lambda^\star - \frac{\lambda}{\lambda_0}\mathbf{u}_{\lambda_0}^\star\right\|_2^2}_{A} + \underbrace{\frac{\alpha}{2}\left\|\mathbf{u}_\lambda^\star - \mathbf{u}_{\lambda_0}^\star\right\|_2^2}_{B} \leq \underbrace{\mathrm{Breg}_{f^{*-}, -\mathbf{A}\mathbf{x}_{\lambda_0}^\star}\left(\frac{\lambda}{\lambda_0}\mathbf{u}_{\lambda_0}^\star, \mathbf{u}_{\lambda_0}^\star\right)}_{C}. \tag{3.45-SFER-b-ineq}$$

This is an instance of (3.33-ABCD3), with $D = 0$ with similar reason as (3.29). □

Corollary 3.1.16 (SLORES ball is a superset of FBI ball)**.** *Consider the strong duality* (3.32)*, if one chooses* $(\mathbf{x}, \mathbf{u}) = \left(\mathbf{x}^\star_{\lambda_0}, \frac{\lambda}{\lambda_0}\mathbf{u}^\star_{\lambda_0}\right)$ *the obtained FBI ball is a subset of the so-called* SLORES ball

$$B_{\texttt{FBI}}\left(\mathbf{x}^\star_{\lambda_0}, \frac{\lambda}{\lambda_0}\mathbf{u}^\star_{\lambda_0}\right) \subset B_{\texttt{SLORES}}(\mathbf{u}^\star_{\lambda_0}).$$

Proof of Corollary 3.1.16. Recall from (2.52), the safeness inequality of SLORES ball is given by:

$$\underbrace{\tfrac{\alpha}{2}\left\|\mathbf{u}^\star_\lambda - \mathbf{u}^\star_{\lambda_0}\right\|_2^2}_{B} \leq \underbrace{\mathrm{Breg}_{f^*-,-\mathbf{A}\mathbf{x}^\star_{\lambda_0}}\left(\tfrac{\lambda}{\lambda_0}\mathbf{u}^\star_{\lambda_0}, \mathbf{u}^\star_{\lambda_0}\right)}_{C}. \tag{3.46-SLORES-b-ineq}$$

This is a relaxation of (3.45-SFER-b-ineq) with $A \geq 0$. Thus FBI ball is a subset of SLORES ball. □

3.2 Hölder half-space and FBI dome

In this section, we introduce a safe "Hölder half-space" tailored for gauge penalization problem. This half-space is proven to contain the dual feasible set and generalize the existing safe half-spaces regions proposed in the literature. By taking intersection with the proposed FBI ball in the previous section, we derive a dome region referred to as "FBI dome" which also unifies existing safe dome regions in the literature.

3.2.1 Definition

Let $\kappa : \mathscr{M} \to \mathbb{R} \cup \{+\infty\}$ be a gauge function (see Definition B.1.11) and its polar κ° (see Definition B.1.17). Let $f : \mathscr{H} \to \mathbb{R} \cup \{+\infty\}$ be a convex function, $\mathbf{A} : \mathscr{M} \to \mathscr{H}$ be a linear operator and $\lambda > 0$ be penalization parameter. Let us consider the following Fenchel-Rockafellar weak duality:

$$\inf_{\mathbf{x}\in\mathscr{M}} \quad f(\mathbf{A}\mathbf{x}) + \lambda\kappa(\mathbf{x}) \geq \max_{\mathbf{u}\in U_{\lambda\kappa}} \quad -f^*(-\mathbf{u}), \tag{3.47}$$

where $U_{\lambda\kappa} = \{\mathbf{u} \in \mathscr{H} : \kappa^\circ(\mathbf{A}^*\mathbf{u}) \leq \lambda\}$.

Theorem 3.2.1 (Hölder half-space)**.** *In Fenchel-Rockafellar weak duality (3.47), we assume that the RHS of (3.47) admits at least a maximizer denoted by* $\mathbf{u}_\lambda^\star$*. Then*

$$\mathbf{u}_\lambda^\star \in H_{\texttt{Hö}}(\mathbf{x}') \triangleq H(\mathbf{A}\mathbf{x}', \lambda\kappa(\mathbf{x}')). \tag{3.48}$$

for any $\mathbf{x}' \in \mathscr{M}$*. We call* $H_{\texttt{Hö}}$ *a* Hölder half-space*.*

Proof of Theorem 3.2.1. Note that $\mathbf{u}_\lambda^\star \in U_{\lambda\kappa}$. Therefore, to prove (3.48), it is sufficient to show that

$$U_{\lambda\kappa} \subset H(\mathbf{A}\mathbf{x}', \lambda\kappa(\mathbf{x}')), \tag{3.49}$$

for all $\mathbf{x}' \in \mathscr{M}$. For any $\mathbf{u} \in U_{\lambda\kappa}$, we have

$$\langle \mathbf{A}\mathbf{x}', \mathbf{u} \rangle \leq \kappa^\circ(\mathbf{A}^*\mathbf{u})\kappa(\mathbf{x}') \leq \lambda\kappa(\mathbf{x}'), \tag{3.50}$$

where the first upper bound follows from the polar inequality (see Proposition B.1.18), and the second upper bound holds since $\mathbf{u} \in U_{\lambda\kappa}$. □

Remark 3.2.2. *Note that the safeness of Hölder half-space (3.50) has been established in two parallel works [99, 87]. In [87], we consider* $\kappa = \|\cdot\|_1$ *and the first inequality in (3.50) therefore resembles the Hölder inequality, hence, the name "Hölder" half-space.*

Remark 3.2.3 (Canonical characterization of dual feasible set)**.** *In the context of LASSO, i.e.,* $\mathscr{M} = \mathbb{R}^n$*,* $\mathscr{H} = \mathbb{R}^m$*,* $f = \frac{1}{2}\|\mathbf{b} - \cdot\|_2^2$ *for some* $\mathbf{b} \in \mathbb{R}^m$*,* $\kappa = \|\cdot\|_1$ *and* $\mathbf{A} \in \mathbb{R}^{m\times n}$ *we show that in inclusion (3.49) is actually a consequence of the following identity [87, Lemma 1]:*

$$U_{\lambda\|\cdot\|_1} = \bigcap_{\mathbf{x}\in\mathbb{R}^n} H(\mathbf{A}\mathbf{x}, \lambda\|\mathbf{x}\|_1). \tag{3.51}$$

We refer to (3.51) as the canonical characterization of dual feasible set $U_{\lambda\|\cdot\|_1}$ *using the primal information* $\mathbf{x} \in \mathbb{R}^n$*.*

By using the Hölder half-space to intersect *any* safe ball, we can derive a safe dome region. Particularizing to FBI ball, we refer to the resulting safe dome region as the FBI dome.

Theorem 3.2.4 (FBI dome)**.** *Assume that the strong duality (3.47) and the hypotheses (H1), (H2) and (H3) hold true. For* $(\mathbf{x}', \mathbf{x}, \mathbf{u}) \in \mathscr{M} \times \mathscr{M} \times \mathscr{H}$*, we have*

$$\mathbf{u}_\lambda^\star \in D_{\texttt{FBI}}(\mathbf{x}', \mathbf{x}, \mathbf{u}) \triangleq H_{\texttt{Hö}}(\mathbf{x}') \cap B_{\texttt{FBI}}(\mathbf{x}, \mathbf{u}). \tag{3.52}$$

We call this safe region FBI dome.

3.2.2 Zero-radius property

In this section we demonstrate the tightness of FBI dome by showing that there exist choices of $(\mathbf{x}', \mathbf{x}, \mathbf{u})$ such that $D_{\texttt{FBI}}(\mathbf{x}', \mathbf{x}, \mathbf{u})$ contains only $\mathbf{u}^\star_\lambda$ as a unique point. The trivial case is to choose $(\mathbf{x}, \mathbf{u})$ as an optimal pair, *i.e.*, $D_{\texttt{FBI}}(\mathbf{x}', \mathbf{x}^\star_\lambda, \mathbf{u}^\star_\lambda) = \{\mathbf{u}^\star_\lambda\}$ for any $\mathbf{x}' \in \mathscr{M}$. This is clear since we have from Proposition 3.1.4 that $\{\mathbf{u}^\star_\lambda\} = B_{\texttt{FBI}}(\mathbf{x}^\star_\lambda, \mathbf{u}^\star_\lambda) \subset H_{\texttt{Hö}}(\mathbf{x}')$.

In the following we provide a non-trivial and probably surprising result, which claims the singleton of $D_{\texttt{FBI}}(\mathbf{x}^\star_\lambda, \mathbf{0}_{\mathscr{M}}, \mathbf{u}^\star_\lambda)$ in the strong duality of LASSO-like problem (3.11).

Theorem 3.2.5 (Zero-radius property FBI dome)**.** *Consider the LASSO-like's strong duality* (3.11)*, we have*

$$\{\mathbf{u}^\star_\lambda\} = D_{\texttt{FBI}}(\mathbf{x}^\star_\lambda, \mathbf{0}_{\mathscr{M}}, \mathbf{u}^\star_\lambda).$$

Proof. We have

$$H_{\texttt{Hö}}(\mathbf{x}^\star_\lambda) = H(\mathbf{A}\mathbf{x}^\star_\lambda, \lambda\kappa(\mathbf{x}^\star_\lambda)) = H(\mathbf{b} - \mathbf{u}^\star_\lambda, \langle \mathbf{b} - \mathbf{u}^\star_\lambda, \mathbf{u}^\star_\lambda \rangle)$$

and

$$B_{\texttt{FBI}}(\mathbf{0}_{\mathscr{M}}, \mathbf{u}^\star_\lambda) = B\left(\frac{\mathbf{u}^\star_\lambda + \mathbf{b}}{2}, \frac{\|\mathbf{u}^\star_\lambda - \mathbf{b}\|_{\mathscr{H}}}{2}\right)$$

Therefore, it is clear that the boundary of $H_{\texttt{Hö}}(\mathbf{x}^\star_\lambda)$ is the tangent hyper-plane of $B_{\texttt{FBI}}(\mathbf{0}_{\mathscr{M}}, \mathbf{u}^\star_\lambda)$ at $\mathbf{u}^\star_\lambda$. Since moreover $B_{\texttt{FBI}}(\mathbf{0}_{\mathscr{M}}, \mathbf{u}^\star_\lambda)$ is not as subset of $H_{\texttt{Hö}}(\mathbf{x}^\star_\lambda)$ (hint: consider the point $\mathbf{b}$) these two observations imply that $\mathbf{u}^\star_\lambda$ is the unique point in the intersection of the two regions. Therefore, FBI dome contains $\mathbf{u}^\star_\lambda$ as the unique point. □

3.2.3 Comparisons

Safe half-spaces

Corollary 3.2.6 (ST half-space is a special case of Hölder half-space)**.** *Consider LASSO's strong duality* (3.17)*, ST half-space is a special case of Hölder half-space.*

$$H_{\texttt{Hö}}(\mathbf{e}_{i_0}) = H_{\texttt{ST}}(i_0) \overset{\text{def.}}{=} H(\mathbf{a}_{i_0}, \lambda) \tag{3.53}$$

for any unit basic vector $\mathbf{e}_{i_0} \in \mathbb{R}^n$ *and* $i_0 \in \{1, \ldots, n\}$.

Proof of Corollary 3.2.6. Notice that $\mathbf{A}\mathbf{e}_{i_0} = \mathbf{a}_{i_0}$ and $\|\mathbf{e}_{i_0}\|_1 = 1$, thus,

$$H_{\texttt{Hö}}(\mathbf{e}_{i_0}) \overset{\text{def.}}{=} H(\mathbf{A}\mathbf{e}_{i_0}, \lambda \|\mathbf{e}_{i_0}\|_1) = H(\mathbf{a}_{i_0}, \lambda) \overset{\text{def.}}{=} H_{\texttt{ST}}(i_0).$$

□

Corollary 3.2.7 (SASVI half-space is a special case of Hölder half-space)**.** *Consider LASSO's strong duality (3.17), SASVI half-space is a special case of Hölder half-space*

$$H_{\texttt{Hö}}(\mathbf{x}^\star_{\lambda_0}) = H_{\texttt{SASVI}}(\mathbf{u}^\star_{\lambda_0}) \overset{\text{def.}}{=} H\left(\mathbf{b} - \mathbf{u}^\star_{\lambda_0}, \left\langle \mathbf{b} - \mathbf{u}^\star_{\lambda_0}, \frac{\lambda}{\lambda_0}\mathbf{u}^\star_{\lambda_0} \right\rangle\right). \tag{3.54}$$

Proof of Corollary 3.2.7. By the optimality (3.18) and (3.19), we have $\mathbf{u}^\star_{\lambda_0} = \mathbf{b} - \mathbf{A}\mathbf{x}^\star_{\lambda_0}$ and $\lambda_0 \left\|\mathbf{x}^\star_{\lambda_0}\right\|_1 = \left\langle \mathbf{A}\mathbf{x}^\star_{\lambda_0}, \mathbf{u}^\star_{\lambda_0} \right\rangle$. This implies

$$H_{\texttt{Hö}}(\mathbf{x}^\star_{\lambda_0}) \overset{\text{def.}}{=} H\left(\mathbf{A}\mathbf{x}^\star_{\lambda_0}, \lambda \left\|\mathbf{x}^\star_{\lambda_0}\right\|_1\right) = H\left(\mathbf{b} - \mathbf{u}^\star_{\lambda_0}, \left\langle \mathbf{b} - \mathbf{u}^\star_{\lambda_0}, \frac{\lambda}{\lambda_0}\mathbf{u}^\star_{\lambda_0} \right\rangle\right) \overset{\text{def.}}{=} H_{\texttt{SASVI}}(\mathbf{u}^\star_{\lambda_0}).$$

□

Safe domes

In the following we compare FBI dome and

- ST dome
- SASVI dome
- DSASVI dome
- GAP moon and dome

A summary of the comparison results is presented in Table 1.1 page 23.

Corollary 3.2.8 (ST dome is a superset of FBI dome)**.** *Consider LASSO's strong duality (3.17), for $\mathbf{u} \in U_{\lambda\|\cdot\|_1}$, we have*

$$D_{\texttt{FBI}}(\mathbf{e}_{i_0}, \mathbf{0}, \mathbf{u}) \subset D_{\texttt{ST}}(i_0, \mathbf{u}) \overset{\text{def.}}{=} H(\mathbf{a}_{i_0}, \lambda) \cap B(\mathbf{b}, \|\mathbf{b} - \mathbf{u}\|_2).$$

Proof. We have

$$D_{\texttt{FBI}}(\mathbf{e}_{i_0}, \mathbf{0}, \mathbf{u}) \overset{\text{def.}}{=} H_{\texttt{Hö}}(\mathbf{e}_{i_0}) \cap B_{\texttt{FBI}}(\mathbf{0}, \mathbf{u}) \subset H(\mathbf{a}_{i_0}, \lambda) \cap B(\mathbf{b}, \|\mathbf{b} - \mathbf{u}\|_2),$$

where the inclusion follows from (3.53) and (3.25). □

Corollary 3.2.9 (SASVI dome is special case of FBI dome)**.** *Consider LASSO's strong duality* (3.17)*, we have*

$$D_{\texttt{FBI}}\left(\mathbf{x}^\star_{\lambda_0}, \mathbf{0}, \frac{\lambda}{\lambda_0}\mathbf{u}^\star_{\lambda_0}\right) = D_{\texttt{SASVI}}(\mathbf{u}^\star_{\lambda_0}) \overset{\text{def.}}{=} H_{\texttt{SASVI}}(\mathbf{u}^\star_{\lambda_0}) \cap B_{\texttt{SASVI}}(\mathbf{u}^\star_{\lambda_0}).$$

Proof of Corollary 3.2.9. We have

$$D_{\texttt{FBI}}\left(\mathbf{x}^\star_{\lambda_0}, \mathbf{0}, \frac{\lambda}{\lambda_0}\mathbf{u}^\star_{\lambda_0}\right) \overset{\text{def.}}{=} H_{\texttt{Hö}}(\mathbf{x}^\star_{\lambda_0}) \cap B_{\texttt{FBI}}\left(\mathbf{0}, \frac{\lambda}{\lambda_0}\mathbf{u}^\star_{\lambda_0}\right) = H_{\texttt{SASVI}}(\mathbf{u}^\star_{\lambda_0}) \cap B_{\texttt{SASVI}}(\mathbf{u}^\star_{\lambda_0}),$$

where the last equality follows from (3.54) and (3.22). Thus, in this case, FBI and SASVI dome are the same. □

The Dynamic SASVI (DSASVI) dome was introduced simultaneously in [87, 99], and defined as the intersection of the Hölder half-space and the SASVI ball. It turns out that this is also a particularization of the FBI dome.

Corollary 3.2.10 (DSASVI dome is a special case of FBI dome)**.** *Consider LASSO's strong duality* (3.17)*, DSASVI dome is a special case of FBI dome.*

$$D_{\texttt{FBI}}(\mathbf{x}, \mathbf{0}, \mathbf{u}) = D_{\texttt{DSASVI}}(\mathbf{x}, \mathbf{u}) \overset{\text{def.}}{=} H_{\texttt{Hö}}(\mathbf{x}) \cap B_{\texttt{SASVI}}(\mathbf{u}),$$

for $\mathbf{u} \in U_{\lambda\|\cdot\|_1}$.

Proof of Corollary 3.2.10.

$$D_{\texttt{FBI}}(\mathbf{x}, \mathbf{0}, \mathbf{u}) \overset{\text{def.}}{=} H_{\texttt{Hö}}(\mathbf{x}) \cap B_{\texttt{FBI}}(\mathbf{0}, \mathbf{u}) = H_{\texttt{Hö}}(\mathbf{x}) \cap B_{\texttt{SASVI}}(\mathbf{u}).$$

Here the last equality follows from the comparison of FBI and SASVI ball (3.22). □

Corollary 3.2.11 (GAP regions are supersets of FBI dome)**.** *Consider LASSO's strong duality* (3.17)*, for* $(\mathbf{x}, \mathbf{u}) \in \mathbb{R}^n \times U_{\lambda\|\cdot\|_1}$*, then FBI dome* $D_{\texttt{FBI}}(\mathbf{x}, \mathbf{0}, \mathbf{u})$ *is the smallest one compared to GAP safe regions:*

$$D_{\texttt{FBI}}(\mathbf{x}, \mathbf{0}, \mathbf{u}) \subset M_{\texttt{GAP}}(\mathbf{x}, \mathbf{u}) \subset D_{\texttt{GAP}}(\mathbf{x}, \mathbf{u}) \subset B_{\texttt{GAP}}(\mathbf{x}, \mathbf{u}).$$

Proof. Here, it is sufficient to show that $D_{\texttt{FBI}}(\mathbf{x}, \mathbf{0}, \mathbf{u}) \subset M_{\texttt{GAP}}(\mathbf{x}, \mathbf{u})$. We now re-produce the proof in [99]. Notice that $D_{\texttt{FBI}}(\mathbf{x}, \mathbf{0}, \mathbf{u}) = B_{\texttt{FBI}}(\mathbf{u}) \cap H_{\texttt{Hö}}(\mathbf{x})$ and $M_{\texttt{GAP}}(\mathbf{x}, \mathbf{u}) = B_{\texttt{FBI}}(\mathbf{u}) \cap E_{\texttt{GAP}}(\mathbf{x})$. Let $\mathbf{p} \in H_{\texttt{Hö}}(\mathbf{x})$, we aim to show that $\mathbf{p} \in E_{\texttt{GAP}}(\mathbf{x})$. By definition of $H_{\texttt{Hö}}(\mathbf{x})$ and $E_{\texttt{GAP}}(\mathbf{x})$, this implication holds because of the following observation:

$$d(\mathbf{p}) \leq p(\mathbf{x}) \iff -\frac{1}{2} \|\mathbf{p} - \mathbf{r}_{\mathbf{x}}\|_2^2 \leq \lambda \|\mathbf{x}\|_1 - \langle \mathbf{A}\mathbf{x}, \mathbf{p} \rangle.$$

The proof is completed. □

3.3 Geometric ball

Given a dome region and an arbitrary point $\mathbf{v}$, this section discusses how to to construct a ball centered at $\mathbf{v}$ and has smallest radius so that it contains the given dome. We refer too this ball as a "geometric ball".

3.3.1 Definition

From a practical standpoint, implementing dimensionality reduction methods using a ball is considerably simpler than utilizing a dome. Motivated by this, several studies have proposed deriving the "smallest" ball (with a pre-specified center) that contains a given dome region. For example, the ST2 and ST3 balls have been derived from the ST dome [95, 96], the GAP ball from the GAP dome [45], and the Dynamic EDPP (DEDPP) ball from the Dynamic SASVI (DSASVI) dome [99]. As the safe region should be as small as possible, its radius should be minimized. We define such ball regions as *geometric balls*.

Definition 3.3.1 (Geometric ball)**.** *Let $\mathbf{v} \in \mathscr{H}$ be a point and $D \subset \mathscr{H}$ be a non-empty dome region. Define $B(\mathbf{v}, R)$ as a ball corresponding to $\mathbf{v}$ and D which has center located at $\mathbf{v}$ and has smallest radius, denoted by R, so that it contains the dome D, i.e.,*

$$R \triangleq \sup_{\mathbf{u} \in D} \|\mathbf{v} - \mathbf{u}\|_{\mathscr{H}}.$$

We call $B(\mathbf{v}, R)$ a geometric ball.

Note that R can be evaluated explicitly:

$$R = \begin{cases} \|\mathbf{v}-\mathbf{c}\|_{\mathscr{H}} + r, & \text{if } \psi_{\mathbf{v}} \geq -\psi_D, \\ \sqrt{\|\mathbf{v}-\mathbf{v}_P\|_{\mathscr{H}}^2 + \left(\|\mathbf{v}_P-\mathbf{c}_P\|_{\mathscr{H}} + \sqrt{1-\psi_D^2}\right)^2}, & \text{otherwise,} \end{cases} \tag{3.55}$$

where $\mathbf{v}_P$ denotes the projection of $\mathbf{v}$ onto the hyperplane P associated with half-space $H(\mathbf{g}, s)$, $\psi_{\mathbf{v}} \triangleq \frac{\langle \mathbf{g}, \mathbf{v}-\mathbf{c}\rangle}{\|\mathbf{g}\|_{\mathscr{H}}\|\mathbf{v}-\mathbf{c}\|_{\mathscr{H}}}$ denotes the cosine between the two vectors and $\psi_D \triangleq \dfrac{s-\langle \mathbf{g}, \mathbf{c}\rangle}{r\|\mathbf{g}\|_{\mathscr{H}}}$ denotes the intersection index of dome region D, see (A.8). The proof for this result is presented in Proposition A.3.5.

By this definition and the generality of the FBI dome established in the previous section, existing safe ball regions (ST2, ST3, GAP, DEDPP) can be considered as instances of the geometric ball. Surprisingly, we demonstrate in the next section that, under certain conditions, the FBI ball can also be viewed as a geometric ball.

3.3.2 Comparisons

Theorem 3.3.2 (Relation of FBI ball and FBI dome)**.** *Consider the strong duality in the LASSO-like setup* (3.11) *and* $(\mathbf{x}, \mathbf{u}) \in \mathscr{M} \times U_{\lambda\kappa}$*, then FBI ball* $B_{\texttt{FBI}}(\mathbf{x}, \mathbf{u})$ *is the ball centered at* $\dfrac{\mathbf{u}+\mathbf{r}_{\mathbf{x}}}{2}$ *with smallest radius containing FBI dome* $D_{\texttt{FBI}}(\mathbf{x}, \mathbf{0}, \mathbf{u})$*, i.e.,*

$$D_{\texttt{FBI}}(\mathbf{x}, \mathbf{0}, \mathbf{u}) \subset B_{\texttt{FBI}}(\mathbf{x}, \mathbf{u})$$

and

$$\operatorname{rad} B_{\texttt{FBI}}(\mathbf{x}, \mathbf{u}) = \max_{\mathbf{p} \in D_{\texttt{FBI}}(\mathbf{x}, \mathbf{0}, \mathbf{u})} \left\| \frac{\mathbf{u}+\mathbf{r}_{\mathbf{x}}}{2} - \mathbf{p} \right\|_{\mathscr{H}}.$$

In other words, the FBI ball $B_{\texttt{FBI}}(\mathbf{x}, \mathbf{u})$ *is the geometric ball associated with center* $\dfrac{\mathbf{u}+\mathbf{r}_{\mathbf{x}}}{2}$ *and FBI dome* $D_{\texttt{FBI}}(\mathbf{x}, \mathbf{0}, \mathbf{u})$*.*

Proof of Theorem 3.3.2. We prove this result by using Proposition A.3.3, which asserts that that the ball $B(r_\theta, r_\theta)$ forms a geometric ball encompassing the dome $D = B(\mathbf{c}, r) \cap H(\mathbf{g}, s)$ if the six parameters $\mathbf{c}, r, \mathbf{g}, s, r_\theta$ and r_θ satisfy (A.9) and (A.10) for some $\theta \leq 0$.

To apply this result, we choose the parameter of dome region as follows:

$$\begin{aligned}\mathbf{c} &= \frac{\mathbf{b}+\mathbf{u}}{2}\\ r &= \frac{\|\mathbf{b}-\mathbf{u}\|_{\mathscr{H}}}{2}\\ \mathbf{g} &= \mathbf{A}\mathbf{x} = \mathbf{b}-\mathbf{r}_{\mathbf{x}}\\ s &= \lambda\kappa(\mathbf{x})\end{aligned}$$

and the parameters of the smallest ball:

$$\begin{aligned}\mathbf{c}_\theta &= \frac{\mathbf{u}+\mathbf{r}_{\mathbf{x}}}{2}\\ r_\theta &= \operatorname{rad} B_{\texttt{FBI}}(\mathbf{x},\mathbf{u})\\ \theta &= \frac{-\|\mathbf{b}-\mathbf{r}_{\mathbf{x}}\|_{\mathscr{H}}}{\|\mathbf{b}-\mathbf{u}\|_{\mathscr{H}}}\end{aligned}$$

The remaining is to show that (A.9) and (A.10) hold true *w.r.t.* to above choice of parameters. We first notice that (A.9) holds true since

$$\mathbf{c}_\theta = \frac{\mathbf{u}+\mathbf{r}_{\mathbf{x}}}{2} = \mathbf{c} + \theta r\frac{\mathbf{g}}{\|\mathbf{g}\|}. \tag{3.56}$$

To prove (A.10), we recall that $\psi_D = \frac{s-\langle\mathbf{g},\mathbf{c}\rangle}{r\|\mathbf{g}\|_{\mathscr{H}}}$ denotes the dome index of dome D. Now, we have

$$\begin{aligned}&r^2((\psi_D-\theta)^2+(1-\psi_D^2))\\ =&r^2(\theta^2-2\theta\psi_D+1)\\ =&\frac{1}{4}\|\mathbf{b}-\mathbf{u}\|^2\left(\frac{\|\mathbf{b}-\mathbf{r}_{\mathbf{x}}\|^2}{\|\mathbf{b}-\mathbf{u}\|^2}+2\frac{\|\mathbf{b}-\mathbf{r}_{\mathbf{x}}\|}{\|\mathbf{b}-\mathbf{u}\|}\frac{\lambda\kappa(\mathbf{x})-\frac{1}{2}\langle\mathbf{A}\mathbf{x},\mathbf{b}+\mathbf{u}\rangle}{\|\mathbf{A}\mathbf{x}\|\frac{1}{2}\|\mathbf{b}+\mathbf{u}\|}+1\right)\\ =&\frac{1}{4}\|\mathbf{b}-\mathbf{r}_{\mathbf{x}}\|^2+\lambda\kappa(\mathbf{x})-\frac{1}{2}\langle\mathbf{A}\mathbf{x},\mathbf{b}+\mathbf{u}\rangle+\frac{1}{4}\|\mathbf{b}-\mathbf{u}\|^2\\ =&\lambda\kappa(\mathbf{x})-\langle\mathbf{A}\mathbf{x},\mathbf{u}\rangle+\frac{1}{4}\|\mathbf{u}-\mathbf{r}_{\mathbf{x}}\|^2\end{aligned}$$

By applying (3.14), we have

$$\begin{aligned}
&= \mathrm{GAP}(\mathbf{x}, \mathbf{u}) - \frac{1}{4} \left\| \mathbf{u} - \mathbf{r}_{\mathbf{x}} \right\|^2 \\
&= (\mathrm{rad}\, B_{\mathtt{FBI}}(\mathbf{x}, \mathbf{u}))^2 \\
&= r_\theta^2.
\end{aligned}$$

Hence, we complete the proof. □

Chapter 4

Extending safe screening principle to the space of measures

Abstract. *In this chapter, we extend the safe screening principle to the total variation norm penalization problem defined on the space of Radon measures, presenting an efficient method to eliminate the support region of optimal measures. We first propose a single-parameter elimination using the safe screening rule. Building upon this, we present a batch parameter screening method referred to as Joint Safe Screening (JSS). Moreover, we investigate the application of this safe screening rule to reduce the complexity of a recently introduced solver known as the Refined Grid Based (RGB) method. Additionally, we establish a consistency result, ensuring that integrating JSS into RGB does not alter the iterative solutions, thus maintaining the convergence analysis previously established for RGB.*

In Chapter 2, we discussed how the safe screening rule (2.9) and its relaxed version (2.11) using safe region can effectively reduce the dimension of ℓ_1-norm penalization problems (2.1). The purpose of this chapter is to extend these safe screening rules to address the following infinite-dimensional counterpart of ℓ_1-norm penalization problem:

$$\min_{\mathbf{x}\in\mathscr{M}} \quad f(\mathbf{A}\mathbf{x}) + \lambda \|\mathbf{x}\|_{TV}\,, \tag{4.1}$$

which is known as a "total-variation norm" penalized problem. Here $\mathscr{H}$ denotes some Hilbert space while $\mathscr{M}$ denotes the space of Radon measures, $f : \mathscr{H} \to \mathbb{R} \cup \{+\infty\}$ is a convex function, $\mathbf{A} : \mathscr{M} \to \mathscr{C}$ is a linear operator called "dictionary operator", $\lambda > 0$, and $\|\cdot\|_{TV}$ denotes the total variation norm of Radon measures.

In Section 4.1, we provide a recap of essential concepts to rigorously define (4.1). In Section 4.2, we introduce a safe screening rule for (4.1). In Section 4.3, we delve into the application of this safe screening rule, accompanied by a theoretical guarantee, to reduce the complexity of a recently proposed solver for (4.1) known as the Refinement Grid Based method [48, Algorithm 2].

4.1 Preliminaries

In this part, we recall the concepts essential to properly define problem (4.1), including the space of Radon measures $\mathscr{M}$ and the dictionary operator $\mathbf{A}$. We then conclude this section with a brief review of several available solving methods for (4.1).

4.1.1 Radon measures

Space of Radon measures. One can encounter two (equivalent) definitions of the space of "Radon measures", see [2, Section 4.2] for a detailed discussion. The first approach defines Radon measures as set functions over Borel sets that satisfy specific regularity conditions, see *e.g.*, [2, Definition 4.2.1] or [46, Definition 2.3]. In this thesis, we rather follow the second approach which defines Radon measures as continuous linear functionals over the space of continuous functions [2, Section 4.2.2]. This approach is consistent with the duality framework that we will exploit in the next section.

Let $T \subset \mathbb{R}^d$ be a *compact* set. We call T the *parameter set*. Let $\mathscr{C} = \mathscr{C}(T, \mathbb{R})$ be the space of continuous functions from T to $\mathbb{R}$. $\mathscr{C}$ is a Banach space endowed with the

max-norm defined as follows:

$$\|\mathbf{z}\|_\infty \triangleq \max\{|\mathbf{z}(\mathbf{t})| : \mathbf{t} \in T\},$$

for any $\mathbf{z} \in \mathscr{C}$. Here, the maximum is well-defined since T is compact and $\mathbf{z}$ is continuous. We denote the strong topology in $\mathscr{C}$ induced by the max-norm by $\tau_{\mathscr{C}}$. It is important to notice that $(\mathscr{C}, \tau_{\mathscr{C}})$ is non-reflexive. [1]

The space of *Radon measures*, denoted by $\mathscr{M} = \mathscr{M}(T, \mathbb{R})$, is defined as the topological dual space of $\mathscr{C}$, *i.e.*, $\mathscr{M} \triangleq (\mathscr{C}, \tau_{\mathscr{C}})^*$. We now use the canonical pairing to denote the action of $\mathbf{x} \in \mathscr{M}$ on $\mathbf{z} \in \mathscr{C}$, *i.e.*,

$$\langle \mathbf{x}, \mathbf{z} \rangle_{\mathscr{M},\mathscr{C}} \triangleq \int_{\mathbf{t}\in T} \mathbf{z}(\mathbf{t})\mathbf{x}(\mathrm{d}\mathbf{t}).$$

To simplify notations, if the spaces of $\mathbf{x}$ and $\mathbf{z}$ are clearly identified from the context, we will drop the subscript in the pairing and ignore the order, *i.e.*, we write $\langle \mathbf{x}, \mathbf{z} \rangle = \langle \mathbf{z}, \mathbf{x} \rangle = \langle \mathbf{x}, \mathbf{z} \rangle_{\mathscr{M},\mathscr{C}}$. [2] Note that the space of Radon measures is also a Banach space endowed with the natural dual norm called *total variation norm (TV-norm)*:

$$\|\mathbf{x}\|_{TV} \triangleq \sup\Big\{ \langle \mathbf{x}, \mathbf{z} \rangle_{\mathscr{M},\mathscr{C}} : \|\mathbf{z}\|_\infty \leq 1 \Big\} \tag{4.2}$$

for any $\mathbf{x} \in \mathscr{M}$. We denote by $\tau_{\mathscr{M}}$ the topology on $\mathscr{M}$ induced by the TV-norm. Here $(\mathscr{M}, \tau_{\mathscr{M}}) = (\mathscr{C}, \tau_{\mathscr{C}})^*$. Recall that $(\mathscr{C}, \tau_{\mathscr{C}})$ is non-reflexive, *i.e.*, the topological dual of $(\mathscr{M}, \tau_{\mathscr{M}})$ is distinct from $\mathscr{C}$ and is not thoroughly understood. This observation is crucial in guiding our approach to utilizing duality results in the subsequent sections.

An important example of a Radon measure is the *Dirac mass*, denoted by $\delta_{\mathbf{t}}$ for some $\mathbf{t} \in T$. The Dirac mass $\delta_{\mathbf{t}}$ acts on a continuous function $\mathbf{z} \in \mathscr{C}$ as follows:

$$\langle \delta_{\mathbf{t}}, \mathbf{z} \rangle \triangleq \mathbf{z}(\mathbf{t}),$$

that is, $\langle \delta_{\mathbf{t}}, \mathbf{z} \rangle$ returns the evaluation of $\mathbf{z}$ at $\mathbf{t}$. The Dirac mass has a unit TV-norm, *i.e.*, $\|\delta_{\mathbf{t}}\|_{TV} = 1$. In general, for a discrete measure defined as a combination of weighted Dirac masses, say $\mathbf{x} = \sum_{i=1}^n w_i \delta_{\mathbf{t}_i}$ where $(w_i, \mathbf{t}_i) \in \mathbb{R} \times T$, the TV-norm of $\mathbf{x}$ is the sum of its component masses: $\|\mathbf{x}\|_{TV} = \sum_{i=1}^n |w_i|$. This remark highlights that TV-norm is essentially an infinite-dimensional counterpart of ℓ_1-norm.

1. That is $\mathscr{C} \subsetneq (\mathscr{C}, \tau_{\mathscr{C}})^{**}$.
2. The notations of canonical dual pairing and the inner product in Hilbert space can be distinguished using their arguments.

The *total variation measure* of $\mathbf{x} \in \mathscr{M}$, denoted by $|\mathbf{x}|$, is a measure defined for any Borel set $\Theta \subset T$ as [56, Section 29]:

$$|\mathbf{x}|(\Theta) \triangleq \sup\left\{ \int_{\mathbf{t}\in\Theta} \mathbf{z}(\mathbf{t})\mathbf{x}(\mathrm{d}\mathbf{t}) : \mathbf{z} \text{ is } \mathbf{x}\text{-measurable and } \operatorname*{ess\,sup}_{\mathbf{t}'\in T} |\mathbf{z}(\mathbf{t}')| \leq 1 \right\}.$$

In particular, the total variation measure evaluated on the whole parameter set T equals to the TV-norm, *i.e.*,

$$|\mathbf{x}|(T) = \|\mathbf{x}\|_{TV}.$$

The support of a measure $\mathbf{x} \in \mathscr{M}$ is the smallest closed set in T, denoted by $\mathrm{supp}(\mathbf{x})$, such that $|\mathbf{x}|(T \setminus \mathrm{supp}(\mathbf{x})) = 0$ [2, page 124]. In other words,

$$\mathrm{supp}(\mathbf{x}) = \{\mathbf{t} \in T : |\mathbf{x}|(\Theta) > 0 \text{ for any open set } \Theta \text{ containing } \mathbf{t}\}. \tag{4.3}$$

4.1.2 Dictionary operator

Recall that, in this section, we denote $\mathscr{H}$ a Hilbert space and $\mathscr{C}$ the space of continuous functions defined on a compact set T. Our objective is to introduce the so-called "dictionary operator" $\mathbf{A}$ appearing in (4.1). Here, we follow the intuitive construction proposed by Flinth [46, Definition 2.1 and 2.13], where the dictionary operator $\mathbf{A}$ is defined using the concepts of "atom" and "test operator".

In this thesis, we consider atom as a function defined on T which satisfies two regularity conditions detailed in the following definition.

Definition 4.1.1 (Atom)**.** *An* atom $\mathbf{a}$ *is a map* $\mathbf{a} : \mathbf{t} \in T \mapsto \mathbf{a}_\mathbf{t} \in \mathscr{H}$ *satisfying the following two conditions:*

(A1) ***Lipschitz continuity.*** *For all* $\mathbf{t}, \mathbf{t}' \in T$, $\|\mathbf{a}_\mathbf{t} - \mathbf{a}_{\mathbf{t}'}\|_\mathscr{H} \leq L \|\mathbf{t} - \mathbf{t}'\|_2$ *for some* $L > 0$.

(A2) ***Boundedness.*** *For all* $\mathbf{t} \in T$, $\|\mathbf{a}_\mathbf{t}\|_\mathscr{H} \leq M$ *for some* $M > 0$.

Here, a brief note is warranted regarding the utilization of the two hypotheses concerning the atom. In Definition 4.1.1, the assumption of Lipschitz continuity (A1) plays a pivotal role in deriving the practical safe screening rule discussed in the subsequent section, see Theorem 4.2.2) The boundedness assumption (A2) ensures the continuity of the "test operator" $\mathbf{K}$, as defined immediately below.

Example 4.1.2. *Let T be a compact subset in $\mathbb{R}^d$ and $\mathscr{H} = L^2(\mathbb{R}^d)$ be the space of squared integrable functions on $\mathbb{R}^n$, then the Gaussian mapping $\mathbf{t} \mapsto \mathbf{a}_\mathbf{t}(\cdot) = \exp\left(-\gamma \left\|\cdot - \mathbf{t}\right\|_2^2\right)$ for some $\gamma > 0$ satisfies the definition of atom.*

We now define the *test operator* $\mathbf{K}\colon \mathscr{H} \to \mathscr{C}$, which is a linear operator such that:

$$(\mathbf{K}\mathbf{u})(\mathbf{t}) \triangleq \langle \mathbf{u}, \mathbf{a}_\mathbf{t} \rangle,$$

for all $\mathbf{t} \in T$. Note that (A2) implies that $\mathbf{K}$ is bounded since

$$\left\|\mathbf{K}\mathbf{u}\right\|_\mathscr{C} = \max_{\mathbf{t}\in T} \left|\langle \mathbf{u}, \mathbf{a}_\mathbf{t} \rangle\right| \leq \max_{\mathbf{t}\in T} \left\|\mathbf{a}_\mathbf{t}\right\|_\mathscr{H} \left\|\mathbf{u}\right\|_\mathscr{H} \leq M \left\|\mathbf{u}\right\|_\mathscr{H}.$$

for all $\mathbf{u} \in \mathscr{H}$. Here, the last inequality follows from (A2).

We define the *dictionary operator* $\mathbf{A} : \mathscr{M} \to \mathscr{H}$ as the adjoint operator of $\mathbf{K}$, *i.e.*,

$$\mathbf{A} \triangleq \mathbf{K}^*.$$

Explicitly, $\mathbf{A}$ can also be defined as the unique linear operator satisfying:

$$\langle \mathbf{u}, \mathbf{A}\mathbf{x} \rangle_{\mathscr{H},\mathscr{H}} = \langle \mathbf{x}, \mathbf{K}\mathbf{u} \rangle_{\mathscr{M},\mathscr{C}} \left(= \int_{\mathbf{t}\in T} \langle \mathbf{u}, \mathbf{a}_\mathbf{t} \rangle \mathbf{x}(\mathrm{d}\mathbf{t}) \right), \tag{4.4}$$

for all $(\mathbf{x}, \mathbf{u}) \in \mathscr{M} \times \mathscr{H}$.

With a slight abuse of terminology, we denote $\mathbf{A}^* \triangleq \mathbf{K}$ and say that $\mathbf{A}$ and $\mathbf{A}^*$ are each other's *adjoint*. From now on, we will use the notation $\mathbf{A}, \mathbf{A}^*$ instead of $\mathbf{K}^*, \mathbf{K}$, respectively.

It is worth noting that the image of a measure via dictionary $\mathbf{A}$ can be understood as a Bochner integral [22] taking value in Hilbert space $\mathscr{H}$, *i.e.*, $\mathbf{A}\mathbf{x} = \int_{\mathbf{t}\in T} \mathbf{a}_\mathbf{t} \mathbf{x}(\mathrm{d}\mathbf{t}) \in \mathscr{H}$ for any measure $\mathbf{x} \in \mathscr{M}$. Particularly, the image of a discrete measure $\mathbf{x} = \sum_{i=1}^n w_i \delta_{\mathbf{t}_i}$ is the linear combination of the corresponding atoms:

$$\mathbf{A}\left(\sum_{i=1}^n w_i \delta_{\mathbf{t}_i}\right) = \sum_{i=1}^n w_i \mathbf{a}_{\mathbf{t}_i}, \tag{4.5}$$

where $(w_i, \mathbf{t}_i) \in \mathbb{R} \times T$ and $i = 1, \ldots, n$. When $n = 1$, the image of a unit Dirac mass is the associated atom, *i.e.*,

$$\mathbf{A}\delta_\mathbf{t} = \mathbf{a}_\mathbf{t}. \tag{4.6}$$

for all $\mathbf{t} \in T$.

Example 4.1.3. *Consider the Gaussian atom defined in Example 4.1.2. For* $\mathbf{x} \in \mathscr{M}$*, then* $\mathbf{A}\mathbf{x} \in L^2(\mathbb{R}^d)$ *is a squared integrable function defined as:*

$$(\mathbf{A}\mathbf{x})(\boldsymbol{\theta}) = \int_{\mathbf{t}\in T} \exp\Big(-\gamma \left\|\boldsymbol{\theta} - \mathbf{t}\right\|_2^2\Big)\mathbf{x}(\mathrm{d}\mathbf{t}),$$

for all $\boldsymbol{\theta} \in \mathbb{R}^d$.

Notice from above discussion, $\mathbf{A}^*$ is continuous from $(\mathscr{H}, \tau_{\mathscr{H}})$ to $(\mathscr{C}, \tau_{\mathscr{C}})$ since it is a bounded linear operator. Additionally, $\mathbf{A}^*$ is also compact as observed in [29, Proof of Theorem 6]. Therefore, $\mathbf{A}$ and $\mathbf{A}^*$ admit several continuity and compactness properties, which are summarized in the following theorem. We also provide a proof for the sake of completeness.

Theorem 4.1.4. *We have the following properties of* $\mathbf{A}$ *and* $\mathbf{A}^*$*:*

1. $\mathbf{A}$ *is compact, continuous and weakly* continuous.*
2. $\mathbf{A}^*$ *is compact, continuous and weakly continuous.*

Proof. Recall that, $\mathbf{A}$ is the adjoint of $\mathbf{A}^*$.We have some basic properties of adjoint operators:

— If $\mathbf{A}^*$ is weakly continuous, then $\mathbf{A}$ is weakly* continuous [69, Theorem 8.10.5].

— If $\mathbf{A}^*$ is weakly continuous if and only if it is continuous [69, Corollary 8.11.4].

— If $\mathbf{A}^*$ is continuous, then $\mathbf{A}$ is also continuous [69, Theorem 8.11.5]

— If $\mathbf{A}^*$ is compact, then $\mathbf{A}$ is also compact [31, Theorem 2].

Recall that $\mathbf{A}^*$ is continuous. Therefore, in the remaining, we only focus on showing that $\mathbf{A}^* : \mathscr{H} \to \mathscr{C}$ is compact, *i.e.*, for any bounded set $G \subset \mathscr{H}$, its image $\mathbf{A}^*G \triangleq \{\mathbf{A}^*\mathbf{u} \mid \mathbf{u} \in G\} \subset \mathscr{C}$ is totally bounded. By Arzelà-Ascoli theorem [31, Theorem 7 page 266], this can be done by showing that $\mathbf{A}^*G$ is a family of pointwise bounded and equicontinuous functions.

Step 1. We first show that $\mathbf{A}^*G$ is pointwise bounded. To this end, we need to prove that, for any fixed $\mathbf{t} \in T$ we have $\sup_{\varphi\in\mathbf{A}^*G} |\varphi(\mathbf{t})| < +\infty$. For any $\varphi \in \mathbf{A}^*G$, there exists some $\mathbf{u} \in G$ so that $\varphi = \mathbf{A}^*\mathbf{u}$. From the boundedness of G, there exists a finite positive number M_G such that $\|\mathbf{u}\|_{\mathscr{H}} \leq M_G$ for all $\mathbf{u} \in G$. Therefore, we have

$$|\varphi(\mathbf{t})| = |(\mathbf{A}^*\mathbf{u})(\mathbf{t})| = |\langle \mathbf{u}, \mathbf{a}_\mathbf{t}\rangle| \leq \|\mathbf{u}\|_{\mathscr{H}} \|\mathbf{a}_\mathbf{t}\|_{\mathscr{H}} \leq M_G M < +\infty,$$

where the second inequality follows from the fact that the atoms $\mathbf{a_t}$ is bounded by M due to (A2). Hence, the family of functions in $\mathbf{A}^*G$ is pointwise bounded.

Step 2. We next prove that the family of functions $\mathbf{A}^*G \subset \mathscr{C}$ is equicontinuous at any fixed $\mathbf{t} \in T$, *i.e.*, for every $\varepsilon > 0$, there exists $\Delta > 0$ such that if for any $\mathbf{t}' \in T$ verifying $\|\mathbf{t} - \mathbf{t}'\| < \Delta$, then we have $|\varphi(\mathbf{t}) - \varphi(\mathbf{t}')| < \varepsilon$ for all $\varphi \in \mathbf{A}^*G$. Since $\varphi \in \mathbf{A}^*G$, there exists $\mathbf{u} \in G$ such that $\varphi = \mathbf{A}^*\mathbf{u}$. Notice that $\mathbf{a}$ is L-Lipschitz continuous by (A1) and G is bounded by some $M_G > 0$, thus

$$\begin{aligned} |\varphi(\mathbf{t}) - \varphi(\mathbf{t}')| &= |\mathbf{A}^*\mathbf{u}(\mathbf{t}) - \mathbf{A}^*\mathbf{u}(\mathbf{t}')| \\ &= |\langle \mathbf{u}, \mathbf{a_t} - \mathbf{a_{t'}} \rangle| \\ &\leq \|\mathbf{u}\|_{\mathscr{H}} \|\mathbf{a_t} - \mathbf{a_{t'}}\|_{\mathscr{H}} \\ &\leq \|\mathbf{u}\|_{\mathscr{H}} L \|\mathbf{t} - \mathbf{t}'\| \\ &< L M_G \Delta. \end{aligned}$$

One then completes the proof by choosing $\Delta = \dfrac{\varepsilon}{L M_G}$.

□

Remark 4.1.5 (Another construction scheme of $\mathbf{A}$ and $\mathbf{A}^*$)**.** *In brief, the so-called "dictionary operator" $\mathbf{A}$ is defined as the adjoint of some test operator, denoted as $\mathbf{A}^*$. Another perspective, as seen in some contributions (e.g., [13]), abstractly assumes the existence of the dictionary operator $\mathbf{A}$ as a weakly* continuous linear operator and then defines $\mathbf{A}^*$ as the pre-adjoint of $\mathbf{A}$. Note that the existence of such a pre-adjoint is guaranteed due to the weak* continuity of $\mathbf{A}$ [94, Theorem 6].*

4.1.3 TV-norm penalization problem

Let Ψ be a closed subset of compact set $T \subset \mathbb{R}^d$.[3] In this section, we denote by $\mathscr{M}(\Psi, \mathbb{R})$ the space of signed Radon measures with support on Ψ. Here, notice that $\mathscr{M}(\Psi, \mathbb{R}) \subset \mathscr{M}(T, \mathbb{R})$, thus the TV-norm $\|\cdot\|_{TV}$ defined on $\mathscr{M}(T, \mathbb{R})$ is still well-defined on $\mathscr{M}(\Psi, \mathbb{R})$. This section is concerned with the following TV-norm penalized problem:

$$\min_{\mathbf{x} \in \mathscr{M}(\Psi, \mathbb{R})} \quad f(\mathbf{A}\mathbf{x}) + \lambda \|\mathbf{x}\|_{TV}, \tag{4.7-p_Ψ}$$

3. Therefore, Ψ is also compact.

where $f : \mathscr{H} \to \mathbb{R} \cup \{+\infty\}$ is a closed proper convex, lower bounded and α^{-1}-strongly smooth [4] function for some $\alpha > 0$, $\mathbf{A}$ is a dictionary operator and $\lambda > 0$.

An intriguing aspect of solving (4.7-p_Ψ) is its capacity to yield sparse solutions. Under specific conditions, as outlined in, for instance, [32, Theorem 2] or [12, Section 4.2.3], there exists an n-sparse optimal solution $\mathbf{x}^\star$ for (4.7-p_Ψ) *i.e.*,

$$\mathbf{x}^\star = \sum_{i=1}^{n} w_i \delta_{\mathbf{t}_i}$$

for some $(w_i, \mathbf{t}_i) \in \mathbb{R} \times T$, $i = 1, \dots, n$.

Note that if one can identify the support of $\mathbf{x}^\star$, say $\Theta = \{\mathbf{t}_i : i = 1, \dots, n\}$, then the weight vector $\mathbf{w} = (w_1, \dots, w_n)$ can be recovered by solving the following finite-dimensional problem:

$$\min_{\mathbf{w} \in \mathbb{R}^n} \quad f(\mathbf{A}_\Theta \mathbf{w}) + \lambda \left\| \mathbf{w} \right\|_1 ,$$

where $\mathbf{A}_\Theta \triangleq [\mathbf{a}_{\mathbf{t}_1}, \dots, \mathbf{a}_{\mathbf{t}_n}]$. Therefore, in order to solve (4.7-p_Ψ) a vast number of solving methods aim at finding Θ, *i.e.*, the support of $\mathbf{x}^\star$.

Below, we present the Fenchel-Rockafellar pre-dual problem associated with (4.7-p_Ψ), along with its optimality conditions. These conditions are essential in the derivation of the safe screening rules detailed in Section 4.2.

Here, the Fenchel-Rockafellar pre-dual problem of (4.7-p_Ψ) is given by

$$\begin{aligned} \max_{\mathbf{u} \in \mathscr{H}} \quad & - f^*(-\mathbf{u}) \\ \text{s.t.} \quad & \mathbf{u} \in U_\Psi , \end{aligned} \tag{4.8-d_Ψ}$$

where

$$U_\Psi = \{\mathbf{u} \in \mathscr{H} : |\langle \mathbf{a}_\mathbf{t}, \mathbf{u} \rangle| \leq \lambda, \forall \mathbf{t} \in \Psi\}. \tag{4.9}$$

From hereafter, a pair $(\mathbf{x}, \mathbf{u}) \in \mathscr{M}(T, \mathbb{R}) \times \mathscr{H}$ is said to be *feasible w.r.t.* $\Psi \subset T$ if

$$\operatorname{supp}(\mathbf{x}) \subset \Psi \tag{4.10a}$$

$$|\langle \mathbf{u}, \mathbf{a}_\mathbf{t} \rangle| \leq \lambda, \forall \mathbf{t} \in \Psi. \tag{4.10b}$$

It is essential to note that the Lipschitz continuity of ∇f implies that the minimum and maximum values in (4.7-p_Ψ) and (4.8-d_Ψ), respectively, can be achieved and the strong

4. See Appendix B.1 for precised definition.

duality holds between the problems, see Proposition B.2.5. Let $\mathbf{x}^\star$ be a minimizer of the primal problem (4.7-p_Ψ) and $\mathbf{u}^\star$ be a maximizer for the pre-dual problem (4.8-d_Ψ). Since ∇f is assumed to be α^{-1}-Lipschitz continuous, f^* is strongly convex. Therefore, the pre-dual problem (4.8-d_Ψ) is strongly concave, thus, implies the existence and uniqueness of $\mathbf{u}^\star$ [100, Proposition 3.5.8]. By Proposition B.2.5, the optimal pair $(\mathbf{x}, \mathbf{u})$ should verify the following optimality conditions.

Theorem 4.1.6. *The pair $(\mathbf{x}^\star, \mathbf{u}^\star) \in \mathscr{M}(T, \mathbb{R}) \times \mathscr{H}$ is an optimal pair w.r.t. (4.7-p_Ψ) and (4.8-d_Ψ) if and only if it verifies the following optimality conditions:*

$$\operatorname{supp}(\mathbf{x}^\star) \subset \Psi \tag{4.11a}$$

$$\mathbf{u}^\star = -\nabla f(\mathbf{A}\mathbf{x}^\star) \tag{4.11b}$$

$$\langle \mathbf{A}\mathbf{x}^\star, \mathbf{u}^\star \rangle = \lambda \|\mathbf{x}^\star\|_{TV} \tag{4.11c}$$

$$\max_{\mathbf{t} \in \Psi} |\langle \mathbf{a}_\mathbf{t}, \mathbf{u}^\star \rangle| = \lambda, \tag{4.11d}$$

4.1.4 Solving algorithms

In recent years, there has been active researches focused on developing new efficient solving methods to address (4.7-p_Ψ). We invite the reader to refer to [11, 29, 64] for some discussions on such algorithmic approaches. In the following, we briefly review some of them.

Grid based methods. One of the simplest approaches for solving (4.7-p_Ψ) is to discretize the parameter set using a *regular grid*. In this discretization approach, (4.7-p_Ψ) can be rewritten as an ℓ_1-norm penalization problem (2.1). Advanced algorithms like FISTA [7], Chambolle-Pock [16], and smoothing-parameterization [78] can efficiently solve this finite-dimensional approximation problem.

However, a notable drawback of this approach is the necessity of choosing a fine grid with an extremely small step size to accurately capture the positions of optimal Dirac masses. In sparse spike deconvolution problems using Beurling LASSO, theoretical analysis has shown that regular grid based methods can only recover Dirac masses around the true optimal ones [32], and the number of spikes recovered is approximately twice the number of spikes in the initial measure [33, 34].

Recently, a variant of the grid based approach has been proposed in [48] called *Refinement Grid Based* method. Unlike using a fixed regular grid, this approach uses a grid

partition that is iteratively refined. The approach can significantly enhance the estimation of the locations of optimal Dirac masses compared to using fixed grid. However, in practice, this refinement can lead to an excessively large grid size, resulting in subproblems with extremely high dimensions after each iteration.

Gradient methods. Note that the problem (4.7-p_Ψ) is an optimization problem defined on the space of Radon measures, which is non-Hilbertian. This characteristic restricts the application of many standard gradient-based methods.

The *Frank-Wolfe* algorithm [60], also known as the conditional gradient method, is an approach that doesn't rely on the Hilbertian structure of the space. This method when particularized to TV-norm penalized problems involves adding one Dirac mass in each iteration and then optimizing their masses and locations. The first version of this method was proposed in [13]. Various variants have been developed since then; for example, the masses and locations of Dirac masses can be updated alternatively [11] or simultaneously [30]. The theoretical guarantees ensure that the convergent rate of the Frank-Wolfe method is sublinear [60, Theorem 1]. In [29, Theorem 6], the author demonstrates that, under certain conditions, the (Sliding) Frank-Wolfe method converges after a finite number of steps.

A more recent approach for solving (4.7-p_Ψ) is to perform simple gradient descent within an over-parameterized setup. Specifically, a substantial number of Dirac masses are initialized, and then a straightforward gradient descent is applied to optimize both their masses and locations. Intriguingly, under specific conditions, this approach converges to the globally optimal solutions despite the non-convexity of the discretized problem [21, 20].

Alternative Methods. We mention in the following some other methods that can be used to directly tackle (4.7-p_Ψ) or its variants.

In the history of solving (4.7-p_Ψ), a significant advancement was made by using *semi-definite programming*. This was particularly effective when the atom was defined as a convolution with ideal low-pass filter [15]. In such cases, the dual problem associated with (4.7-p_Ψ) can be interpreted as a semi-definite programming problem with can be solved efficiently. Notably, this approach is among the first methods that eliminate the dependency on grid discretization, a traditional method of solving (4.7-p_Ψ).

Flinth *et al.* [47] note that the dual problem of (4.7-p_Ψ), with its infinite constraints, can be viewed as a *semi-infinite programming*, thus, can be solved using the *exchange*

methods. They also investigate the method that combines the exchange method with gradient descent to enhance efficiency. Furthermore, their study provides a detailed convergence analysis for the proposed methods [47, Theorem 3].

Orthogonal Matching Pursuit (OMP) is an approach that addresss the sparse structure appeared in the optimal solutions of (4.7-p_Ψ) rather than directly solving it. The theoretical results, exemplified in [37, 38], demonstrate the efficacy of OMP in precisely identifying atom parameters within a finite number steps.

Note that there is also a research direction that approximates the dictionary using low dimensional spaces and apply, *e.g.*, OMP, to tackle the transformed problem in the low dimensional space, see [35, 62, 17, 36].

Another recent approach proposed in [90, 8] addresses sparse representation of measures where the optimal Dirac masses must be suitably separated. The authors exploited the *projected gradient descent* method to enforce this separation constraint. Additionally, the projection can also be heuristically implemented by merging Dirac masses that are sufficiently close to each other.

4.2 Safe screening rules on the space of measures

This section introduces two safe screening rules for the TV-norm penalized problem (4.7-p_Ψ) including a basic and a relaxed rule. Let $(\mathbf{x}^\star, \mathbf{u}^\star)$ be an optimal pair *w.r.t.* (4.7-p_Ψ) and (4.8-d_Ψ) where $\Psi = T$.

The basic safe screening rule reads as follows:

Theorem 4.2.1 (Safe screening rule for signed Radon measures)**.** *For $\mathbf{t} \in T$, we have*

$$|\langle \mathbf{a}_\mathbf{t}, \mathbf{u}^\star \rangle| < \lambda \Longrightarrow \mathbf{t} \notin \operatorname{supp}(\mathbf{x}^\star). \tag{4.12-SS-SRM}$$

Proof. Rewrite the two optimality conditions (4.11c) and (4.11d) for $\Psi = T$, we obtain

$$\int_{\mathbf{t}\in T} \langle \mathbf{a}_\mathbf{t}, \mathbf{u}^\star \rangle \mathbf{x}^\star(\mathrm{d}\mathbf{t}) = \lambda \, |\mathbf{x}^\star| \, (T). \tag{4.13a}$$

$$\max_{\mathbf{t}\in T} |\langle \mathbf{a}_\mathbf{t}, \mathbf{u}^\star \rangle| = \lambda, \tag{4.13b}$$

We prove the theorem by contradiction. Assuming that there exists some $\mathbf{t}_0 \in \operatorname{supp}(\mathbf{x}^\star)$ satisfying $|\langle \mathbf{a}_{\mathbf{t}_0}, \mathbf{u}^\star \rangle| < \lambda$. Since $\mathbf{t} \longmapsto |\langle \mathbf{a}_\mathbf{t}, \mathbf{u}^\star \rangle|$ is continuous, there exists $\varepsilon > 0$ and an open neighborhood Θ of $\mathbf{t}_0$ such that $|\langle \mathbf{a}_\mathbf{t}, \mathbf{u}^\star \rangle| < \lambda - \varepsilon$ for all $\mathbf{t} \in \Theta$. Furthermore, the fact

that $\mathbf{t}_0 \in \operatorname{supp}(\mathbf{x}^\star)$ yields $|\mathbf{x}^\star|(\Theta) > 0$ due to the definition of support of measure (4.3). Combining these two observations together with (4.13b), we can see that

$$\begin{aligned}
\int_{\mathbf{t}\in T} \langle \mathbf{a}_\mathbf{t}, \mathbf{u}^\star \rangle \mathbf{x}^\star(\mathrm{d}\mathbf{t}) &\leq \int_{\mathbf{t}\in T} |\langle \mathbf{a}_\mathbf{t}, \mathbf{u}^\star \rangle| \, |\mathbf{x}^\star| \, (\mathrm{d}\mathbf{t}) \\
&= \int_{\mathbf{t}\in \Theta} |\langle \mathbf{a}_\mathbf{t}, \mathbf{u}^\star \rangle| \, |\mathbf{x}^\star| \, (\mathrm{d}\mathbf{t}) + \int_{\mathbf{t}\in T\setminus\Theta} |\langle \mathbf{a}_\mathbf{t}, \mathbf{u}^\star \rangle| \, |\mathbf{x}^\star| \, (\mathrm{d}\mathbf{t}) \\
&< (\lambda - \varepsilon) \, |\mathbf{x}^\star| \, (\Theta) + \lambda \, |\mathbf{x}^\star| \, (T \setminus \Theta) \\
&= \lambda \, |\mathbf{x}^\star| \, (T) - \varepsilon \, |\mathbf{x}^\star| \, (\Theta) \\
&< \lambda \, |\mathbf{x}^\star| \, (T).
\end{aligned}$$

The obtained strict inequality is in contradiction with (4.13a), we therefore finish the proof.

□

The basic safe screening (4.12-SS-SRM) has two practical limitations. First, it lacks precise knowledge of $\mathbf{u}^\star$. This issue can nevertheless be addressed using the concept of safe region, see Definition 2.2.1. Second, screening a single parameter $\mathbf{t}$ at a time is inefficient given the infinitely uncountable number of elements in T. To overcome this issue, we employ the so-called *joint safe screening rule* proposed in [58], which eliminates a region of parameters rather than a single one.

Theorem 4.2.2 (Joint safe screening rule for signed Radon measures)**.** *Let $\Theta \subset T$ and S be a safe region, i.e., $\mathbf{u}^\star \in S$, we have*

$$\sup_{\mathbf{t}\in\Theta, \mathbf{u}\in S} |\langle \mathbf{a}_\mathbf{t}, \mathbf{u} \rangle| < \lambda \Longrightarrow \Theta \cap \operatorname{supp}(\mathbf{x}^\star) = \emptyset. \tag{4.14-JSS-SRM}$$

In particular, if Θ and S are ball regions, i.e., $\Theta = B(\mathbf{t}_0, r_0)$ for some $(\mathbf{t}_0, r_0) \in T \times \mathbb{R}_+$ and $S = B(\mathbf{c}, r)$ for some $(\mathbf{c}, r) \in \mathscr{H} \times \mathbb{R}_+$, then

$$|\langle \mathbf{a}_{\mathbf{t}_0}, \mathbf{c} \rangle| + r_0 L \, \|\mathbf{c}\|_\mathscr{H} + rM < \lambda \Longrightarrow \Theta \cap \operatorname{supp}(\mathbf{x}^\star) = \emptyset, \tag{4.15}$$

where the constants L and M associated with the atom function $\mathbf{a}\colon T \to \mathscr{H}$ are defined in Definition 4.1.1, respectively.

Proof. Notice that (4.14-JSS-SRM) is a direct consequence of (4.12-SS-SRM). We now

prove (4.15). Notice from (A2) that $\mathbf{a}$ is bounded by M, then

$$|\langle \mathbf{a_t}, \mathbf{u} \rangle| \leq |\langle \mathbf{a_t}, \mathbf{c} \rangle| + |\langle \mathbf{a_t}, \mathbf{u} - \mathbf{c} \rangle| \leq |\langle \mathbf{a_t}, \mathbf{c} \rangle| + rM. \tag{4.16}$$

Also notice that the L-Lipschitz continuity of $\mathbf{a}$ implies:

$$|\langle \mathbf{a_t}, \mathbf{c} \rangle| \leq |\langle \mathbf{a_{t_0}}, \mathbf{c} \rangle| + |\langle \mathbf{a_t} - \mathbf{a_{t_0}}, \mathbf{c} \rangle| \leq |\langle \mathbf{a_{t_0}}, \mathbf{c} \rangle| + Lr_0 \|\mathbf{c}\|_{\mathscr{H}}. \tag{4.17}$$

Combining (4.16), (4.17) and (4.14-JSS-SRM), we deduce (4.15). □

4.3 Improving RGB method with joint safe screening

In this section, we study the application of the joint safe screening method proposed in Theorem 4.2.2 in reducing the complexity of a recent method called *Refinement Grid Based method (RGB)* [48, Algorithm 2] for solving problem (4.7-p_Ψ).

In the following, we begin by revisiting the fundamentals of the RGB method in Section 4.3.1. Next, we introduce an enhancement of RGB method, called *RGBJSS*, by incorporating (4.14-JSS-SRM) into the RGB method, see Algorithm 1. We then establish the consistency between RGB and RGBJSS in Theorem 4.3.2. This consistency ensures that implementing the JSS into RGB does not alter the iterative solutions obtained using RGB. In essence, RGBJSS method does not affect the convergence of RGB while reducing the dimension of sub-problems solved during the iterations of the RGB method.

4.3.1 A reminder of Refinement Grid Based (RGB) method

We first describe the basics of the RGB method [48, Algorithm 2]. The main idea of the RGB method is to solve discretized versions of (4.7-p_Ψ) over a sequence of increasingly finer grids that approximate T. More specifically, the finite grid in iteration k ($k \geq 1$) is constructed by refining the grid used in iteration $k-1$.

More formally, let $W^{(k)}$ be a partition of T at iteration $k \geq 0$. We refer to each element of $W^{(k)}$ as a *cell*, which can be a segment in 1D, a square in 2D and a cube in 3D. We call $W^{(k)}$ the set of *working cells*. In RGB method, we update $W^{(k)}$ by selecting a set of *candidate cells* denoted by $C^{(k)}$ and split them into smaller pieces:

$$W^{(k+1)} = \left(W^{(k)} \setminus C^{(k)}\right) \cup \left(\cup \operatorname{split} C^{(k)}\right). \tag{4.18}$$

Here, the "split" operator denotes the process of splitting the cells in $C^{(k)}$ into smaller ones. It is noteworthy that not every cell in $C^{(k)}$ needs to undergo this splitting; only a fraction of them do to prevent unnecessary complexity. [5] It is crucial to emphasize that the splitting operator must adhere to the following "conservation" rule:

$$\cup \operatorname{split} C^{(k)} = \cup C^{(k)}. \tag{4.19}$$

This compels the cells, both before and after the splitting process, still collectively cover the same region.

In the following, we will explain how to identify the candidate cells of $C^{(k)}$.

Given a set of working cells $W^{(k)}$, instead of solving (4.7-p_Ψ) over the whole parameter set T at iteration k, one solves a modified version of the problem restricted to the vertices of cells in $W^{(k)}$ denoted by $\operatorname{vert} W^{(k)}$:

$$\operatorname{vert} W^{(k)} \triangleq \bigcup_{\Theta \in W^{(k)}} \text{vertices of } \Theta. \tag{4.20}$$

Let $\left(\mathbf{x}^{(k)}, \mathbf{u}^{(k)}\right)$ be an optimal pair *w.r.t.* (4.7-p_Ψ)-(4.8-d_Ψ) where $\Psi = \operatorname{vert} W^{(k)}$. They satisfy the optimality conditions (4.11b), (4.11c) and (4.11d) *w.r.t.* $\operatorname{vert} W^{(k)}$, *i.e.*,

$$\mathbf{u}^{(k)} = -\nabla f(\mathbf{A}\mathbf{x}^{(k)}) \tag{4.21a}$$

$$\left\langle \mathbf{A}\mathbf{x}^{(k)}, \mathbf{u}^{(k)} \right\rangle = \lambda \left\| \mathbf{x}^{(k)} \right\|_{TV} \tag{4.21b}$$

$$\left| \left\langle \mathbf{a}_\mathbf{t}, \mathbf{u}^{(k)} \right\rangle \right| \leq \lambda, \ \forall \mathbf{t} \in \operatorname{vert} W^{(k)} \tag{4.21c}$$

If, in (4.21c), we have "$\forall \mathbf{t} \in T$" instead of "$\forall \mathbf{t} \in \operatorname{vert} W^{(k)}$", then $\left(\mathbf{x}^{(k)}, \mathbf{u}^{(k)}\right)$ is a primal-dual solution for (4.7-p_Ψ)-(4.8-d_Ψ) with $\Psi = T$ and we can stop the algorithm. Otherwise, there must exist some parameter $\mathbf{t} \in T \setminus \operatorname{vert} W^{(k)}$ that violates the optimality condition (4.11d), *i.e.*, $\left| \left\langle \mathbf{a}_\mathbf{t}, \mathbf{u}^{(k)} \right\rangle \right| > \lambda$. This suggests that we should identify the cells Θ for which the optimality condition is violated and subdivide them to obtain a finer approximation for T. This guides the choice of $C^{(k)}$:

$$C^{(k)} \triangleq \{\Theta \in W^{(k)} : \sup_{\mathbf{t} \in \Theta} \left| \left\langle \mathbf{a}_\mathbf{t}, \mathbf{u}^{(k)} \right\rangle \right| > \lambda\}.$$

5. In practice, instead of splitting all cells in $C^{(k)}$, we only take into account the cells with largest radius to reduce the grid size in the next iteration.

Details of RGB method is described in Algorithm 1 (excluding the screening steps 7).

In [48, Theorem 7], under certain conditions, the authors provide a detailed analysis for the convergence rate of RGB method. Furthermore, the growth of $\operatorname{vert} W^{(k)}$ can be theoretically controlled.

However, it is important to note that the cardinality of $\operatorname{vert} W^{(k)}$ is a crucial complexity bottleneck of the RGB method in practical implementation even when T is of very low dimension (dimension 1 or 2). In the next section, we propose a new variant of the RGB method that combines with joint safe screening to achieve a potentially significant reduction in the number of vertices in $W^{(k)}$.

4.3.2 The proposed solving method

This section shows how to integrate the joint safe screening method into the RGB method to accelerate the resolution process for solving the TV-norm penalized problem (4.7-p_Ψ) for $\Psi = T$. We refer to the resulting method as the *Refinement Grid Based method with Joint Safe Screening (RGBJSS)*, see Algorithm 1.

Note that in the RGBJSS method, we introduce the boolean variable `ScrOpt`, which is set to true if joint safe screening is performed and false otherwise.

The difference between the RGBJSS method and the RGB method lies in how $W^{(k)}$ is updated (see step 7 and 9 of Algorithm 1). In the RGB method, we update $W^{(k)}$ (step 9) by only splitting the cells in $C^{(k)}$ as shown in (4.18). However, in the RGBJSS method, in addition to splitting the candidate cells in $C^{(k)}$, we also eliminate some cells that pass the joint safe screening test (4.14-JSS-SRM), denoted by $D^{(k)}$. We call the elements in $D^{(k)}$ the *deleted cells*. To construct $D^{(k)}$ using JSS, one uses the parameters including safe region $S^{(k)}$ (4.23), a dual (feasible) point $\mathbf{p}^{(k)}$ (4.24), and a scaling factor $\lambda^{(k)}$ (4.25).

Remark 4.3.1. *In RGBJSS Algorithm 1, one needs to find $C^{(k)}, D^{(k)}$ and $\lambda^{(k)}$. These tasks essentially involve the evaluation of $\sup_{\mathbf{t}\in\Theta} |\langle \mathbf{a}_\mathbf{t}, \mathbf{u}\rangle|$. However, in practice, obtaining the exact value of this supremum is challenging. As a substitute, we can use relaxations for it. For each Θ, we can determine the* balls *Θ_1 and Θ_2 such that $\Theta_1 \subset \Theta \subset \Theta_2$. In this way, the supremum involving Θ can be replaced by the supremum over the suitable ball Θ_1*

Algorithm 1 Refinement Grid Based with Joint Safe Screening (RGBJSS)

Setup:
- working cells $W^{(0)}$ a cover of T, *i.e.*, $\cup W^{(0)} = T$
- candidate cells $C^{(0)}$
- deleted cells $D^{(0)}$
- screening option `ScrOpt` (boolean)

for $k = 0, ..., +\infty$ **do**
  Determine an optimal pair $\left(\mathbf{x}^{(k)}, \mathbf{u}^{(k)}\right)$ of (4.7-p_Ψ)-(4.8-d_Ψ) with $\Psi = \operatorname{vert} W^{(k)}$
  If $\sup_{\mathbf{t}\in T} \left|\left\langle \mathbf{a_t}, \mathbf{u}^{(k)} \right\rangle\right| \leq \lambda$ then $\left(\mathbf{x}^{(k)}, \mathbf{u}^{(k)}\right)$ is optimal. We stop the algorithm
  Find candidate cells $C^{(k)} = \{\Theta \in W^{(k)} : \sup_{\mathbf{t}\in\Theta} \left|\left\langle \mathbf{a_t}, \mathbf{u}^{(k)} \right\rangle\right| > \lambda\}$ which contain parameters violating the stopping condition
  if `ScrOpt` is true **then**
    Update $W^{(k+1)} = \left(W^{(k)} \setminus \left(C^{(k)} \cup D^{(k)}\right)\right) \cup \left(\cup \operatorname{split} C^{(k)}\right)$ where

$$D^{(k)} = \{\Theta \in W^{(k)} : \sup_{(\mathbf{t},\mathbf{u})\in\Theta\times S^{(k)}} |\langle \mathbf{a_t}, \mathbf{u}\rangle| < \lambda\} \tag{4.22}$$

$$S^{(k)} = S(\mathbf{x}^{(k)}, \mathbf{p}^{(k)}) \tag{4.23}$$

$$\mathbf{p}^{(k)} = \frac{\lambda}{\lambda^{(k)}} \mathbf{u}^{(k)} \tag{4.24}$$

$$\lambda^{(k)} = \max_{\Theta\in C^{(k)}} \sup_{\mathbf{t}\in\Theta} \left|\left\langle \mathbf{a_t}, \mathbf{u}^{(k)} \right\rangle\right| \tag{4.25}$$

  else
    Update $W^{(k+1)} = \left(W^{(k)} \setminus C^{(k)}\right) \cup \left(\cup \operatorname{split} C^{(k)}\right)$
  end if
end for
return $\left(\mathbf{x}^{(k)}, \mathbf{u}^{(k)}\right)$

or Θ_2. *Specifically, the practical implementation is*

$$\begin{aligned}
C^{(k)} &= \{\Theta \in W^{(k)} : \sup_{\mathbf{t}\in\Theta_1} \left|\left\langle \mathbf{a_t}, \mathbf{u}^{(k)} \right\rangle\right| > \lambda\},\\
D^{(k)} &= \{\Theta \in W^{(k)} : \sup_{(\mathbf{t},\mathbf{u})\in\Theta_2\times S^{(k)}} |\langle \mathbf{a_t}, \mathbf{u}\rangle| < \lambda\},\\
\lambda^{(k)} &= \max_{\Theta\in C^{(k)}} \sup_{\mathbf{t}\in\Theta_2} \left|\left\langle \mathbf{a_t}, \mathbf{u}^{(k)} \right\rangle\right|.
\end{aligned}$$

In this case, our analysis of RGBJSS discussed in the next section still applies.

4.3.3 Consistence guarantee

Let us denote the quantities obtained during the iterations of Algorithm 1 as follows:

$$\begin{aligned}&\left(\mathbf{x}_0^{(k)}, \mathbf{u}_0^{(k)}, C_0^{(k)}, W_0^{(k)}\right)_{k\geq 0}, \text{ if } \texttt{ScrOpt} \text{ is false,}\\ &\left(\mathbf{x}_1^{(k)}, \mathbf{u}_1^{(k)}, C_1^{(k)}, W_1^{(k)}\right)_{k\geq 0}, \text{ otherwise.}\end{aligned}$$

As emphasized in the previous section, the abundance of vertices in $W^{(k)}$ can pose a challenge, impacting the practical performance of the RGB method. The integration of joint safe screening in RGBJSS overcomes this by eliminating irrelevant cells at each iteration so that $\operatorname{vert} W_1^{(k)} \subset \operatorname{vert} W_0^{(k)}$ (the proper proof is provided in the theorem below). However, this integration raises two essential questions.

The first question is: *Does RGBJSS, in comparison with RGB, increase the number of candidate cells being selected?* For instance, if $C_0^{(k)} \subset C_1^{(k)}$, it means that RGBJSS would introduce a larger number of vertices for the next iteration. This scenario is not desirable.

Fortunately, the answer to this question is "no". In the following, we demonstrate that the candidate cells identified by RGB and RGBJSS are the same, *i.e.*, $C_0^{(k)} = C_1^{(k)}$; in other words, joint safe screening does not affect the candidate cell selection process of RGB method.

The second question is: *Does RGBJSS alter the iterative solutions in comparison to RGB?* If the iterative pairs of solutions change, joint safe screening may affect the convergence analysis of RGB. The phenomenon of altering iterative solutions is common when integrating (joint) safe screening into many solving methods. However, we prove in the following that the RGB and RGBJSS method yield identical iterative solutions, *i.e.*, $\left(\mathbf{x}_0^{(k)}, \mathbf{u}_0^{(k)}\right) = \left(\mathbf{x}_1^{(k)}, \mathbf{u}_1^{(k)}\right)$ for all $k \geq 0$. Therefore, JSS preserves the validity of the convergence analysis already established for the RGB method [48, Theorem 7].

We now consolidate these statements into the following theorem and refer to them as the *consistency* guarantee of applying joint safe screening into RGB method.

Theorem 4.3.2 (Consistency)**.** *Consider RGB and RGBJSS method. For all $k \geq 0$, we have*

$$\left(\mathbf{x}_1^{(k)}, \mathbf{u}_1^{(k)}, C_1^{(k)}\right) = \left(\mathbf{x}_0^{(k)}, \mathbf{u}_0^{(k)}, C_0^{(k)}\right) \tag{4.26}$$

and

$$\operatorname{vert} W_1^{(k)} \subset \operatorname{vert} W_0^{(k)}. \tag{4.27}$$

In the remaining of this section, we focus on the (quite technical) proof of Theo-

rem 4.3.2. In the subsequent analysis, we use the following notations for the data in the screening step of Algorithm 1:

$$\begin{aligned}&\left(D_0^{(k)}, S_0^{(k)}, \mathbf{p}_0^{(k)}, \lambda_0^{(k)}\right)_{k\geq 0}, \text{ if } \texttt{ScrOpt} \text{ is false,}\\ &\left(D_1^{(k)}, S_1^{(k)}, \mathbf{p}_1^{(k)}, \lambda_1^{(k)}\right)_{k\geq 0}, \text{ otherwise.}\end{aligned}$$

Here, it is worth noting that the data with subscript 1 is formally defined when JSS is applied (with `ScrOpt` is true). However, the data with subscript 0 is loosely defined since we do not need it if JSS is not applied. However, its definition aligns analogously with the one employed when JSS is applied.

We now prove the following technical lemma.

Lemma 4.3.3. *We have:*

1. *The set of working cells $W_0^{(i)}$ is a cover of T, i.e., $\cup W_0^{(i)} = T$ for all $i \geq 0$.*
2. *The primal-dual pair $\left(\mathbf{x}_0^{(i)}, \mathbf{p}_0^{(i)}\right)$ is feasible w.r.t. $\operatorname{vert} W_0^{(k)}$ for all $k \geq i \geq 0$.*
3. *The primal-dual pair $\left(\mathbf{x}_1^{(i)}, \mathbf{p}_1^{(i)}\right)$ is feasible w.r.t. $\operatorname{vert} W_1^{(i)}$ for all $i \geq 0$.*
4. *The candidate cells will not be screened, i.e., $C_1^{(i)} \cap D_1^{(i)} = \emptyset$, for all $i \geq 0$.*

Proof of Lemma 4.3.3. We now prove the four items.

Item 1. Here, we consider Algorithm 1 without screening. Notice that

$$\cup W_0^{(i)} = \left(\cup W_0^{(i-1)} \setminus \cup C_0^{(i-1)}\right) \cup \left(\cup \operatorname{split} C_0^{(i)}\right) = \cup W_0^{(i-1)}. \tag{4.28}$$

where the last equality follows from the property of splitting operator (4.19). Applying (4.28) recursively and notice that $\cup W_0^{(0)} = T$ by the setup, we conclude that $\cup W_0^{(i)} = T$ for all $i \geq 0$.

Item 2. We still consider Algorithm 1 without screening. We first notice that

$$\operatorname{supp}(\mathbf{x}_0^{(i)}) \subset \operatorname{vert} W_0^{(i)} \subset \operatorname{vert} W_0^{(k)},$$

where the first inclusion follows from the feasibility of $\mathbf{x}_0^{(i)}$ *w.r.t.* $\operatorname{vert} W_0^{(i)}$ and the second inclusion follows from the fact that $W_0^{(i)}$ is finer than $W_0^{(k)}$ for $i \leq k$. We now prove that $\mathbf{p}_0^{(i)}$ is feasible *w.r.t.* $\operatorname{vert} W_0^{(k)}$. First,

$$\max_{\mathbf{t}\in \operatorname{vert} W_0^{(k)}} \left|\left\langle \mathbf{a}_\mathbf{t}, \mathbf{p}_0^{(i)}\right\rangle\right| \leq \max_{\mathbf{t}\in T} \left|\left\langle \mathbf{a}_\mathbf{t}, \mathbf{p}_0^{(i)}\right\rangle\right| = \max_{\Theta\in W_0^{(i)}} \sup_{\mathbf{t}\in\Theta} \left|\left\langle \mathbf{a}_\mathbf{t}, \mathbf{p}_0^{(i)}\right\rangle\right|, \tag{4.29}$$

where the inequality follows from $\operatorname{vert} W_0^{(k)} \subset T$ and the equality holds since $T = \cup W_0^{(i)}$ (see Item 1). We further observe that

$$\max_{\Theta \in W_0^{(i)}} \sup_{\mathbf{t} \in \Theta} \left| \left\langle \mathbf{a_t}, \mathbf{p}_0^{(i)} \right\rangle \right| = \max_{\Theta \in C_0^{(i)}} \sup_{\mathbf{t} \in \Theta} \left| \left\langle \mathbf{a_t}, \frac{\lambda}{\lambda_0^{(i)}} \mathbf{u}_0^{(i)} \right\rangle \right| = \lambda, \tag{4.30}$$

here the first equality is a consequence of the definition of $C_0^{(i)}$ and (4.24); the second equality holds true by applying (4.25). By combining (4.29) and (4.30), we conclude that $\mathbf{p}_0^{(i)}$ is feasible *w.r.t.* $\operatorname{vert} W_0^{(k)}$.

Item 3. Now, we consider the algorithm with screening mode. We first notice that $\mathbf{x}_1^{(i)}$ is feasible *w.r.t.* $W_1^{(i)}$ due to its optimality. On the other hand,

$$\max_{\mathbf{t} \in \operatorname{vert} W_1^{(i)}} \left| \left\langle \mathbf{a_t}, \mathbf{p}_1^{(i)} \right\rangle \right| \leq \max_{\Theta \in W_1^{(i)}} \sup_{\mathbf{t} \in \Theta} \left| \left\langle \mathbf{a_t}, \mathbf{p}_1^{(i)} \right\rangle \right| = \lambda, \tag{4.31}$$

where the first inequality follows from the fact that $\operatorname{vert} W_1^{(i)} \subset \cup W_1^{(i)}$, and the second equality holds by applying similar arguments as in deriving (4.30). Therefore, $\mathbf{p}_1^{(i)}$ is feasible *w.r.t.* $\operatorname{vert} W_1^{(k)}$.

Item 4. Now, we consider the algorithm with screening mode and aim to show that $C_1^{(i)} \cap D_1^{(i)} = \emptyset$. By definition of $C_1^{(i)}$ and $D_1^{(i)}$, we have

$$\max_{\mathbf{t} \in \Theta} \left| \left\langle \mathbf{a_t}, \mathbf{u}_1^{(i)} \right\rangle \right| \geq \lambda \Longleftrightarrow \Theta \in C_1^{(i)}$$

and

$$\max_{(\mathbf{t}, \mathbf{u}) \in \Theta \times S_1^{(i)}} |\langle \mathbf{a_t}, \mathbf{u} \rangle| < \lambda \Longleftrightarrow \Theta \in D_1^{(i)}.$$

To demonstrate that there is no Θ belonging to the intersection of $C_1^{(i)}$ and $D_1^{(i)}$, it suffices to show that $\mathbf{u}_1^{(i)}$ belongs to the safe regions $S_1^{(i)} = S\left(\mathbf{x}_1^{(i)}, \mathbf{p}_1^{(i)}\right)$. Indeed, notice that $S_1^{(i)} = S\left(\mathbf{x}_1^{(i)}, \mathbf{p}_1^{(i)}\right)$ is a safe region with $\left(\mathbf{x}_1^{(i)}, \mathbf{p}_1^{(i)}\right)$ feasible *w.r.t.* $\operatorname{vert} W_1^{(i)}$ (see Item 3), it therefore contains the maximizer $\mathbf{u}_1^{(i)}$ of the dual problem associated with $\operatorname{vert} W_1^{(i)}$. □

We now prove the consistence result presented in Theorem 4.3.2 based on the results obtained from Lemma 4.3.3.

Proof of Theorem 4.3.2. The result holds for $k = 0$. We assume by induction that the result holds for $0, \ldots, k-1$ where $k > 0$.

Step 1. To prove that $\mathbf{x}_0^{(k)} = \mathbf{x}_1^{(k)}$, it is equivalent to show that they are equal on $\operatorname{vert} W_1^{(k)}$ and zero elsewhere. It is therefore sufficient to verify that

$$\operatorname{supp}\left(\mathbf{x}_0^{(k)}\right) \subset \operatorname{vert} W_1^{(k)}. \tag{4.32}$$

By exploiting the empty intersection of the set of candidate and deleted cells in Item 4 of Lemma 4.3.3, and the fact that $\cup C_1^{(i)} = \cup \operatorname{split} C_1^{(i)}$, one derives

$$\cup W_1^{(i)} = \left(\cup W_1^{(i-1)} \setminus \left(\cup C_1^{(i-1)} \cup D_1^{(i-1)}\right)\right) \cup \operatorname{split} C_1^{(i)} = \cup W_1^{(i-1)} \setminus \cup D_1^{(i-1)}, \tag{4.33}$$

Applying (4.33) recursively for $i = k, k-1, ..., 1$, we obtain

$$\cup W_1^{(k)} = \cup W_1^{(k-1)} \setminus \cup D_1^{(k-1)} = \cdots = T \setminus \cup\left(D_1^{(k-1)} \cup \cdots \cup D_1^{(0)}\right). \tag{4.34}$$

From the view of (4.34), one can prove (4.32) by showing that

$$\left(\cup D_1^{(i)}\right) \cap \operatorname{supp}\left(\mathbf{x}_0^{(k)}\right) = \emptyset, \, \forall i \leq k-1. \tag{4.35}$$

By joint safe screening rule (4.14-JSS-SRM), (4.35) holds if one can show that $\mathbf{u}_0^{(k)} \in S_1^{(i)}$ for all $i \leq k-1$. This inclusion holds by observing that:

$$\mathbf{u}_0^{(k)} \in S\left(\mathbf{x}_0^{(i)}, \mathbf{p}_0^{(i)}\right) = S\left(\mathbf{x}_1^{(i)}, \mathbf{p}_1^{(i)}\right) = S_1^{(i)}. \tag{4.36}$$

Here, the inclusion holds since $S\left(\mathbf{x}_0^{(i)}, \mathbf{p}_0^{(i)}\right)$ is a safe region [6] containing the dual optimal solution $\mathbf{u}_0^{(k)}$ *w.r.t.* $\operatorname{vert} W_0^{(k)}$ for any $i \leq k-1$, the first equality is true according to the induction's assumption, and the last equality follows from (4.23).

Step 2. From the optimality (4.21a), $\mathbf{x}_0^{(k)} = \mathbf{x}_1^{(k)}$ implies $\mathbf{u}_0^{(k)} = \mathbf{u}_1^{(k)}$.

Step 3. Proving $C_0^{(k)} = C_1^{(k)}$ is equivalent to showing that

$$\{\Theta \in W_0^{(k)} : \sup_{\mathbf{t} \in \Theta} \left|\left\langle \mathbf{a}_\mathbf{t}, \mathbf{u}_0^{(k)} \right\rangle\right| > \lambda\} = \{\Theta \in W_1^{(k)} : \sup_{\mathbf{t} \in \Theta} \left|\left\langle \mathbf{a}_\mathbf{t}, \mathbf{u}_1^{(k)} \right\rangle\right| > \lambda\}.$$

Since $\mathbf{u}_0^{(k)} = \mathbf{u}_1^{(k)}$, above equality holds if $\sup_{\mathbf{t} \in \Theta} \left|\left\langle \mathbf{a}_\mathbf{t}, \mathbf{u}_0^{(k)} \right\rangle\right| \leq \lambda$ for all $\Theta \in D_1^{(i)}$ and $i \leq k-1$. This is true since $\mathbf{u}_0^{(k)} \in S_1^{(i)}$ as shown in (4.36).

6. Here the safe region is well-defined since $\left(\mathbf{x}_0^{(i)}, \mathbf{p}_0^{(i)}\right)$ is feasible *w.r.t.* $W_0^{(k)}$ due to Item 2 of Lemma 4.3.3.

Step 4. Finally, notice that

$$\begin{aligned}\operatorname{vert} W_1^{(k)} &= \left(W_1^{(k-1)} \setminus \left(C_1^{(k-1)} \cup D_1^{(k-1)}\right)\right) \cup \operatorname{split} C_1^{(k-1)} \\ &\subset \left(W_0^{(k-1)} \setminus C_0^{(k-1)}\right) \cup \operatorname{split} C_0^{(k-1)} \\ &= \operatorname{vert} W_0^{(k)}.\end{aligned}$$

where the inclusion holds since $W_1^{(k-1)} = W_0^{(k-1)}$ due to induction and $C_0^{(k)} = C_1^{(k)}$ due to Step 3. The proof is completed. □

Conclusion

Contributions

This thesis, titled *"Some Contributions on Safe Regions and Safe Screening in Convex Optimization"*, embodies two principal contributions to the domain of convex optimization. The major contributions include the introduction of a novel family of safe regions, termed FBI regions, and an extension of the safe screening methodology from finite-dimensional to infinite-dimensional problems.

The first significant contribution presents a new family of safe regions encompassing *FBI ball, Hölder half-space, FBI dome and geometric ball*. We construct these safe regions in a general framework in which the FBI ball is proven to be safe for general convex penalization functions, while the other regions are safe if the gauge penalization is considered. This framework therefore includes norm penalized optimization problems as specific cases. Furthermore, our framework also provides a unifying perspective, demonstrating that existing safe regions can be viewed as special cases or supersets of the proposed FBI regions. This contribution not only introduces novel safe regions crucial for addressing high-dimensional optimization problems, but also enhances the theoretical understanding of the intricate relationships of existing safe regions introduced over the last decade.

The second major contribution extends the scope of *Joint Safe Screening (JSS)* rules, expanding from being applicable to ℓ_1-norm penalized problems (a finite-dimensional context) to now encompass total variation norm (TV-norm) penalized problems defined in the space of Radon measures (an infinite-dimensional context). Building upon this result, the thesis integrates JSS into the Refinement Grid Based (RGB) method, a recently introduced algorithm tailored for TV-norm problems. By doing so, computational bottlenecks associated with solving high-dimensional subproblems of RGB are significantly reduced. Furthermore, we provide a *consistency guarantee*, affirming that implementing JSS does not alter the iterative solutions compared to using only RGB. This contribution not only underscores but also lays the foundation for the potential of leveraging safe screening to accelerate the resolution of other infinite-dimensional problems in the future.

Perspectives

Note that there are several perspectives for extending the two main contributions of this thesis. In the subsequent discussion, we will highlight two significant potential directions, focusing on key points and omitting technical intricacies.

Extending the application scope of the proposed FBI regions: Recall that our safe regions are tailored for the following broad class of convex optimization problems:

$$\min_{\mathbf{x}\in\mathscr{M}} \quad f(\mathbf{A}\mathbf{x}) + g(\mathbf{x}), \tag{4.37}$$

where f, g are convex functions, $\mathbf{A}$ is a linear operator, and $\mathscr{M}$ is a Banach space. This comprehensive setup allows us to encompass most existing safe regions, as they are constructed to address specific instances of (4.37).

While our contributions pertain to a broad family of optimization problems, it leverages specific assumptions related to f and g. Specifically, we demonstrate that the FBI ball is safe when the conjugate f^* of f exhibits strong convexity on its domain, and the Hölder half-space is safe when g is a gauge function. These insights raise a fundamental question:

Can we weaken or even relax the conditions imposed on f and g?

Recent research have exhibited promising approaches to address this question. In [25], Dantas *et al.* have extended the GAP safe ball framework —similar to the one considered in this thesis— to cases where f^* exhibits only local strong convexity. Additionally, Herzet *et al.* [59] have gone a step further by removing such conditions on f^*, resulting in an innovative approach called *region-free safe screening*, provided g is an ℓ_1-norm. We also emphasize alternative methodologies, akin to safe screening, that have been developed for penalization functions being non-convex (such as the ℓ_0-norm), see *e.g.*, [1, 53, 55].

Exploring the relaxation of these conditions on f and g may significantly broaden the application scope of the safe regions. Delving into this topic presents a promising avenue for future research.

Applying joint safe screening rule for other infinite-dimensional problems and other solvers. The second contribution of this thesis involves the extension of *Joint Safe Screening (JSS) rule* to handling the TV-norm problem:

$$\min_{\mathbf{x}\in\mathscr{M}(T,\mathbb{R})} \quad f(\mathbf{A}\mathbf{x}) + \lambda \|\mathbf{x}\|_{TV}\,, \tag{4.38}$$

where f is convex, $\mathbf{A}$ is linear, $\lambda > 0$, and $\mathscr{M}(T,\mathbb{R})$ is the space of real-valued Radon measures defined on some compact set $T \subset \mathbb{R}^d$. We also demonstrate how JSS can reduce the dimension of subproblems in the RGB method, a recent solver of (4.38).

Based on this contribution, a further question arises:

> *Can we integrate JSS into solvers beyond RGB and extend its applicability to problems beyond the TV-norm problem (4.38)?*

A simple approach for solving (4.38) is to approximate the measure $\mathbf{x}$ by a sufficiently large number of Dirac masses resulting the following approximation problem:

$$\min_{(w_i,\mathbf{t}_i)\in\mathbb{R}\times T} \quad f\left(\sum_{i=1}^{n} w_i \mathbf{a}_{\mathbf{t}_i}\right) + \lambda \sum_{i=1}^{n} |w_i|\,, \tag{4.39}$$

where $\mathbf{x} \approx \sum_{i=1}^{n} w_i \delta_{\mathbf{t}_i}$, $(w_i, \mathbf{t}_i) \in \mathbb{R}\times T$ and $\mathbf{a}_{\mathbf{t}_i} = \mathbf{A}\delta_{\mathbf{t}_i}$ for $i = 1,\ldots,n$. Notably, problem (4.39) also arises in the context of training one-hidden layer neural networks and is referred to as the *mean field limit* [83]. Despite the non-convexity, solving (4.39) using gradient descent methods can achieve the global optimum, provided a diverse initialization with a sufficiently large number of Dirac masses [21, 20].

However, employing a large number of Dirac masses for approximation can incur substantial computational expenses. JSS emerges as a promising approach to tackle this complexity issue, making it a compelling research direction.

Another promising research path is using JSS for different versions of (4.38), *e.g.*, [76], [63]. Let us consider the problem proposed in [63]:

$$\min_{\mathbf{x}\in\mathscr{M}} \quad \frac{1}{2}\|\mathbf{b} - \mathbf{A}\mathbf{x}\|_{\mathscr{H}}^2 + \lambda \|\mathbf{x}\|_{\mathrm{TV}^2} + \lambda \|\mathrm{div}(\mathbf{x})\|_{TV}\,, \tag{4.40}$$

where $\mathbf{b}$ belongs to a Hilbert space $\mathscr{H}$, $\mathbf{A}$ is a linear operator, $\mathscr{M}$ denotes the topological dual space of $\mathscr{C}(T,\mathbb{R}^2)$, the set of $\mathbb{R}^2$-valued continuous functions defined on T, with the dual norm $\|\cdot\|_{\mathrm{TV}^2}$, and div denotes the divergence operator.

In [63], Laville *et al.* demonstrate the existence of a sparse optimal measure for (4.40), with "curves" structure instead of "spikes" as in TV-norm problem (4.38). Leveraging this sparsity to design a JSS for addressing (4.40) presents an challenging avenue for future research.

Appendix A

Geometry in Hilbert spaces

Main results. In this appendix, we explore some geometric expression of shapes (balls, half-spaces and domes) with proofs in a general Hilbert space, see Table A.1 for the summary.

Result	**Location**
Support function over a ball	Proposition A.1.1
Projection onto hyperplane and half-space	Proposition A.2.2
Support function over a dome	Proposition A.3.2
Smallest ball containing a dome - part 1	Proposition A.3.3
Radius of dome	Proposition A.3.4
Smallest ball containing a dome - part 2	Proposition A.3.5

Table A.1 – Some geometric results in Appendix A

We emphasize that these results are likely established, at least in Euclidean spaces, and implicitly used in various articles when examining safe regions, see for instance [95, 45, 99]. However, we were unable to identify a specific reference presenting them for abitrary Hilbert spaces. We therefore present these results here to maintain self-containment and comprehensiveness of this thesis.

Main geometric regions. In this appendix, we consider a Hilbert space $\mathscr{H}$ with inner product $\langle \cdot, \cdot \rangle$ and induced norm $\|\cdot\|$. We define the *ball* with center $\mathbf{c} \in \mathscr{H}$ and radius $r \in [0, +\infty]$ as

$$B(\mathbf{c}, r) \triangleq \{\mathbf{v} \in \mathscr{H} : \|\mathbf{v} - \mathbf{c}\| \leq r\}.$$

Here, we have $B(\mathbf{c}, 0) = \{\mathbf{c}\}$ and $B(\mathbf{c}, +\infty) = \mathscr{H}$. The *half-space* with normal vector $\mathbf{g} \in \mathscr{H}$ and intercept $s \in \mathbb{R}$ is defined by

$$H(\mathbf{g}, s) \triangleq \{\mathbf{v} \in \mathscr{H} : \langle \mathbf{g}, \mathbf{v} \rangle \leq s\}.$$

Notice that $H(\mathbf{0}_{\mathscr{H}}, s)$ equals to $\mathscr{H}$ if $s \geq 0$ and equals to emptyset otherwise. A *dome* is

defined as the intersection of a ball and a half-space

$$D(\mathbf{c}, r, \mathbf{g}, s) \triangleq B(\mathbf{c}, r) \cap H(\mathbf{g}, s).$$

Other geometric notations. We now recap some basic geometric quantities used in this chapter.

— For $R \subset \mathscr{H}$, we denote by $\operatorname{Bd} R$ the boundary of R. The boundary of a half-space is a hyperplane, and the boundary of a ball is a sphere.

— For $\mathbf{v} \in \mathscr{H}$, we denote by $\mathbf{v}^\perp \triangleq \{\mathbf{p} \in \mathscr{H} : \langle \mathbf{v}, \mathbf{p} \rangle = 0\}$ the orthogonal space of $\mathbf{v}$.

— The support function over a region R is $\varphi_R(\mathbf{v}) \triangleq \sup_{\mathbf{u} \in R} \langle \mathbf{v}, \mathbf{u} \rangle$.

— The cosine of two vectors $\mathbf{u}$ and $\mathbf{v}$ in $\mathscr{H}$ is defined as $\cos(\mathbf{u}, \mathbf{v}) \triangleq \frac{\langle \mathbf{u}, \mathbf{v} \rangle}{\|\mathbf{u}\| \|\mathbf{v}\|}$.

— The radius of a set R is denoted by $\operatorname{rad}(R) \triangleq \sup_{\mathbf{u}, \mathbf{v} \in R} \frac{1}{2} \|\mathbf{u} - \mathbf{v}\|$.

— The distance from $\mathbf{v}$ to R is defined by $\operatorname{dist}(\mathbf{v}, R) \triangleq \inf_{\mathbf{v}' \in R} \|\mathbf{v} - \mathbf{v}'\|$.

— Note that if R is a nonempty closed convex set in Hilbert space $\mathscr{H}$, then there exists a unique minimizer for the closest point projection from any point $\mathbf{v} \in \mathscr{H}$ onto R, see *e.g.*, [5, Proposition 3.14]. We denote it by $\operatorname{Proj}(\mathbf{v}, R) \triangleq \arg\min_{\mathbf{v}' \in R} \|\mathbf{v} - \mathbf{v}'\|$.

A.1 Ball

The following proposition presents the closed-form expression for support function over a ball region.

Proposition A.1.1 (Support function over a ball)**.** *For $\mathbf{v}, \mathbf{c} \in \mathscr{H}$ and $r \in \mathbb{R}$, we have*

$$\varphi_{B(\mathbf{c}, r)}(\mathbf{v}) = \langle \mathbf{v}, \mathbf{c} \rangle + r \|\mathbf{v}\| .$$

Proof. For $\mathbf{u} \in B(\mathbf{c}, r)$, we have $\langle \mathbf{v}, \mathbf{u} \rangle \leq \langle \mathbf{v}, \mathbf{c} \rangle + \langle \mathbf{v}, \mathbf{u} - \mathbf{c} \rangle \leq \langle \mathbf{v}, \mathbf{c} \rangle + r \|\mathbf{v}\|$. Thus, $\varphi_{B(\mathbf{c}, r)}(\mathbf{v}) \leq \langle \mathbf{v}, \mathbf{c} \rangle + r \|\mathbf{v}\|$. We now show that the equality holds. It is clear that we obtain the equality if $\mathbf{v} = \mathbf{0}_{\mathscr{H}}$. For $\mathbf{v} \neq \mathbf{0}_{\mathscr{H}}$, the equality holds if we choose $\mathbf{u} = \mathbf{c} + r \frac{\mathbf{v}}{\|\mathbf{v}\|}$. The proof is completed. □

A.2 Half-space

Let P be the hyperplane associated with the half-space $H = H(\mathbf{g}, s)$ with $\mathbf{g} \neq \mathbf{0}_{\mathscr{H}}$. For any vector $\mathbf{v}$, we define the *algebraic distance* from $\mathbf{v}$ to P as

$$\operatorname{algdist}(\mathbf{v}, P) \triangleq \frac{\langle \mathbf{g}, \mathbf{v} \rangle - s}{\|\mathbf{g}\|}.$$

Note that the algebraic distance is non-positive as soon as $\mathbf{v} \in H$ and is positive otherwise. We define the *algebraic projection* from $\mathbf{v}$ to the hyperplane P as

$$\mathbf{v}_P \triangleq \mathbf{v} - \operatorname{algdist}(\mathbf{v}, P) \frac{\mathbf{g}}{\|\mathbf{g}\|}.$$

In this section, we aim to establish the connection between these concepts, which is presented in Proposition A.2.2. To obtain this result, we first introduce Proposition A.2.1, which can be considered as a generalization of Pythagorean theorem. This proposition provides a means of representing the distance between two points in terms of their algebraic distance corresponding to a half-space.

Proposition A.2.1. *Let P be the hyperplane associated with the half-space $H = H(\mathbf{g}, s)$ with $\mathbf{g} \neq \mathbf{0}_{\mathscr{H}}$. For any $\mathbf{v}, \mathbf{u} \in \mathscr{H}$, we have*

$$\|\mathbf{v} - \mathbf{u}\|^2 = \begin{cases} (\|\mathbf{v} - \mathbf{v}_P\| - \|\mathbf{u} - \mathbf{u}_P\|)^2 + \|\mathbf{v}_P - \mathbf{u}_P\|^2 & \text{if } \mathbf{v}, \mathbf{u} \in H \text{ or } \mathbf{v}, \mathbf{u} \notin H, \\ (\|\mathbf{v} - \mathbf{v}_P\| + \|\mathbf{u} - \mathbf{u}_P\|)^2 + \|\mathbf{v}_P - \mathbf{u}_P\|^2 & \text{otherwise.} \end{cases} \tag{A.1}$$

In particular, for $\mathbf{u} \neq \mathbf{v}$, we have

$$\|\mathbf{v}_P - \mathbf{u}_P\| = \|\mathbf{v} - \mathbf{u}\| \sqrt{1 - \cos(\mathbf{g}, \mathbf{v} - \mathbf{u})^2} \tag{A.2}$$

Proof. To prove (A.1), we first notice that

$$\begin{aligned} \|\mathbf{v} - \mathbf{u}\|^2 &= \|(\mathbf{v} - \mathbf{v}_P) + (\mathbf{v}_P - \mathbf{u}_P) + (\mathbf{u}_P - \mathbf{u})\|^2 \\ &= \|(\mathbf{v} - \mathbf{v}_P) + (\mathbf{u}_P - \mathbf{u})\|^2 + \|\mathbf{v}_P - \mathbf{u}_P\|^2 \\ &\quad + 2\langle \mathbf{v} - \mathbf{v}_P, \mathbf{v}_P - \mathbf{u}_P \rangle + 2\langle \mathbf{u}_P - \mathbf{u}, \mathbf{v}_P - \mathbf{u}_P \rangle \\ &= (-\operatorname{algdist}(\mathbf{v}, P) + \operatorname{algdist}(\mathbf{u}, P))^2 + \|\mathbf{v}_P - \mathbf{u}_P\|^2 . \end{aligned} \tag{A.3}$$

The second equality in the equation above follows from the fact that $\langle \mathbf{v} - \mathbf{v}_P, \mathbf{v}_P - \mathbf{u}_P \rangle = 0$

since $\mathbf{v} - \mathbf{v}_P$ can be proved to be orthogonal to P (*i.e.*, aligned with $\mathbf{g}$) and $\mathbf{v}_P, \mathbf{u}_P$ are points in P. Similarly, we have $\langle \mathbf{u}_P - \mathbf{u}, \mathbf{v}_P - \mathbf{u}_P \rangle = 0$. For any vector $\mathbf{p}$, it is important to note that $\operatorname{algdist}(\mathbf{p}, P)$ is equal to $-\|\mathbf{p} - \mathbf{p}_P\|$ if $\mathbf{p} \in H$ and equals to $\|\mathbf{p} - \mathbf{p}_P\|$ otherwise. Therefore, we obtain (A.1).

To prove (A.2), one can exploit the definition of algebraic distance and cosine:

$$|\operatorname{algdist}(\mathbf{v}, P) - \operatorname{algdist}(\mathbf{u}, P)| = \frac{|\langle \mathbf{g}, \mathbf{v} - \mathbf{u} \rangle|}{\|\mathbf{g}\|} = \|\mathbf{v} - \mathbf{u}\| \, |\cos(\mathbf{g}, \mathbf{v} - \mathbf{u})| \, .$$

Substituting this into (A.3), we obtain (A.2).

□

The next proposition characterizes the closest point projection operator and its distance *w.r.t.* hyperplane and half-space using algebraic distance and projection.

Proposition A.2.2 (Projection onto hyperplane and half-space)**.** *Let* $H = H(\mathbf{g}, s)$ *and* $P = \operatorname{Bd} H$*. For any* $\mathbf{v}$*, one has*

$$\operatorname{dist}(\mathbf{v}, P) = |\operatorname{algdist}(\mathbf{v}, P)| \, , \tag{A.4}$$

$$\operatorname{dist}(\mathbf{v}, H) = \max(0, \operatorname{algdist}(\mathbf{v}, P)), \tag{A.5}$$

$$\operatorname{Proj}(\mathbf{v}, P) = \mathbf{v}_P, \tag{A.6}$$

$$\operatorname{Proj}(\mathbf{v}, H) = \begin{cases} \mathbf{v} & \text{if } \mathbf{v} \in H, \\ \mathbf{v}_P & \text{otherwise.} \end{cases} \tag{A.7}$$

Proof. Consider $\mathbf{p} \in P$ such that $\mathbf{p} \neq \mathbf{v}_P$. We have $\mathbf{p} = \mathbf{p}_P$. By Proposition A.2.1, no matter $\mathbf{v}$ belonging to H or not, we have

$$\begin{aligned} \|\mathbf{v} - \mathbf{p}\|^2 &= (\|\mathbf{v} - \mathbf{v}_P\| \pm \|\mathbf{p} - \mathbf{p}_P\|)^2 + \|\mathbf{v}_P - \mathbf{p}_P\|^2 \\ &= \|\mathbf{v} - \mathbf{v}_P\|^2 + \|\mathbf{v}_P - \mathbf{p}\|^2 \\ &> \|\mathbf{v} - \mathbf{v}_P\|^2 \\ &= |\operatorname{algdist}(\mathbf{v}, P)|^2 \, . \end{aligned}$$

Therefore, $\mathbf{v}_P$ is the unique projection of $\mathbf{v}$ on to P. This proves (A.4) and (A.6),

To prove (A.5) and (A.7), we consider two cases. If $\mathbf{v} \in H$, then it is clear that $\operatorname{dist}(\mathbf{v}, H) = 0$ and, thus, $\operatorname{Proj}(\mathbf{v}, H) = \mathbf{v}$. Otherwise, we assume that $\mathbf{v} \notin H$. Considering

any $\mathbf{p} \in H$, we have

$$\|\mathbf{v}-\mathbf{p}\|^2 = (\|\mathbf{v}-\mathbf{v}_P\| + \|\mathbf{p}-\mathbf{p}_P\|)^2 + \|\mathbf{v}_P-\mathbf{p}_P\|^2 \geq \|\mathbf{v}-\mathbf{v}_P\|^2 .$$

Therefore, $\|\mathbf{v}-\mathbf{p}\| \geq \|\mathbf{v}-\mathbf{v}_P\| = \text{algdist}(\mathbf{v}, H)$ for all $\mathbf{p} \in H$. This means $\mathbf{v}_P$ is the projection of $\mathbf{v}$ onto H. The proof is completed. □

A.3 Dome

For a dome $D = B(\mathbf{c}, r) \cap H(\mathbf{g}, s)$ with $r \in (0, \infty)$ and $\mathbf{g} \neq \mathbf{0}_{\mathscr{H}}$, we define its *intersection index* of a as follows:

$$\psi_D \triangleq \frac{s - \langle \mathbf{g}, \mathbf{c} \rangle}{r \|\mathbf{g}\|}, \tag{A.8}$$

In the following, we sometimes drop in subscript and simply write ψ if D is clear from the context. The following proposition summarizes some basic properties of ψ.

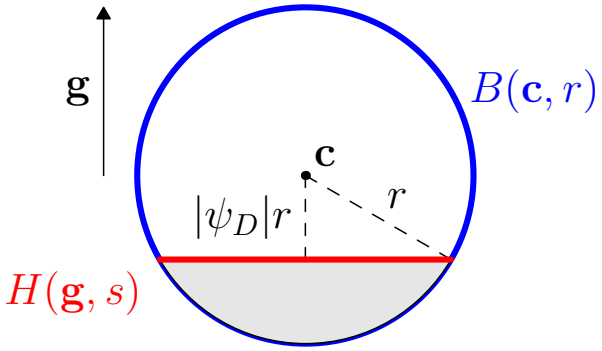

Figure A.1 – A 2D visualization of intersection index (A.8) in case of $\psi_D < 0$.

Proposition A.3.1 (Properties of dome's intersection index)**.** *Let P be the hyperplane associated with H. Then*

1. $\psi = \dfrac{-\text{algdist}(\mathbf{c}, P)}{r}$.
2. $H = \{\mathbf{p} \in \mathscr{H} : \langle \mathbf{g}, \mathbf{p}-\mathbf{c} \rangle \leq \psi r \|\mathbf{g}\|\}$
3. $B \cap H \neq \emptyset$ *iff* $\psi \geq -1$
4. $\mathbf{c} \in H$ *iff* $\psi \geq 0$
5. $B \subset H$ *iff* $\psi \geq 1$

Proof. Note that Item 1, Item 2 and Item 4 are obvious by definition of D. We now prove Item 3 and Item 5.

Item 3. If $\mathbf{c} \in H$, then $\{\mathbf{c}\} \subset B \cap H \neq \emptyset$ and $\psi \geq 0 > -1$. We now consider $\mathbf{c} \notin H$, *i.e.*, $\operatorname{algdist}(\mathbf{c}, P) \geq 0$. In this case, $B \cap H$ is nonempty iff there exists some point $\mathbf{p} \in B \cap H$. This implies $r \geq \|\mathbf{c} - \mathbf{p}\| \geq \operatorname{Proj}(\mathbf{c}, P) = \operatorname{algdist}(\mathbf{c}, P)$, *i.e.*, $-\psi \leq 1$.

Item 5. This is clear since

$$B \subset H \iff s \geq \sup_{\mathbf{v} \in B} \langle \mathbf{v}, \mathbf{g} \rangle = \langle \mathbf{g}, \mathbf{c} \rangle + r \|\mathbf{g}\| \iff \psi \geq 1.$$

The proof is completed. □

Below, we recall a simple formula for support function over a dome region using trigonometry. This formula aligns with [97, Lemma 3]. Note that there are several methodologies employed to derive different formulas for this result, such as using Lagrange duality [52, Appendix A], geometric methods [57, Appendix B], as well as directly solving it [96, Section 3], [66, Theorem 3], and [75, Theorem 2]. The 2D visualization of Proposition A.3.2 can be found in Figure A.2.

Proposition A.3.2 (Support function over a dome)**.** *Let $D = B(\mathbf{c}, r) \cap H(\mathbf{g}, s)$ be a non-empty dome. Its support function evaluated at vector $\mathbf{v}$ is*

$$\varphi_D(\mathbf{v}) = \langle \mathbf{v}, \mathbf{c} \rangle + r \|\mathbf{v}\| \cos([\theta_D - \theta_{\mathbf{v}}]_+)$$

where

$$\theta_{\mathbf{v}} = \arccos \frac{\langle \mathbf{v}, \mathbf{g} \rangle}{\|\mathbf{v}\| \|\mathbf{g}\|}, \quad \theta_D = \arccos\left(\left[\frac{s - \langle \mathbf{g}, \mathbf{c} \rangle}{r \|\mathbf{g}\|} \right]_{[-1,1]} \right).$$

here $[t]_+ = \max(t, 0)$ and $[t]_{[-1,1]} = \max(\min(t, 1), -1)$ is the restriction of t on $[-1, 1]$.

Here, one should notice that θ_D is the arccosine of the intersection index ψ_D restricted on $[-1, 1]$. First $\psi_D \geq -1$ is clear due to the third item of Proposition A.3.1. Second, when $\psi_D > 1$, the result holds true obviously since $D = B$ due to the fifth item of Proposition A.3.1.

The following result provides a closed-form expression for the smallest ball (parameterized by some $\theta \leq 0$) containing a given dome. Here, the ball is constrained so that the line joining its center and the center of the dome is perpendicular to the hyperplane of the dome.

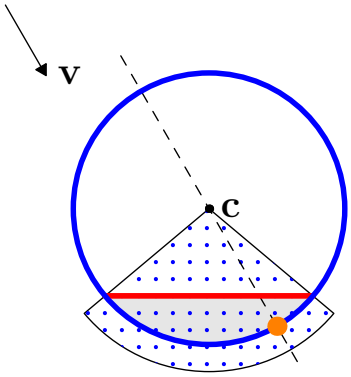

(a) $\theta_D \geq \pi/2, \theta_D \leq \theta_{\mathbf{v}}$

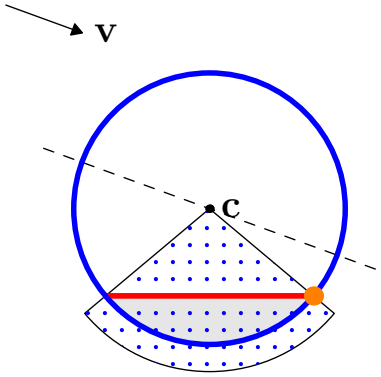

(b) $\theta_D \geq \pi/2, \theta_D > \theta_{\mathbf{v}}$

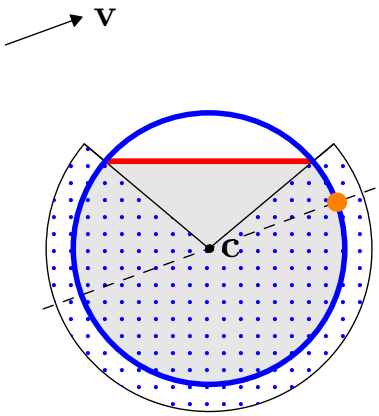

(c) $\theta_D < \pi/2, \theta_D \leq \theta_{\mathbf{v}}$

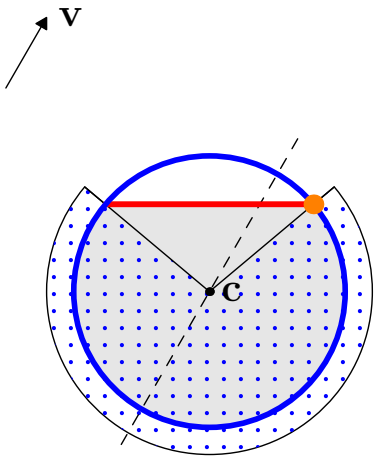

(d) $\theta_D < \pi/2, \theta_D > \theta_{\mathbf{v}}$

Figure A.2 – 2D visualization of Proposition A.3.2. Here the gray region represents the dome and the dotted region represents a (part of) cone region of $\mathbf{v}$ such that $\theta_D \leq \theta_{\mathbf{v}}$. The orange dot denotes the $\arg\max_{\mathbf{u} \in D} \langle \mathbf{v}, \mathbf{u} \rangle$.

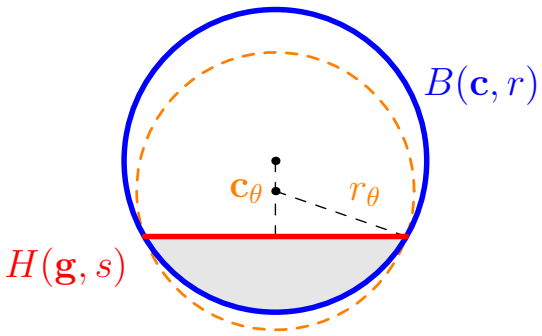

Figure A.3 – 2D visualization of the smallest ball $B(\mathbf{c}_\theta, r_\theta)$ (dashed orange circle) in Proposition A.3.3.

Proposition A.3.3 (Smallest ball containing a dome - part 1)**.** *Consider the dome* $D = B(\mathbf{c}, r) \cap H(\mathbf{g}, s)$ *with* $\mathbf{g} \neq \mathbf{0}_{\mathscr{H}}$ *and* $r > 0$ *with an intersection index of* D *satisfying* $\psi \in [-1, 1]$*. We consider the parameterized ball* $B(\mathbf{c}_\theta, r_\theta)$ *for some* $\theta \leq 0$*, where*

$$\mathbf{c}_\theta = \mathbf{c} + \theta r \frac{\mathbf{g}}{\|\mathbf{g}\|}, \tag{A.9}$$

$$r_\theta = r\sqrt{(\theta - \psi)^2 + 1 - \psi^2}. \tag{A.10}$$

Then

$$D \subset B(\mathbf{c}_\theta, r_\theta). \tag{A.11}$$

Furthermore, $B(\mathbf{c}_\theta, r_\theta)$ *is the smallest ball centered at* $\mathbf{c}_\theta$ *containing* D*, i.e.,*[1]

$$r_\theta = \max_{\mathbf{p} \in D} \|\mathbf{c}_\theta - \mathbf{p}\| . \tag{A.12}$$

Proof of Proposition A.3.3. For $\mathbf{v} \in D$, we have $\|\mathbf{v} - \mathbf{c}\| \leq r$ and $\langle \mathbf{g}, \mathbf{v} - \mathbf{c} \rangle \leq \psi r \|\mathbf{g}\|$ with equality if $\mathbf{v} \in \operatorname{Bd} B(\mathbf{c}, r)$ and $\mathbf{v} \in \operatorname{Bd} H(\mathbf{g}, s)$, respectively. Also notice that if $\theta \leq 0$,

1. In other words, $B(\mathbf{c}_\theta, r_\theta)$ is a geometric ball associated with $\mathbf{c}_\theta$ and D, see Definition 3.3.1.

we have

$$\begin{aligned}\|\mathbf{v}-\mathbf{c}_\theta\|^2 &= \left\|\mathbf{v}-\mathbf{c}-\frac{\theta r}{\|\mathbf{g}\|}\mathbf{g}\right\|^2 \\ &= \|\mathbf{v}-\mathbf{c}\|^2 - 2\frac{\theta r}{\|\mathbf{g}\|}\langle \mathbf{v}-\mathbf{c},\mathbf{g}\rangle + \theta^2 r^2 \\ &\le r^2 - 2\theta\psi r^2 + \theta^2 r^2 \\ &= r^2((\theta-\psi)^2 + 1 - \psi^2) \\ &= r_\theta^2.\end{aligned}$$

Here the inequality follows from the assumption that $\theta \le 0$. From this estimation, one can see that $\mathbf{v} \in B_\theta$ and therefore (A.11) holds true.

From this estimation, one can notice that (A.12) holds true if $\mathbf{v} \in \operatorname{Bd} H(\mathbf{g},s) \cap \operatorname{Bd} B(\mathbf{c},r)$. The remaining is dedicated to show that $\operatorname{Bd} H(\mathbf{g},s) \cap \operatorname{Bd} B(\mathbf{c},r)$ is non empty. We choose $\mathbf{v} = \mathbf{c}_{\operatorname{Bd} H} + r\sqrt{1-\psi^2}\mathbf{v}_0$ for some unit vector $\mathbf{v}_0 \in \mathbf{g}^\perp$ and $\mathbf{c}_{\operatorname{Bd} H}$ the projection of $\mathbf{c}$ onto $\operatorname{Bd} H$ given by the expression $\mathbf{c}_{\operatorname{Bd} H} = \mathbf{c} + r\psi\frac{\mathbf{g}}{\|\mathbf{g}\|}$. By this choice of $\mathbf{v}$, it not difficult to verify that $\mathbf{v} \in \operatorname{Bd} H(\mathbf{g},s) \cap \operatorname{Bd} B(\mathbf{c},r)$. This completes the proof. □

In the following, we show how to evaluate the radius of dome in a closed-form expression using the intersection index.

Proposition A.3.4 (Radius of dome)**.** *Let D be a non-empty dome with intersection index ψ ($\psi \ge -1$). Its radius is given by the following formula:*

$$\operatorname{rad}(D) = \begin{cases} r\sqrt{1-\psi^2} & \text{if } \psi \le 0, \\ r & \text{otherwise.} \end{cases} \tag{A.13}$$

In particular, if $\psi \le 0$, then $\operatorname{rad}(D) = \operatorname{rad}(\operatorname{Bd} B \cap \operatorname{Bd} H)$.

Proof. Let $D = B \cap H$ where $B = B(\mathbf{c},r)$ and $H = H(\mathbf{g},s)$. Consider unit vector $\mathbf{v} \in \mathbf{g}^\perp$, *i.e.*, $\langle \mathbf{v},\mathbf{g}\rangle = 0$ and $\|\mathbf{v}\| = 1$. We prove (A.13) by considering two cases of ψ.

Case 1: $\psi > 0$**.** consider $\mathbf{v}_1 = \mathbf{c} + r\mathbf{v}$ and $\mathbf{v}_2 = \mathbf{c} - r\mathbf{v}$. Then it is not hard to see that $\mathbf{v}_1, \mathbf{v}_2 \in D$. Indeed, we have $\mathbf{v}_1, \mathbf{v}_2 \in B$ since $\|\mathbf{v}_1 - \mathbf{c}\| = \|\mathbf{v}_2 - \mathbf{c}\| = r$. We also have $\langle \mathbf{g}, \mathbf{v}_1 - \mathbf{c}\rangle = 0 \le \psi r \|\mathbf{g}\|$ since $\mathbf{v} \in \mathbf{g}^\perp$ and $\psi > 0$. This means $\mathbf{v}_1 \in H$ due to characterization of H in Proposition A.3.1, and similar for $\mathbf{v}_2$. We can also observe that $2r = \|\mathbf{v}_1 - \mathbf{v}_2\| \le 2\operatorname{rad} D \le 2\operatorname{rad} B = 2r$, thus, $\operatorname{rad}(D) = r$.

Case 2: $\psi \leq 0$**.** Here $\psi \in [-1, 0]$. Let $\kappa \triangleq r\sqrt{1-\psi^2}$ and $\mathbf{v}_1 \triangleq \mathbf{c}_P + \kappa\mathbf{v}$ and $\mathbf{v}_2 \triangleq \mathbf{c}_P - \kappa\mathbf{v}$ where $\mathbf{c}_P$ is the projection of $\mathbf{c}$ onto $P = \operatorname{Bd} H$. Here κ is well-defined since $\psi \in [-1, 0]$. We now show that $\mathbf{v}_1, \mathbf{v}_2 \in D$. Indeed, it is easy to see that $\mathbf{v}_1, \mathbf{v}_2 \in P \subset H$ since $\langle \mathbf{g}, \mathbf{v}_1 - \mathbf{c} \rangle = \langle \mathbf{g}, \mathbf{v}_1 - \mathbf{c} \rangle = s$. To see that $\mathbf{v}_1, \mathbf{v}_2 \in B$, we notice that $\|\mathbf{c} - \mathbf{v}_1\|^2 = \|\mathbf{c} - \mathbf{c}_P\|^2 + \|\kappa\mathbf{v}\|^2 = r^2\psi^2 + r^2(1-\psi^2) = r^2$, *i.e.*, $\mathbf{v}_1 \in B$. Similarly, $\mathbf{v}_2 \in B$. Therefore, $2\kappa = \|\mathbf{v}_1 - \mathbf{v}_2\| \leq 2\operatorname{rad}(D)$. Now the remaining is to show that $\operatorname{rad}(D) \leq \kappa$. This can be done using Proposition A.3.3. Let B_ψ be the ball parameterized by ψ and r_ψ be its radius defined in Proposition A.3.3 containing D. We have $\operatorname{rad}(D) \leq \operatorname{rad} B_\psi = r_\psi = r\sqrt{1-\psi^2}$. due to (A.9). Thus $\operatorname{rad}(D) = \kappa = r\sqrt{1-\psi^2}$.

Notice that in Case 2. we have $\mathbf{v}_1, \mathbf{v}_2 \in \operatorname{Bd} B \cap \operatorname{Bd} H$. The proof is completed.

□

We finally conclude this chapter with a general expression of the ball with the smallest radius containing a dome with an arbitrary choice of center. Although the proof of this result relies on Proposition A.3.3, it is, in fact, a generalization of Proposition A.3.3 by relaxing the constraint that the line connecting the center (of the smallest ball) and the center of the dome is perpendicular to the hyperplane of the dome. A 2D visualization of Proposition A.3.5 is depicted in Figure A.4.

Proposition A.3.5 (Smallest ball containing a dome - part 2)**.** *Let $D = B \cap H$ be a non-empty dome with intersection index ψ, where $B = B(\mathbf{c}, r)$ and $H = H(\mathbf{g}, s)$. For $\mathbf{v} \neq \mathbf{c}$ in $\mathscr{H}$, define $B_\mathbf{v} = B(\mathbf{v}, R)$ as the ball centered at $\mathbf{v}$ with smallest radius containing the dome D. Then*

$$R = \begin{cases} \|\mathbf{v} - \mathbf{c}\| + r & \text{if } \cos(\mathbf{g}, \mathbf{v} - \mathbf{c}) \geq -\psi \\ \sqrt{\|\mathbf{v} - \mathbf{v}_P\|^2 + (\|\mathbf{v}_P - \mathbf{c}_P\| + r\sqrt{1-\psi^2})^2} & \text{otherwise} \end{cases} \tag{A.14}$$

Proof of Proposition A.3.5. Since $D \neq \emptyset$, we have $\psi \geq -1$. If $\psi \geq 1$, then $D = B$ and $\cos(\mathbf{g}, \mathbf{v} - \mathbf{c}) \geq -1 \geq -\psi$ and $r_\mathbf{v} \triangleq \max_{\mathbf{p} \in D} \|\mathbf{v} - \mathbf{p}\| = \max_{\mathbf{p} \in B} \|\mathbf{v} - \mathbf{p}\| = \|\mathbf{v} - \mathbf{c}\| + r$. In this case, the result is obviously true. Thus, *w.l.o.g.* we assume that $\psi \in [-1, 1)$. We now consider two cases.

Case 1. Assume that $\cos(\mathbf{v} - \mathbf{c}, \mathbf{g}) \geq -\psi$. Define

$$\overline{\mathbf{v}} \triangleq \mathbf{c} + \frac{R}{\|\mathbf{c} - \mathbf{v}\|}(\mathbf{c} - \mathbf{v}). \tag{A.15}$$

We now show that

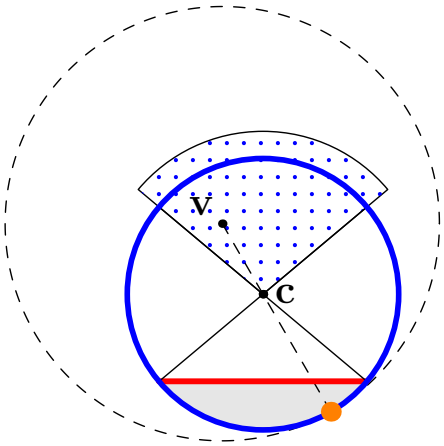

(a) $\psi_D \leq 0, \psi_{\mathbf{v}} \geq -\psi_D$

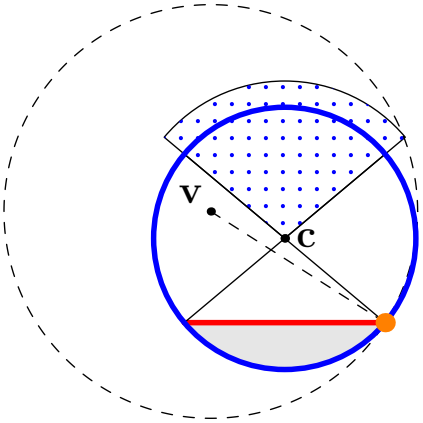

(b) $\psi_D \leq 0, \psi_{\mathbf{v}} < -\psi_D$

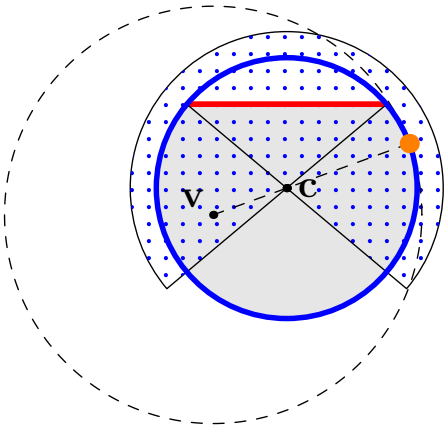

(c) $\psi_D > 0, \psi_{\mathbf{v}} \geq -\psi_D$

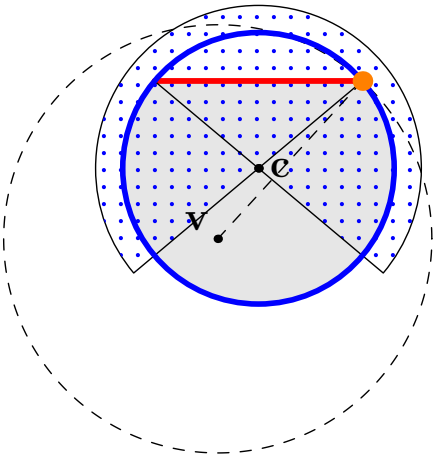

(d) $\psi_D > 0, \psi_{\mathbf{v}} < -\psi_D$

Figure A.4 – 2D visualization of geometric ball (dashed circle) in Proposition A.3.5. Here the gray region represents the dome and the dotted region represents a (part of) cone region of $\mathbf{v}$ such that $\psi_{\mathbf{v}} \geq -\psi_D$. The orange dot denotes the $\arg\max_{\mathbf{u} \in D} \|\mathbf{v} - \mathbf{u}\|$.

1. $\|\mathbf{v}-\overline{\mathbf{v}}\| = \|\mathbf{v}-\mathbf{c}\| + R$

2. $\|\mathbf{v}-\mathbf{p}\| \leq \|\mathbf{v}-\overline{\mathbf{v}}\|$ for all $\mathbf{p} \in D$

3. $\overline{\mathbf{v}} \in D$

The first item is clear. For second item, we have

$$\begin{aligned}\|\mathbf{v}-\mathbf{p}\| &\leq \|\mathbf{v}-\mathbf{c}\| + \|\mathbf{c}-\mathbf{p}\| \\ &\leq \|\mathbf{v}-\mathbf{c}\| + R \\ &= \|\mathbf{v}-\overline{\mathbf{v}}\|.\end{aligned}$$

for any $\mathbf{p} \in D$. The last item follows from the observations: 1) $\overline{\mathbf{v}} \in B(\mathbf{c}, R)$ since $\|\mathbf{c}-\overline{\mathbf{v}}\| = R$ and 2) $\overline{\mathbf{v}} \in H(\mathbf{g}, L)$ since

$$\begin{aligned}\langle \mathbf{g}, \overline{\mathbf{v}} \rangle - L &= \langle \mathbf{g}, \mathbf{c} \rangle + \frac{R}{\|\mathbf{c}-\mathbf{v}\|}\langle \mathbf{g}, \mathbf{c}-\mathbf{v} \rangle - L \\ &= R\|\mathbf{g}\|\left(\cos(\mathbf{c}-\mathbf{v}, \mathbf{g}) + \frac{\langle \mathbf{g}, \mathbf{c} \rangle - L}{R\|\mathbf{g}\|}\right) \\ &= R\|\mathbf{g}\|\left(-\cos(\mathbf{v}-\mathbf{c}, \mathbf{g}) - \psi\right) \leq 0.\end{aligned}$$

Step 2. We assume that $\cos(\mathbf{v}-\mathbf{c}, \mathbf{g}) \leq -\psi$. Define

$$\overline{\mathbf{v}} \triangleq \mathbf{c}_P + \frac{\sqrt{1-\psi^2}}{\|\mathbf{c}_P - \mathbf{v}_P\|}(\mathbf{c}_P - \mathbf{v}_P)$$

and

$$\kappa \triangleq \sqrt{\|\mathbf{v}-\mathbf{v}_P\|^2 + (\|\mathbf{v}_P - \mathbf{c}_P\| + r\sqrt{1-\psi^2})^2}.$$

It is sufficient to show that

1. $\|\mathbf{v}-\overline{\mathbf{v}}\| = \kappa$

2. $\|\mathbf{v}-\mathbf{p}\| \leq \|\mathbf{v}-\overline{\mathbf{v}}\|$ for all $\mathbf{p} \in D$

3. $\overline{\mathbf{v}} \in D$

The first is simple, since

$$\begin{aligned}\|\mathbf{v}-\overline{\mathbf{v}}\|^2 &= \|\mathbf{v}-\mathbf{v}_P\|^2 + \|\mathbf{v}_P-\overline{\mathbf{v}}\|^2 \\ &= \|\mathbf{v}-\mathbf{v}_P\|^2 + \|\mathbf{c}_P-\mathbf{v}_P\|^2\left(\frac{r\sqrt{1-\psi^2}}{\|\mathbf{c}_P-\mathbf{v}_P\|}+1\right)^2 \\ &= \kappa^2.\end{aligned}$$

For the third, we show that $\overline{\mathbf{v}} \in P \cap \operatorname{Bd} B$. Indeed, it is easy to show that $\overline{\mathbf{v}} \in P$ since $\mathbf{c}_P, \mathbf{v}_P \in P$. We also have $\|\overline{\mathbf{v}}-\mathbf{c}\|^2 = \|\mathbf{c}-\mathbf{c}_P\|^2 + \|\mathbf{c}_P-\overline{\mathbf{v}}\|^2 = R^2\psi^2 + R(1-\psi^2) = R^2$, *i.e.*, $\overline{\mathbf{v}} \in \operatorname{Bd} B$. To prove 2., consider $B_\theta \triangleq B(\mathbf{c}_\theta, r_\theta)$ where $\mathbf{c}_\theta, r_\theta$ is defined by for some $\theta \leq 0$ to be chosen latter such that

$$\|\mathbf{v}-\mathbf{c}_\theta\| + R_\theta = \kappa \tag{A.16}$$

In this case, we have, for all $\mathbf{p} \in D$,

$$\|\mathbf{p}-\mathbf{v}\| \leq \|\mathbf{v}-\mathbf{c}_\theta\| + R_\theta = \kappa = \|\mathbf{v}-\overline{\mathbf{v}}\|.$$

since $D \subset B_\theta$, (A.16) and item 1. For simplicity, define $a \triangleq \operatorname{algdist}(\mathbf{v}, P)$, $b \triangleq \|\mathbf{v}_P-\mathbf{c}_P\|$ and $c \triangleq r\sqrt{1-\psi^2}$. First, we have $\kappa = \sqrt{a^2+(b+c)^2}$.

Now, it is time to choose θ,

$$\theta \triangleq \psi + \frac{t}{R} \tag{A.17}$$

where $t \triangleq \frac{ac}{b+c}$. We also observe that $t = \operatorname{algdist}(\mathbf{c}_\theta, P)$ since

$$\begin{aligned}&\operatorname{algdist}(\mathbf{c}_\theta, P) \\ &= \frac{\langle \mathbf{g}, \mathbf{c}_\theta\rangle - L}{\|\mathbf{g}\|} \\ &= \frac{\langle \mathbf{g}, \mathbf{c}_\theta\rangle - \langle \mathbf{g}, \mathbf{c}_P\rangle}{\|\mathbf{g}\|} \\ &= R(\theta-\psi) \\ &= t.\end{aligned}$$

Hence

$$\|\mathbf{v}-\mathbf{c}_\theta\| + R_\theta = \sqrt{(a-t)^2+b^2} + \sqrt{t^2+c^2} = \sqrt{a^2+(b+c)^2} = \kappa. \tag{A.18}$$

Where the first equality follows from (A.1) and (A.10), the second one follows from definition of t. It remains to show that $\theta \leq 0$ under our assumption. Let

$$\xi \triangleq \cos(\mathbf{v} - \mathbf{c}, \mathbf{g}) \tag{A.19}$$

Then

$$\theta \leq 0 \iff t \leq -R\psi \tag{A.20}$$

Indeed, since $\text{algdist}(\mathbf{c}_\theta, P) = \frac{\text{algdist}(\mathbf{v},P)r\sqrt{1-\psi^2}}{\|\mathbf{v}_P - \mathbf{c}_P\| + r\sqrt{1-\psi^2}}$, $\|\mathbf{v}_P - \mathbf{c}_P\| = R\sqrt{1-\xi^2}$, $\text{algdist}(\mathbf{v}, P) = R(\xi - \psi)$, hence $t \leq -R\psi$ is equivalent to

$$\frac{(\xi - \psi)\sqrt{1-\psi^2}}{\sqrt{1-\xi^2} + \sqrt{1-\psi^2}} \leq -\psi \iff \frac{\xi}{\sqrt{1-\xi^2}} \leq \frac{-\psi}{\sqrt{1-\psi^2}} \iff \xi \leq -\psi. \tag{A.21}$$

This is true due to our assumption. The proof is completed.

□

Appendix B

Fenchel-Rockafellar duality

This appendix chapter aims to recap the fundamental results in convex optimization necessary for establishing the main contributions presented in Chapters 3 and 4. In Appendix B.1, we recall the essential concepts and their properties in convex optimization. In Appendix B.2, we first revisit the hypotheses in the standard Fenchel-Rockafellar duality framework to establish the strong duality result. Subsequently, we introduce two propositions with easily verifiable conditions for establishing Fenchel-Rockafellar strong duality in specific setups.

B.1 Some concepts in convex optimization

In this section, we review some basic concepts in convex optimization.

— Topological dual spaces, weak and weak* topologies [1]

— Convex set, convex function and their topological properties

— Conjugate function

— Gradient and subgradient

— Strong smoothness (gradient Lipschitz) and strong convexity

— Fenchel and Bregman divergence

— Gauge function

In this section, we set $\inf \emptyset = +\infty$ and $\sup \emptyset = -\infty$.

Topological dual spaces, weak and weak* topologies

Let $\mathscr{V}$ be a Banach space with norm $\|\cdot\|_{\mathscr{V}}$. We denote by $\tau_{\mathscr{V}}$ the norm induced topology of $\mathscr{V}$ induced by the norm $\|\cdot\|_{\mathscr{V}}$. Let $\mathscr{V}^*$ be its topological dual space of $(\mathscr{V}, \tau_{\mathscr{V}})$, *i.e.*,

1. In finite-dimensional settings, the weak (or weak*) topology is equivalent to the standard topology. Consequently, readers with a specific interest in finite-dimensional problems may skip this discussion.

$\mathscr{V}^* = (\mathscr{V}, \tau_{\mathscr{V}})^*$. Then $\mathscr{V}^*$ is also a Banach space endowed with the dual norm denoted by $\|\cdot\|_{\mathscr{V}^*}$. We denote the topology in $\mathscr{V}^*$ generated by the dual norm by $\tau_{\mathscr{V}^*}$. The topologies $\tau_{\mathscr{V}}$ and $\tau_{\mathscr{V}^*}$ are called *strong topologies* in $\mathscr{V}$ and $\mathscr{V}^*$, respectively.

We now use the canonical pairing to denote the evaluation of $\mathbf{x} \in \mathscr{V}^*$ on $\mathbf{z} \in \mathscr{V}$, *i.e.*,

$$\langle \mathbf{x}, \mathbf{z} \rangle_{\mathscr{V},\mathscr{V}^*} \triangleq \mathbf{x}(\mathbf{z}).$$

Note that if $\mathscr{V}$ is a Hilbert space, then $\mathscr{V} = \mathscr{V}^*$, $\tau_{\mathscr{V}} = \tau_{\mathscr{V}^*}$ and the canonical pairing becomes the inner product. In the following, we will drop the subscript of canonical pairing if the spaces of $\mathbf{x}$ and $\mathbf{z}$ can be easily identified in the context.

However, note that the strong topologies are not necessarily symmetric. Specifically, the dual of $\mathscr{V}^*$ with respect to $\tau_{\mathscr{V}^*}$ is not always $\mathscr{V}$, i.e., $\mathscr{V} \neq (\mathscr{V}^*, \tau_{\mathscr{V}^*})^*$. If this symmetry holds, the space $\mathscr{V}$ is said to be *reflexive*. The typical reflexive space is Hilbert space. It is important to note that Euclidean spaces $\mathbb{R}^m$ are examples of Hilbert spaces.

The non-symmetry of $\tau_{\mathscr{V}}$ and $\tau_{\mathscr{V}^*}$ may be unsuitable for investigating certain concepts in convex optimization. [2] The standard approach to obtain symmetry is to work with the weak and weak* topology. We now discuss the these two topologies below.

Let $\omega_{\mathscr{V}}$ be the coarsest topology for which each element in $\mathscr{V}^*$ (called linear functional on $\mathscr{V}$) is $\omega_{\mathscr{V}}$-continuous. So $\omega_{\mathscr{V}}$ is called *the weak topology* of $\mathscr{V}$. Similarly, let $\omega_{\mathscr{V}^*}$ be the coarsest topology for which each element in $\mathscr{V}$ (which can be considered as a linear functional on $\mathscr{V}^*$) is $\omega_{\mathscr{V}^*}$-continuous. Then $\omega_{\mathscr{V}^*}$ is called *weak* topology* in $\mathscr{V}^*$.

The weak and weak* topology are symmetric, *i.e.*, $\mathscr{V}^* = (\mathscr{V}, \omega_{\mathscr{V}})^*$ and $\mathscr{V} = (\mathscr{V}^*, \omega_{\mathscr{V}^*})^*$. As we will see in the following, the symmetric role of weak and weak* topologies will naturally appear for establishing nice symmetric results for sets, functions and operators in convex analysis.

Note that if $\mathscr{V}$ is a Hilbert space then weak and weak* topology are identical, *i.e.*, $\omega_{\mathscr{V}} = \omega_{\mathscr{V}^*}$. In particular, if $\mathscr{V} = \mathbb{R}^m$ then all the topologies coincide, and are denoted $\tau_{\mathbb{R}^m}$. In other words, when working with finite-dimensional setups, there is no need to distinguish the strong, weak and weak* topologies.

In the following, when we say "A set in $\mathscr{V}$ is closed", "a function is continuous on $\mathscr{V}$" of a "a linear operator from $\mathscr{V}_1$ to $\mathscr{V}_2$ is continuous" we implicitly assume that the strong topologies is being used. If the weak or weak* topology is considered, we will explicitly mention it. For example, when considering weak topologies, we say "A set in $\mathscr{V}$ is weakly

2. In Chapter 4, we work with the space of Radon measures, which is non-reflexive.

closed" or "a function is weakly continuous on $\mathscr{V}$" or "a linear operator from $\mathscr{V}_1$ to $\mathscr{V}_2$ is weak-to-weak continuous".

Convex set, convex function and their topological properties

Let $\mathscr{V}$ be a Banach space. A set K in $\mathscr{V}$ is convex iff for all $\mathbf{v}, \mathbf{u} \in K$ and $\tau \in [0,1]$, we have $\tau\mathbf{v} + (1-\tau)\mathbf{u} \in K$.

In general a weakly closed set is always closed. However, the converse is not true. Interestingly, the converse holds for convex sets.

Theorem B.1.1 ([14, Theorem 3.7]). *A convex subset of $\mathscr{V}$ is closed iff it is weakly closed.*

For a function $f\colon \mathscr{V} \to \mathbb{R} \cup \{\pm\infty\}$, we define its *domain* as the set of positions that f admits finite value,

$$\mathrm{dom}(f) \triangleq \{\mathbf{v} \in \mathscr{V} : -\infty < f(\mathbf{v}) < +\infty\}.$$

A function f is said to be *closed proper convex* if it satisfies the following properties:

1. Convexity. $f(\tau\mathbf{v} + (1-\tau)\mathbf{u}) \leq \tau f(\mathbf{v}) + (1-\tau) f(\mathbf{u})$ for all $\mathbf{v}, \mathbf{u} \in \mathscr{V}$ and $\tau \in [0,1]$
2. Properness. $f(\mathbf{v}) > -\infty$ for all $\mathbf{v} \in \mathscr{V}$ and there exists $\mathbf{v}_0 \in \mathscr{V}$ so that $f(\mathbf{v}_0) < +\infty$
3. Closedness.[3] The epigraph of f, denoted by $\mathrm{epi}f = \{(\mathbf{v}, \tau) \in \mathscr{V} \times \mathbb{R} : f(\mathbf{v}) \leq \tau\}$, is closed[4]

Note that the convexity and properness of f can be defined using the $\mathrm{epi}f$. Indeed, it is not hard to see that f is convex iff $\mathrm{epi}f$ is convex. In particular, the properness of f implies that its domain is non-empty.

Assuming that $\mathrm{epi}f$ is convex, then it is closed iff weakly closed due to Theorem B.1.1. This fact is reformulated in terms of function f as follows.

Theorem B.1.2. *([4, Proposition 20]) The function $f\colon \mathscr{V} \to \mathbb{R} \cup \{\pm\infty\}$ is closed proper convex if and only if it is weakly closed proper convex.*

Conjugate function. The *(convex) conjugate* of $f\colon \mathscr{V} \to \mathbb{R} \cup \{\pm\infty\}$ is a function $f^*\colon \mathscr{V}^* \to \mathbb{R} \cup \{\pm\infty\}$ defined by

$$f^*(\mathbf{u}) \triangleq \sup_{\mathbf{v} \in \mathscr{V}} \langle \mathbf{u}, \mathbf{v} \rangle - f(\mathbf{v}), \quad \forall \mathbf{u} \in \mathscr{V}^*.$$

3. f is closed iff it is lower-semi continuous [68, Proposition 2.159].
4. More precisely, the epigraph $\mathrm{epi}f$ is assumed to be closed in the product topology of the strong topology of $\mathscr{V}$ and the usual topology of $\mathbb{R}$, *i.e.*, $\tau_{\mathscr{V}} \times \tau_{\mathbb{R}}$.

The *biconjugate* of f, say $f^{**}\colon \mathscr{V} \to \mathbb{R} \cup \{\pm\infty\}$, is a function defined on $\mathscr{V}$ (not $\mathscr{V}^{**}$) such that:

$$f^{**}(\mathbf{v}) \triangleq \sup_{\mathbf{u}\in\mathscr{V}^*} \langle \mathbf{v}, \mathbf{u}\rangle - f^*(\mathbf{u}), \quad \forall \mathbf{v} \in \mathscr{V}.$$

The functions that are closed proper convex play an essential role in convex analysis with desirable properties.

Theorem B.1.3 (Biconjugate theorem [4, Theorem 2.22 p. 79])**.** *If f is closed proper convex, then $f^{**} = f$.*

Remark B.1.4. *Similar to function defined on $\mathscr{V}$, one can define conjugate and biconjugate for function h defined on $\mathscr{V}^*$, say $h\colon \mathscr{V}^* \to \mathbb{R} \cup \{\pm\infty\}$, as follows,*

$$h^*(\mathbf{v}) \triangleq \sup_{\mathbf{u}\in\mathscr{V}^*} \langle \mathbf{v}, \mathbf{u}\rangle - h(\mathbf{u}), \quad \forall \mathbf{v} \in \mathscr{V}$$
$$h^{**}(\mathbf{u}) \triangleq \sup_{\mathbf{v}\in\mathscr{V}} \langle \mathbf{u}, \mathbf{v}\rangle - h^*(\mathbf{v}), \quad \forall \mathbf{u} \in \mathscr{V}^*.$$

Here, it is crucial to notice that h^* is defined on $\mathscr{V}$ not $\mathscr{V}^{**}$. In this case, the biconjugate theorem should be stated: If $h\colon \mathscr{V}^* \to \mathbb{R} \cup \{\pm\infty\}$ is weakly closed proper convex, then h^* is (weakly) closed proper convex and $h = h^{**}$. More generally, the convex conjugacy operator defines a one-to-one map from the space of (weakly) closed proper convex functions to the space of weakly* closed proper convex functions, [2, Theorem 9.3.5].*

Gradient and subgradient. A function $f\colon \mathscr{V} \to \mathbb{R} \cup \{\pm\infty\}$ is said to be differentiable at $\mathbf{v}$ (belonging to the interior of $\mathrm{dom}(f)$) if there exists a continuous linear functional $\mathbf{g}_\mathbf{v} \in \mathscr{V}^*$ such that [5]

$$\lim_{\|\mathbf{p}\|_\mathscr{V}\to 0_+} \frac{|f(\mathbf{v}+\mathbf{p}) - f(\mathbf{v}) - \langle \mathbf{g}_\mathbf{v}, \mathbf{p}\rangle|}{\|\mathbf{p}\|_\mathscr{V}} = 0. \tag{B.1}$$

In this case, we denote $\nabla f(\mathbf{v}) = \mathbf{g}_\mathbf{v}$ and call it the *gradient* of f at $\mathbf{v}$ [68, Definition 5.39].

In various applications, f is not differentiable. In such cases, we need a general concept of gradient called "subgradient" and the collection of subgradients is called "subdifferential". Specifically, the *subdifferential* of a convex function f at $\mathbf{v}$ is defined as

$$\partial f(\mathbf{v}) \triangleq \{\mathbf{g} \in \mathscr{V}^* : f(\mathbf{u}) \geq f(\mathbf{v}) + \langle \mathbf{g}, \mathbf{u}-\mathbf{v}\rangle, \forall \mathbf{u} \in \mathscr{V}\}.$$

5. Here, $\mathbf{g}_\mathbf{v}$ defined by (B.1) is also referred to as the Fréchet derivative. It's important to distinguish it from the Gâteaux derivative. It's worth noting that all Fréchet derivatives are Gâteaux derivatives, but for the applications in this thesis, using the Fréchet derivative is sufficient.

Each vector $\mathbf{g} \in \partial f(\mathbf{v})$ is called a *subgradient*. We define the domain of ∂f the region where the subdifferential is non-empty:

$$\mathrm{dom}(\partial f) \triangleq \{\mathbf{v} \in \mathscr{V} : \partial f(\mathbf{v}) \neq \emptyset\}.$$

In particular, if f is differentiable, then its gradient is the unique subgradient, *i.e.*, $\partial f(\mathbf{v}) = \{\nabla f(\mathbf{v})\}$ [4, Proposition 2.40]. It is important to notice that subgradients provide an elegant way to characterize the minimizers of a convex function, that is $\mathbf{v}^\star \in \arg\min_{\mathbf{v}\in\mathscr{V}} f(\mathbf{v})$ iff $0 \in \partial f(\mathbf{v}^\star)$, this is known as the *Fermat's rule* [4, Section 2.2.1].

Theorem B.1.5. *([4, Proposition 2.33]) If f is (weakly) closed proper convex, then the following relations are equivalent:*

- $\mathbf{r} \in \partial f^*(\mathbf{v})$
- $\mathbf{v} \in \partial f(\mathbf{r})$
- $f(\mathbf{r}) + f^*(\mathbf{v}) = \langle \mathbf{v}, \mathbf{r} \rangle$

Loosely speaking, ∂f and ∂f^* are said to be "inverses" of each other.

Strong smoothness and strong convexity. A function f is said to be *α-strongly convex* (on its domain) for some $\alpha > 0$ if, for all $\mathbf{v} \in \mathscr{V}$, $\mathbf{v}_0 \in \mathrm{dom}(\partial f)$ and $\mathbf{g}_0 \in \partial f(\mathbf{v}_0)$,

$$f(\mathbf{v}) \geq f(\mathbf{v}_0) + \langle \mathbf{g}_0, \mathbf{v} - \mathbf{v}_0 \rangle + \frac{\alpha}{2} \|\mathbf{v} - \mathbf{v}_0\|_{\mathscr{V}}^2 . \tag{B.2}$$

Here, we note that $f(\mathbf{v}_0)$ is finite since $\mathbf{v}_0 \in \mathrm{dom}(\partial f) \subset \mathrm{dom}(f)$ but $f(\mathbf{v})$ can equal to $+\infty$ if $\mathbf{v} \notin \mathrm{dom}(f)$.

A function f is called *β-strongly smooth* (on the entire space) for some $\beta > 0$ if $\mathrm{dom}(f) = \mathscr{V}$, f is Fréchet differentiable on $\mathscr{V}$ and verifies the following inequality, for all $\mathbf{v}, \mathbf{v}_0 \in \mathscr{V}$,

$$f(\mathbf{v}) \leq f(\mathbf{v}_0) + \langle \nabla f(\mathbf{v}_0), \mathbf{v} - \mathbf{v}_0 \rangle + \frac{\beta}{2} \|\mathbf{v} - \mathbf{v}_0\|_{\mathscr{V}}^2 .$$

Note that β-strong smoothness is also known as *β-smoothness*, see *e.g.*, [61].

For a comprehensive equivalent definitions of strong convexity and smoothness, please refer to, *e.g.*, [68, Section 6.1], [6, Chapter 5] or [100, Section 3.5].

It is important to notice the following equivalent definition of strong smoothness using gradient.

Theorem B.1.6 ([68, Corollary 6.9]). *Let $f\colon \mathscr{V} \to \mathbb{R} \cup \{\pm\infty\}$ be a closed proper convex function. It is β-strongly smooth iff it is differentiable with gradient ∇f being β-Lipschitz continuous on the entire space $\mathscr{V}$.*

It is well known that there is a nice duality between the strong convexity and smoothness [6, Theorem 5.26], which is stated as follows.

Theorem B.1.7 (Duality between strong convexity and strong smoothness). *f is β-strongly smooth w.r.t. $\|\cdot\|_{\mathscr{V}}$ on $\mathscr{V}$ iff f^* is β^{-1}-strongly convex w.r.t. $\|\cdot\|_{\mathscr{V}^*}$ on $\operatorname{dom}(f^*)$.*

Remark B.1.8. *Note that the proof of Theorem B.1.7 can be found in [100, Proposition 3.5.3], in which the author consider the duality of a more general concept called uniform convexity and uniform smoothness in the general vector spaces. However, in the context of finite-dimensional setups e.g., in many machine learning problems, the result is well-known and has a simpler proof, as shown in [61, Theorem 6].*

Remark B.1.9. *In finite-dimensional spaces, the strong smoothness and convexity can be characterized easily using the eigenvalues of Hessian matrix of twice differentiable convex functions [6, Theorem 5.12]. Let $\mathscr{V} = \mathbb{R}^m$, let $\nabla^2 f$ be the Hessian of f. If all the eigenvalues of $\nabla^2 f$ are all lower bounded by some $\alpha > 0$, then f is α-strongly convex on its domain. Similarly, if all eigenvalues $\nabla^2 f$ are upper bounded by some $\beta \geq 0$ on $\mathbb{R}^m$, then f is β-strongly smooth on the whole space $\mathbb{R}^m$ [68, Corollary 6.4].*

Fenchel and Bregman divergence. Let f be a closed proper convex function. The *Fenchel divergence* $\operatorname{Fen}_f\colon \mathscr{V} \times \mathscr{V}^* \to \mathbb{R}_+ \cup \{+\infty\}$ associated with f is defined as follows, for all $\mathbf{u} \in \mathscr{V}, \mathbf{v} \in \mathscr{V}^*$,

$$\operatorname{Fen}_f(\mathbf{u}, \mathbf{v}) \triangleq f(\mathbf{u}) + f^*(\mathbf{v}) - \langle \mathbf{u}, \mathbf{v} \rangle. \tag{B.3}$$

Fenchel divergence is always non-negative[6] by definition of conjugate and equals to zero iff $\mathbf{v} \in \partial f(\mathbf{u})$, see (by Theorem B.1.5). Note that $\operatorname{Fen}_f(\mathbf{u}, \mathbf{v}) < +\infty$ iff $(\mathbf{u}, \mathbf{v}) \in \operatorname{dom}(f) \times \operatorname{dom}(f^*)$.

For a convex function f, $\mathbf{u}_0 \in \operatorname{dom}(\partial f)$ and $\mathbf{g}_0 \in \partial f(\mathbf{u}_0)$, one defines the *Bregman divergence* at $\mathbf{u}_0$ as a function $\operatorname{Breg}_{f,\mathbf{g}_0}(\cdot, \mathbf{u}_0)\colon \mathscr{V} \to \mathbb{R}_+ \cup \{+\infty\}$ such that

$$\operatorname{Breg}_{f,\mathbf{g}_0}(\mathbf{u}, \mathbf{u}_0) \triangleq f(\mathbf{u}) - f(\mathbf{u}_0) - \langle \mathbf{g}_{\mathbf{u}_0}, \mathbf{u} - \mathbf{u}_0 \rangle, \tag{B.4}$$

6. This is known as the Fenchel-Young inequality.

for $\mathbf{u} \in \mathscr{H}$. By the convexity of f and definition of subgradient, it is clear that the Bregman divergence is non-negative and equal to zero if $\mathbf{u} = \mathbf{u}_0$. If f is differentiable, *i.e.*, $\partial f = \{\nabla f\}$, we simply write Breg_f instead of $\mathrm{Breg}_{f,\nabla f}$.

Note that if f is α-strongly convex, then

$$\mathrm{Breg}_{f,\mathbf{g}_0}(\mathbf{u}, \mathbf{u}_0) \geq \frac{\alpha}{2} \|\mathbf{u} - \mathbf{u}_0\|_{\mathscr{H}}^2 ,$$

by the definition of strong convexity (B.2).

We demonstrate in the following an important relationship between Fenchel and Bregman divergences.

Proposition B.1.10 (Relationship between Fenchel and Bregman divergence)**.** *Let f is closed proper convex function. For $\mathbf{u}, \mathbf{v} \in \mathscr{H}$, we have*

$$\mathrm{Fen}_f(\mathbf{u}, \mathbf{v}) = \mathrm{Breg}_{f,\mathbf{v}}(\mathbf{u}, \mathbf{r}), \quad \forall \mathbf{r} \in \partial f^*(\mathbf{v}). \tag{B.5}$$

Proof. Since f is closed proper convex, one can apply Theorem B.1.5 to derive

$$\mathbf{r} \in \partial f^*(\mathbf{v}) \iff f(\mathbf{r}) + f^*(\mathbf{v}) = \langle \mathbf{r}, \mathbf{v} \rangle.$$

Therefore,

$$\begin{aligned}
\mathrm{Fen}_f(\mathbf{u}, \mathbf{v}) &= f(\mathbf{u}) + f^*(\mathbf{v}) - \langle \mathbf{u}, \mathbf{v} \rangle \\
&= f(\mathbf{u}) + (\langle \mathbf{r}, \mathbf{v} \rangle - f(\mathbf{r})) - \langle \mathbf{u}, \mathbf{v} \rangle \\
&= f(\mathbf{u}) - f(\mathbf{r}) - \langle \mathbf{v}, \mathbf{u} - \mathbf{r} \rangle \\
&= \mathrm{Breg}_{f,\mathbf{v}}(\mathbf{u}, \mathbf{r}).
\end{aligned}$$

□

Gauge function. Gauge is a generalized concept of norm. Its definition is provided below.

Definition B.1.11 (Gauge function [51])**.** *A function $\kappa : \mathscr{V} \to \mathbb{R} \cup \{+\infty\}$ is said to be gauge function if it satisfies the following properties*

1. *non-negative, $\kappa(\mathbf{z}) \geq 0$, for all $\mathbf{z} \in \mathscr{V}$,*
2. *vanishing at origin, i.e., $\kappa(\mathbf{0}_{\mathscr{V}}) = 0$,*

3. *positively homogeneous, i.e.,* $\kappa(t\mathbf{z}) = t\kappa(\mathbf{z})$, *for all* $t \geq 0$ *and* $\mathbf{z} \in \mathscr{V}$,

4. *subadditive, i.e.,* $\kappa(\mathbf{z}+\mathbf{x}) \leq \kappa(\mathbf{z}) + \kappa(\mathbf{x})$, *for all* $\mathbf{z}, \mathbf{x} \in \mathscr{V}$.

From this definition, it is clear that:

Proposition B.1.12. *If* κ *is a gauge function, then it is proper and convex.*

Example B.1.13 (Norms are gauge functions)**.** *Let* $\|\cdot\|_{\mathscr{V}}$ *be a norm in* $\mathscr{V}$*, then it is a gauge function. Recall that* $\|\cdot\|_{\mathscr{V}}$ *is a norm if it satisfies the following properties for all* $\mathbf{z} \in \mathscr{V}$*: 1) subadditive, 2) absolutely homogenous i.e.,* $\|t\mathbf{z}\|_{\mathscr{V}} = |t| \, \|\mathbf{z}\|_{\mathscr{V}}$ *for all* $t \in \mathbb{R}$*, and 3)* $\|\mathbf{z}\|_{\mathscr{V}} = 0$ *iff* $\mathbf{z} = \mathbf{0}_{\mathscr{V}}$*. Note that the properties 1) and 2) imply that* $\|\mathbf{z}\|_{\mathscr{V}} \geq 0$ *and* $\|\mathbf{0}_{\mathscr{V}}\|_{\mathscr{V}} = 0$.

Example B.1.14 (Seminorms are gauge functions)**.** *Let* $|\cdot|_{\mathscr{V}}$ *be a seminorm in* $\mathscr{V}$*, then it is a gauge function. Recall that* $|\cdot|_{\mathscr{V}}$ *is a seminorm if it satisfies the following properties for all* $\mathbf{z} \in \mathscr{V}$*: 1) subadditive, 2) absolutely homogenous. Note that the properties 1) and 2) imply that* $|\mathbf{z}|_{\mathscr{V}} \geq 0$ *and* $|\mathbf{0}_{\mathscr{V}}|_{\mathscr{V}} = 0$*. Note that if* $|\cdot|_{\mathscr{V}}$ *additionally satisfies the point-separating property, i.e.,* $|\mathbf{z}|_{\mathscr{V}} = 0 \Rightarrow \mathbf{z} = \mathbf{0}_{\mathscr{V}}$ *then* $|\cdot|_{\mathscr{V}}$ *is a norm.*

Note that every norm is a seminorm, but the converse is not true. To illustrate, consider $\mathbf{z} \in \mathscr{V} = \mathbb{R}^2$ *and define* $|\mathbf{z}|_{\mathscr{V}} = |\mathbf{z}(1)|$*. In this case,* $|\cdot|_{\mathscr{V}}$ *is a seminorm, but not a norm.*

Example B.1.15 (Indicator function over a cone is a gauge functions)**.** *Let* C *be a pointed convex cone, i.e., it is a convex set and satisfies the property that:* $t\mathbf{c} \in C$ *for all* $t \geq 0$ *and* $\mathbf{c} \in C$*. In this definition, we note that* $\mathbf{0}_{\mathscr{V}} \in C$*. Then the indicator function over* C *is a gauge function.*

Example B.1.16 (Combination of gauge functions is a gauge function)**.** *It is clear that combination of gauge functions is again a gauge function. For example, let us consider* $\mathscr{V} = \mathbb{R}^n$*. Then the norm with non-negative constraint* $\|\cdot\|_2 + \iota_{\mathbb{R}^n_+}(\cdot)$ *is a gauge function since it is the sum of two gauge functions with convex cone* $\mathbb{R}^n_+$.

We now recall the definition of the polar of gauge function.

Definition B.1.17 (Polar of gauge function)**.** *The polar of gauge function* $\kappa : \mathscr{V} \to \mathbb{R} \cup \{+\infty\}$*, say* $\kappa^\circ : \mathscr{V}^* \to \mathbb{R} \cup \{+\infty\}$*, is defined as*

$$\kappa^\circ(\mathbf{z}') \triangleq \sup\{\langle \mathbf{z}', \mathbf{z} \rangle : \kappa(\mathbf{z}) \leq 1, \mathbf{z} \in \mathscr{V}\},$$

for any $\mathbf{z}' \in \mathscr{V}^*$.

From the definition of polar function, we obtain the following result.

Proposition B.1.18 (Polar inequality)**.** *For* $\mathbf{z} \in \mathscr{V}$ *and* $\mathbf{z}' \in \mathscr{V}^*$*, we have*

$$\langle \mathbf{z}', \mathbf{z} \rangle \leq \kappa^\circ(\mathbf{z}')\kappa(\mathbf{z}).$$

B.2 Fenchel-Rockafellar duality

In this section, we first revisit the standard hypotheses employed in establishing the so-called" Fenchel-Rockafellar strong duality". Subsequently, we introduce two specific results with easy-to-verify conditions to establish this strong duality.

Let $\mathscr{H}$ be a Hilbert space and $\mathscr{C}$ be a possibly non-reflexive Banach space. Recall that $\tau_{\mathscr{C}}$ and $\omega_{\mathscr{C}}$ represent the strong and weak topologies on $\mathscr{C}$, while $\tau_{\mathscr{C}^*}$ and $\omega_{\mathscr{C}^*}$ denote the strong and weak* topologies on $\mathscr{C}^*$. Regarding $\mathscr{H}$, we denote by $\tau_{\mathscr{H}}$ and $\omega_{\mathscr{H}}$ the strong and the weak topology on $\mathscr{H}$, respectively. Note that the weak and weak* topology on $\mathscr{H}$ coincide.

Let $f : \mathscr{H} \to \mathbb{R} \cup \{+\infty\}$ and $k : \mathscr{C} \to \mathbb{R} \cup \{+\infty\}$ be convex functions and $\mathbf{K} : \mathscr{H} \to \mathscr{C}$ be a linear operator. From the definition of conjugate function, it is clear that

$$\underbrace{h(\mathbf{u}) + h^*(-\mathbf{K}^*\mathbf{x})}_{\geq \langle -\mathbf{K}\mathbf{u}, \mathbf{x} \rangle} + \underbrace{k(\mathbf{K}\mathbf{u}) + k^*(\mathbf{x})}_{\geq \langle \mathbf{K}\mathbf{u}, \mathbf{x} \rangle} \geq 0,$$

for any $\mathbf{u} \in \mathscr{H}$ and $\mathbf{x} \in \mathscr{C}^*$. In other words, we obtain the so-called *Fenchel-Rockafellar duality*:

$$\inf_{\mathbf{u} \in \mathscr{H}} \quad h(\mathbf{u}) + k(\mathbf{K}\mathbf{u}) \geq \sup_{\mathbf{x} \in \mathscr{C}^*} \quad -h^*(-\mathbf{K}^*\mathbf{x}) - k^*(\mathbf{x}). \tag{B.6}$$

Here, (B.6) is known as the *weak duality*. It is called *strong duality* if the LHS and RHS are equal.

The following theorem, which is known as the *Fenchel-Rockafellar strong duality*, provides the sufficient conditions so that the strong duality holds.

Theorem B.2.1 (Fenchel-Rockafellar strong duality [77, Theorem 3.51])**.** *If* h, k *and* $\mathbf{K}$ *verify the following hypotheses:*

(D1) $h \colon (\mathscr{H}, \tau_{\mathscr{H}}) \to \mathbb{R} \cup \{+\infty\}$ *is closed proper convex*

(D2) $k \colon (\mathscr{C}, \tau_{\mathscr{C}}) \to \mathbb{R} \cup \{+\infty\}$ *is closed proper convex*

(D3) $\mathbf{K} \colon (\mathscr{H}, \tau_{\mathscr{H}}) \to (\mathscr{C}, \tau_{\mathscr{C}})$ *is linear and continuous*

(D4) there exists $\mathbf{u}_0 \in \mathscr{H}$ *such that* h *is finite at* $\mathbf{u}_0$ *and* k *is* $\tau_{\mathscr{C}}$*-continuous at* $\mathbf{K}\mathbf{u}_0$*, then the following strong duality holds,*

$$\inf_{\mathbf{u}\in\mathscr{H}} \quad h(\mathbf{u}) + k(\mathbf{K}\mathbf{u}) = \max_{\mathbf{x}\in\mathscr{C}^*} \quad -h^*(-\mathbf{K}^*\mathbf{x}) - k^*(\mathbf{x}). \tag{B.7}$$

Here the RHS of (B.7) *admits at least a maximizer denoted by* $\mathbf{x}^\star$*. Furthermore, if there exists a minimizer, say* $\mathbf{u}^\star$*, for the LHS of* (B.7)*, then* $(\mathbf{x}^\star, \mathbf{u}^\star)$ *satisfies the following optimality conditions:*

$$-\mathbf{K}^*\mathbf{x}^\star \in \partial h(\mathbf{u}^\star), \tag{B.8a}$$

$$\mathbf{x}^\star \in \partial k(\mathbf{K}\mathbf{u}^\star). \tag{B.8b}$$

Conversely, any $(\mathbf{x}^\star, \mathbf{u}^\star)$ *satisfying* (B.8a)-(B.8b) *is an optimal pair w.r.t.* (B.7)*.*

It is essential to note that the standard strong duality presented in Theorem B.2.1 is *non-symmetric*. Firstly, a solution for the LHS of (B.7) is guaranteed, but such assurance does not hold for the RHS. Secondly, while the hypotheses (D1), (D2), (D3), and the optimality conditions (B.8a) and (B.8b) associated with h, k, and $\mathbf{K}$ can be readily translated to h^*, k^*, and $\mathbf{K}^*$, hypothesis (D4) cannot be similarly transferred.

In Remark B.2.2 and Remark B.2.3, we elaborate on how the optimality conditions and hypotheses (D1), (D2), (D3) can be equivalently formulated in terms of h^*, k^*, and $\mathbf{K}^*$. Subsequently, in Remark B.2.4, we present equivalently sufficient conditions that the LHS in (B.7) achieves its minimum value.

We then conclude this section by specializing the Fenchel-Rockafellar strong duality to specific problems where the hypotheses (D1), (D2), (D3), (D4) can be substituted with conditions that are easier to verify and the LHS of (B.7) admits the minimum value.

Remark B.2.2 (Equivalence of optimality conditions (B.8a)-(B.8b))**.** *By (D1), (D2) and Theorem B.1.5, one can notice that the optimality condition* (B.8a) *and* (B.8a) *can be equivalently rewritten in terms of* h^* *and* k^* *as follows:*

$$\mathbf{u}^\star \in \partial h^*(-\mathbf{K}^*\mathbf{x}^\star), \tag{B.9a}$$

$$\mathbf{K}\mathbf{u}^\star \in \partial k^*(\mathbf{x}^\star). \tag{B.9b}$$

Remark B.2.3 (Equivalence of hypotheses (D1), (D2), (D3))**.** *Notice that the conditions imposed on* h*,* k*, and* $\mathbf{K}$ *as in (D1),(D2) and(D3) can be equivalently transformed into*

conditions of the conjugate functions h^*, k^*, and the adjoint operator $\mathbf{K}^*$. However, to achieve this, the topological properties w.r.t. strong topologies in (D1),(D2), and(D3) need to be replaced by the corresponding topological properties in the weak (and weak) topologies. Specifically, by Theorem B.1.2, the hypotheses (D1) and (D2) are equivalent to the following (D5) and (D6), respectively.*

(D5) $h^* \colon \mathscr{H} \to \mathbb{R} \cup \{+\infty\}$ *is closed proper convex*

(D6) $k^* \colon \mathscr{C}^* \to \mathbb{R} \cup \{+\infty\}$ *is weakly* closed proper convex*

and by [69, Theorem 8.10.5], (D3) is equivalent to (D7):

(D7) $\mathbf{K}^* \colon \mathscr{C}^* \to \mathscr{H}$ *is linear and weak*-to-weak continuous*

Remark B.2.4. *Assume that, in addition to the hypotheses (D1), (D2), (D3) (D4), if one of the following (equivalent) hypotheses holds true:*

(D8) $h \colon \mathscr{H} \to \mathbb{R} \cup \{+\infty\}$ *is strongly convex,*

(D9) $h^* \colon \mathscr{H} \to \mathbb{R} \cup \{+\infty\}$ *is strongly smooth,*

(D10) $h^* \colon \mathscr{H} \to \mathbb{R} \cup \{+\infty\}$ *is gradient Lipschitz on $\mathscr{H}$,*

then the LHS of (B.7) is strongly convex, thus, admits unique optimal solution denoted by $\mathbf{u}^\star$.

In the following, let $\mathscr{C}$ be a (possibly non-reflexive) Banach space and $\mathscr{M}$ be its topological dual space. Let $\mathscr{H}$ be a Hilbert space. The following result provides easy-to-verify conditions that establishes the strong duality for norm penalized problems over the space $\mathscr{M}$.

Proposition B.2.5. *Let us consider*

- $f : \mathscr{H} \to \mathbb{R} \cup \{+\infty\}$ *is convex, lower bounded and gradient Lipschitz on the whole space $\mathscr{H}$,*
- $\|\cdot\|_{\mathscr{M}}$ *is a norm in $\mathscr{M}$,*
- $\mathbf{A} : \mathscr{M} \to \mathscr{H}$ *is linear and weak*-to-weak continuous,*
- $\lambda > 0$.

Then the following Fenchel-Rockafellar strong duality holds

$$\min_{\mathbf{x} \in \mathscr{M}} \quad f(\mathbf{A}\mathbf{x}) + \lambda \|\mathbf{x}\|_{\mathscr{M}} = \max_{\mathbf{u} \in U_{\lambda \|\cdot\|_{\mathscr{M}}}} \quad -f^*(-\mathbf{u}) \tag{B.10}$$

where and $U_{\lambda\|\cdot\|_{\mathscr{M}}} = \{\mathbf{u} \in \mathscr{H} : \|\mathbf{A}^*\mathbf{u}\|_{\mathscr{C}} \leq \lambda\}$. *Furthermore, the RHS of* (B.10) *admits a unique optimal solution. The optimal pair verifies the following optimality conditions:*

$$\mathbf{u}^\star = -\nabla f(\mathbf{A}\mathbf{x}^\star) \tag{B.11}$$

$$\mathbf{A}^*\mathbf{u}^\star \in (\partial\lambda \|\cdot\|_{\mathscr{M}})(\mathbf{x}^\star) \tag{B.12}$$

where

$$(\partial\lambda \|\cdot\|_{\mathscr{M}})(\mathbf{x}) = \Big(\mathbf{z} \in \mathscr{C} : \|\mathbf{z}\|_{\mathscr{C}} \leq \lambda \text{ and } \langle \mathbf{x}, \mathbf{z}\rangle_{\mathscr{M},\mathscr{C}} = \lambda \|\mathbf{x}\|_{\mathscr{M}}\Big),$$

for any $\mathbf{x} \in \mathscr{M}$.

Proof. By swapping min and max, one can notice that (B.10) can be rewritten as follows:

$$\min_{\mathbf{u}\in\mathscr{H}} \quad f^*(-\mathbf{u}) + \iota_K(\mathbf{A}^*\mathbf{u}) = \max_{\mathbf{x}\in\mathscr{M}} \quad -f(\mathbf{A}\mathbf{x}) - \lambda \|\mathbf{x}\|_{\mathscr{M}}\,, \tag{B.13}$$

where $K = \{\mathbf{z} \in \mathscr{C} : \|\mathbf{z}\|_{\mathscr{C}} \leq \lambda\}$. By choosing $h(\cdot) = f^*(-\cdot)$, $g(\cdot) = \iota_K(\cdot)$ and $\mathbf{K} = \mathbf{A}^*$, then one can verify that $h^*(\cdot) = f(-\cdot)$, $g^*(\cdot) = \lambda \|\cdot\|_{\mathscr{M}}$ and $\mathbf{K}^* = \mathbf{A}$. In this case, (B.13) can be rewritten in the form of (B.7) of Theorem B.2.1 but with "inf" is now replaced by "min". Therefore, to obtain the proof for (B.13), one can combine Theorem B.2.1 and Remark B.2.4. The remaining of this proof is dedicated to show that the choice of h, k and $\mathbf{K}$ satisfies (D1), (D2), (D3), (D4) (in Theorem B.2.1) and (D10) (in Remark B.2.4).

Proof of (D1). Note that f is closed and proper since it is differentiable. Thus, $h^*(\cdot) = f(-\cdot)$ is closed proper convex. Thus, we deduce that h is also closed proper convex.

Proof of (D2). It is known that dual norm is weakly* closed [2, Proposition 2.4.12 (ii)(c)]. Therefore, $g^* = \lambda \|\cdot\|_{\mathscr{M}}$ is weakly* closed proper convex and, thus, g is closed proper convex.

Proof of (D3). Since $\mathbf{K}^* = \mathbf{A}$ is weak*-to-weak* continuous, $\mathbf{K}$ is therefore weak-to-weak continuous [69, Theorem 8.10.5]. Hence, $\mathbf{K}$ is continuous [69, Corollary 8.11.4].

Proof of (D4). To prove (D4), we choose $\mathbf{u}_0 = \mathbf{0}_{\mathscr{H}}$. We first observe that $h(\mathbf{0}_{\mathscr{H}}) = f^*(\mathbf{0}_{\mathscr{H}}) = \sup_{\mathbf{v}\in\mathscr{H}} f(\mathbf{v}) < +\infty$ since f is lower bounded. Second, we observe that $k = \iota_K$ is continuous on its interior domain, which is the interior K, and that $\mathbf{K}\mathbf{u}_0 = \mathbf{0}_{\mathscr{C}}$ belongs the interior of of the unit ball K. Thus, (D4) holds true.

Proof of (D10). Finally, $h^*(\cdot) = f(-\cdot)$ is gradient Lipschitz.

Finally, we remark that the optimality condition (B.11) follows from (B.8a) and the fact that f is differentiable and the optimality condition (B.12) holds by applying the equivalence of (B.12) and (B.9b).

This completes the proof. □

In finite-dimensional setting, we have the a strong duality result under weaker conditions of functions.

Proposition B.2.6. *Let $f : \mathbb{R}^m \to \mathbb{R} \cup \{+\infty\}$ be a convex and gradient Lipschitz on $\mathbb{R}^m$, $g : \mathbb{R}^n \to \mathbb{R} \cup \{+\infty\}$ is closed proper convex and $\mathbf{A} \in \mathbb{R}^{m\times n}$. Then the following Fenchel-Rockafellar strong duality holds*

$$\min_{\mathbf{x}\in\mathbb{R}^n} \quad f(\mathbf{A}\mathbf{x}) + g(\mathbf{x}) = \max_{\mathbf{u}\in\mathbb{R}^m} \quad -f^*(-\mathbf{u}) - g^*(\mathbf{A}^{\mathrm{T}}\mathbf{u}) \tag{B.14}$$

In particular, the maximizer $\mathbf{u}^\star$ of the RHS of (B.14) is unique.

Proof. Let $\widetilde{f}(\cdot) = f(\mathbf{A}\cdot)$, we notice that $\widetilde{f}$ is closed and proper since f is differentiable. Therefore, by applying [80, Theorem 3.1], we can prove (B.14) if

$$\operatorname{relint}\operatorname{dom}(\widetilde{f}) \cap \operatorname{relint}\operatorname{dom}(g) \neq \emptyset. \tag{B.15}$$

where "relint" denotes the relative interior of a set. First, we observe that $\operatorname{dom}(\widetilde{f}) = \mathbb{R}^m$ since f is differentiable on $\mathbb{R}^m$, thus, $\operatorname{relint}\operatorname{dom}(\widetilde{f}) = \mathbb{R}^m$. Second, $\operatorname{dom}(g)$ is a non-empty convex set since g is proper convex function. Notice that the relative interior of non-empty convex set is non-empty [6, Theorem 3.17]. Thus, $\operatorname{relint}\operatorname{dom}(g) \neq \emptyset$. Hence, the intersection in (B.15) is non-empty. The uniqueness of $\mathbf{u}^\star$ follows directly from the strong convexity of f^* (which is equivalent to the gradient Lipschitz of f on $\mathbb{R}^m$). □

BIBLIOGRAPHY

[1] Alper Atamturk and Andrés Gómez, « Safe screening rules for l0-regression from perspective relaxations », *in*: *International conference on machine learning*, PMLR, 2020, pp. 421–430.

[2] Hedy Attouch, Giuseppe Buttazzo, and Gérard Michaille, *Variational analysis in sobolev and bv spaces*, 2nd ed., Philadelphia, PA: Society for Industrial and Applied Mathematics, 2014, DOI: 10.1137/1.9781611973488.

[3] Runxue Bao, Bin Gu, and Heng Huang, « Fast oscar and owl regression via safe screening rules », *in*: *International conference on machine learning*, PMLR, 2020, pp. 653–663.

[4] Viorel Barbu and Teodor Precupanu, *Convexity and optimization in banach spaces*, Springer Science & Business Media, 2012.

[5] Heinz H. Bauschke and Patrick L. Combettes, *Convex analysis and monotone operator theory in hilbert spaces*, Springer International Publishing, 2017, DOI: 10.1007/978-3-319-48311-5.

[6] Amir Beck, *First-order methods in optimization*, Philadelphia, PA: Society for Industrial and Applied Mathematics, 2017, DOI: 10.1137/1.9781611974997.

[7] Amir Beck and Marc Teboulle, « A fast iterative shrinkage-thresholding algorithm for linear inverse problems », *in*: *Siam journal on imaging sciences* 2.*1* (2009), pp. 183–202.

[8] Pierre-Jean Bénard, Yann Traonmilin, and Jean-François Aujol, « Fast off-the-grid sparse recovery with over-parametrized projected gradient descent », *in*: *2022 30th european signal processing conference (eusipco)*, IEEE, 2022, pp. 2206–2210.

[9] Howard D Bondell and Brian J Reich, « Simultaneous regression shrinkage, variable selection, and supervised clustering of predictors with oscar », *in*: *Biometrics* 64.*1* (2008), pp. 115–123.

[10] Antoine Bonnefoy, Valentin Emiya, Liva Ralaivola, and Rémi Gribonval, « A dynamic screening principle for the lasso », *in*: *2014 22nd european signal processing conference (eusipco)*, IEEE, 2014, pp. 6–10.

[11] Nicholas Boyd, Geoffrey Schiebinger, and Benjamin Recht, « The alternating descent conditional gradient method for sparse inverse problems », *in*: *Siam journal on optimization* 27.*2* (2017), pp. 616–639.

[12] Claire Boyer, Antonin Chambolle, Yohann De Castro, Vincent Duval, Frédéric De Gournay, and Pierre Weiss, « On representer theorems and convex regularization », *in*: *Siam journal on optimization* 29.*2* (2019), pp. 1260–1281.

[13] Kristian Bredies and Hanna Katriina Pikkarainen, « Inverse problems in spaces of measures », *in*: *Esaim: control, optimisation and calculus of variations* 19.*1* (2013), pp. 190–218.

[14] Haim Brezis and Haim Brézis, *Functional analysis, sobolev spaces and partial differential equations*, vol. 2, 3, Springer, 2011.

[15] Emmanuel J Candès and Carlos Fernandez-Granda, « Towards a mathematical theory of super-resolution », *in*: *Communications on pure and applied mathematics* 67.*6* (2014), pp. 906–956.

[16] Antonin Chambolle and Thomas Pock, « A first-order primal-dual algorithm for convex problems with applications to imaging », *in*: *Journal of mathematical imaging and vision* 40 (2011), pp. 120–145.

[17] Frédéric Champagnat and Cédric Herzet, « Interpolating and translation-invariant approximations of parametric dictionaries », *in*: *2020 28th european signal processing conference (eusipco)*, IEEE, 2021, pp. 2011–2015.

[18] Huangyue Chen, Lingchen Kong, Pan Shang, and Shanshan Pan, « Safe feature screening rules for the regularized huber regression », *in*: *Applied mathematics and computation* 386 (2020), p. 125500.

[19] Shaobing Chen and David Donoho, « Basis pursuit », *in*: *Proceedings of 1994 28th asilomar conference on signals, systems and computers*, vol. 1, IEEE, 1994, pp. 41–44.

[20] Lenaic Chizat, « Sparse optimization on measures with over-parameterized gradient descent », *in*: *Mathematical programming* 194.*1-2* (2022), pp. 487–532.

[21] Lenaic Chizat and Francis Bach, « On the global convergence of gradient descent for over-parameterized models using optimal transport », *in*: *Advances in neural information processing systems* 31 (2018).

[22] Donald L Cohn, *Measure theory*, vol. 1, Springer, 2013.

[23] Liang Dai and Kristiaan Pelckmans, « An ellipsoid based, two-stage screening test for BPDN », *in*: 2012, pp. 654–658.

[24] Cassio Dantas, Emmanuel Soubies, and Cédric Févotte, « Accelerating non-negative and bounded-variable linear regression algorithms with safe screening », *in*: *Arxiv preprint arxiv:2202.07258* (2022).

[25] Cassio F Dantas, Emmanuel Soubies, and Cédric Févotte, « Expanding boundaries of gap safe screening », *in*: *The journal of machine learning research* 22.*1* (2021), pp. 10665–10721.

[26] Cassio F Dantas, Emmanuel Soubies, and Cédric Févotte, « Safe screening for sparse regression with the kullback-leibler divergence », *in*: *Icassp 2021-2021 ieee international conference on acoustics, speech and signal processing (icassp)*, IEEE, 2021, pp. 5544–5548.

[27] Cassio F Dantas, Emmanuel Soubies, and Cédric Févotte, « Sphere refinement in gap safe screening », *in*: *Ieee signal processing letters* (2023).

[28] Cassio Fraga Dantas and Rémi Gribonval, « Stable safe screening and structured dictionaries for faster l1 regularization », *in*: *Ieee transactions on signal processing* 67.*14* (2019), pp. 3756–3769.

[29] Quentin Denoyelle, « Theoretical and numerical analysis of super-resolution without grid », PhD thesis, Université Paris sciences et lettres, 2018.

[30] Quentin Denoyelle, Vincent Duval, Gabriel Peyré, and Emmanuel Soubies, « The sliding frank–wolfe algorithm and its application to super-resolution microscopy », *in*: *Inverse problems* 36.*1* (2019), p. 014001.

[31] Nelson Dunford and Jacob T Schwartz, *Linear operators, part 1: general theory*, vol. 10, John Wiley & Sons, 1988.

[32] Vincent Duval and Gabriel Peyré, « Exact support recovery for sparse spikes deconvolution », *in*: *Foundations of computational mathematics* 15.*5* (2015), pp. 1315–1355.

[33] Vincent Duval and Gabriel Peyré, « Sparse regularization on thin grids i: the lasso », *in*: *Inverse problems* 33.*5* (2017), p. 055008.

[34] Vincent Duval and Gabriel Peyré, « Sparse spikes super-resolution on thin grids ii: the continuous basis pursuit », *in*: *Inverse problems* 33.*9* (2017), p. 095008.

[35] Chaitanya Ekanadham, Daniel Tranchina, and Eero P Simoncelli, « Recovery of sparse translation-invariant signals with continuous basis pursuit », *in*: *Ieee transactions on signal processing* 59.*10* (2011), pp. 4735–4744.

[36] Clément Elvira, Jérémy E Cohen, Cédric Herzet, and Rémi Gribonval, « Continuous dictionaries meet low-rank tensor approximations », *in*: *Arxiv preprint arxiv:2009.06340* (2020).

[37] Clément Elvira, Rémi Gribonval, Charles Soussen, and Cédric Herzet, « Omp and continuous dictionaries: is k-step recovery possible? », *in*: *Icassp 2019-2019 ieee international conference on acoustics, speech and signal processing (icassp)*, IEEE, 2019, pp. 5546–5550.

[38] Clément Elvira, Rémi Gribonval, Charles Soussen, and Cédric Herzet, « When does omp achieve exact recovery with continuous dictionaries? », *in*: *Applied and computational harmonic analysis* 51 (2021), pp. 374–413.

[39] Clément Elvira and Cédric Herzet, « A response to “fast oscar and owl regression via safe screening rules” by bao et al. », PhD thesis, CentraleSupelec; Inria Rennes–Bretagne Atlantique, 2021.

[40] Clément Elvira and Cédric Herzet, « Safe rules for the identification of zeros in the solutions of the slope problem », *in*: *Siam journal on mathematics of data science* 5.*1* (2023), pp. 147–173, DOI: 10.1137/21M1457631.

[41] Clément Elvira and Cédric Herzet, *Safe rules for the identification of zeros in the solutions of the SLOPE problem*, Oct. 2021.

[42] Clément Elvira and Cédric Herzet, « Safe squeezing for antisparse coding », *in*: 68 (2020), pp. 3252–3265.

[43] Clément Elvira and Cédric Herzet, « Short and squeezed: accelerating the computation of antisparse representations with safe squeezing », *in*: 2020, DOI: 10.1109/ICASSP40776.2020.9053156.

[44] Jianqing Fan and Jinchi Lv, « Sure independence screening », *in*: *Wiley statsref: statistics reference online* (2018).

[45] Olivier Fercoq, Alexandre Gramfort, and Joseph Salmon, « Mind the duality gap: safer rules for the lasso », *in*: *International conference on machine learning*, PMLR, 2015, pp. 333–342.

[46] Axel Flinth, *Exact and soft recovery of structured signals from atomic and total variation norm regularization*, Technische Universitaet Berlin (Germany), 2018.

[47] Axel Flinth, Frédéric De Gournay, and Pierre Weiss, « On the linear convergence rates of exchange and continuous methods for total variation minimization », *in*: *Mathematical programming* 190.*1-2* (2021), pp. 221–257.

[48] Axel Flinth, Frédéric de Gournay, and Pierre Weiss, « Grid is good: adaptive refinement algorithms for off-the-grid total variation minimization », *in*: *Arxiv preprint arxiv:2301.07555* (2023).

[49] Simon Foucart, *Mathematical pictures at a data science exhibition*, Cambridge University Press, 2022.

[50] Simon Foucart and Holger Rauhut, *A mathematical introduction to compressive sensing*, Springer New York, 2013, ISBN: 9780817649487, DOI: 10.1007/978-0-8176-4948-7.

[51] Michael P Friedlander, Ives Macedo, and Ting Kei Pong, « Gauge optimization and duality », *in*: *Siam journal on optimization* 24.*4* (2014), pp. 1999–2022.

[52] Laurent El Ghaoui, Vivian Viallon, and Tarek Rabbani, « Safe feature elimination for the lasso and sparse supervised learning problems », *in*: *Arxiv preprint arxiv:1009.4219* (2010).

[53] Theo Guyard, Cédric Herzet, and Clément Elvira, « Node-screening tests for the l0-penalized least-squares problem », *in*: *Icassp 2022-2022 ieee international conference on acoustics, speech and signal processing (icassp)*, IEEE, 2022, pp. 5448–5452.

[54] Théo Guyard, Cédric Herzet, and Clément Elvira, « Screen & relax: accelerating the resolution of elastic-net by safe identification of the solution support », *in*: *Icassp 2022 - 2022 ieee international conference on acoustics, speech and signal processing (icassp)*, 2022, pp. 5443–5447, DOI: 10.1109/ICASSP43922.2022.9747412.

[55] Théo Guyard, Gilles Monnoyer, Clément Elvira, and Cédric Herzet, « Safe peeling for l0-regularized least-squares with supplementary material », *in*: *Arxiv preprint arxiv:2302.14471* (2023).

[56] Paul R Halmos, *Measure theory*, vol. 18, Springer, 2013.

[57] Cédric Herzet, Clément Dorffer, and Angélique Drémeau, « Gather and conquer: region-based strategies to accelerate safe screening tests », *in*: *Ieee transactions on signal processing* 67.*12* (2019), pp. 3300–3315.

[58] Cédric Herzet and Angélique Drémeau, « Joint screening tests for lasso », *in*: *2018 ieee international conference on acoustics, speech and signal processing (icassp)*, IEEE, 2018, pp. 4084–4088.

[59] Cédric Herzet, Clément Elvira, and Hong-Phuong Dang, « Region-free safe screening tests for l1-penalized convex problems », *in*: *2022 30th european signal processing conference (eusipco)*, IEEE, 2022, pp. 2061–2065.

[60] Martin Jaggi, « Revisiting frank-wolfe: projection-free sparse convex optimization », *in*: *International conference on machine learning*, PMLR, 2013, pp. 427–435.

[61] Sham Kakade, Shai Shalev-Shwartz, Ambuj Tewari, et al., « On the duality of strong convexity and strong smoothness: learning applications and matrix regularization », *in*: 2.*1* (2009), p. 35.

[62] Karin C Knudson, Jacob Yates, Alexander Huk, and Jonathan W Pillow, « Inferring sparse representations of continuous signals with continuous orthogonal matching pursuit », *in*: *Advances in neural information processing systems* 27 (2014).

[63] Bastien Laville, Laure Blanc-Féraud, and Gilles Aubert, « Off-the-grid curve reconstruction through divergence regularization: an extreme point result », *in*: *Siam journal on imaging sciences* 16.*2* (2023), pp. 867–885.

[64] Bastien Laville, Laure Blanc-Féraud, and Gilles Aubert, « Off-the-grid variational sparse spike recovery: methods and algorithms », *in*: *Journal of imaging* 7.*12* (2021), ISSN: 2313-433X, DOI: 10.3390/jimaging7120266, URL: https://www.mdpi.com/2313-433X/7/12/266.

[65] Jingwei Liang and Clarice Poon, « Screening for sparse online learning », *in*: *Arxiv preprint arxiv:2101.06982* (2021).

[66] Jun Liu, Zheng Zhao, Jie Wang, and Jieping Ye, « Safe screening with variational inequalities and its application to lasso », *in*: *International conference on machine learning*, PMLR, 2014, pp. 289–297.

[67] Abed Malti and Cédric Herzet, « Safe screening tests for lasso based on firmly non-expansiveness », *in*: *2016 ieee international conference on acoustics, speech and signal processing (icassp)*, IEEE, 2016, pp. 4732–4736.

[68] Boris S Mordukhovich and Nguyen Mau Nam, *Convex analysis and beyond: volume i: basic theory*, Springer Nature, 2022.

[69] Lawrence Narici and Edward Beckenstein, *Topological vector spaces*, Chapman and Hall/CRC, 2010.

[70] Eugene Ndiaye, « Safe optimization algorithms for variable selection and hyperparameter tuning », PhD thesis, Université Paris-Saclay (ComUE), 2018.

[71] Eugene Ndiaye, Olivier Fercoq, Alexandre Gramfort, and Joseph Salmon, « Gap safe screening rules for sparse-group lasso », *in*: *Advances in neural information processing systems* 29 (2016).

[72] Eugene Ndiaye, Olivier Fercoq, Alexandre Gramfort, and Joseph Salmon, « Gap safe screening rules for sparsity enforcing penalties », *in*: *The journal of machine learning research* 18.*1* (2017), pp. 4671–4703.

[73] Eugene Ndiaye, Olivier Fercoq, and Joseph Salmon, « Screening Rules and its Complexity for Active Set Identification », *in*: *Journal of Convex Analysis* 28.*4* (2021), pp. 1053–1072.

[74] Xianli Pan, Xinying Pang, Hongmei Wang, and Yitian Xu, « A safe screening based framework for support vector regression », *in*: *Neurocomputing* 287 (2018), pp. 163–172.

[75] Xianli Pan and Yitian Xu, « A safe feature elimination rule for l1-regularized logistic regression », *in*: *Ieee transactions on pattern analysis and machine intelligence* 44.*9* (2021), pp. 4544–4554.

[76] Romain Petit, « Reconstruction of piecewise constant images via total variation regularization: exact support recovery and grid-free numerical methods », PhD thesis, Université Paris Dauphine-PSL, 2022.

[77] Juan Peypouquet, *Convex optimization in normed spaces*, Springer International Publishing, 2015, DOI: 10.1007/978-3-319-13710-0.

[78] Clarice Poon and Gabriel Peyré, « Smooth over-parameterized solvers for non-smooth structured optimization », *in*: *Mathematical programming* (2023), pp. 1–56.

[79] Shaogang Ren, Shuai Huang, Jieping Ye, and Xiaoning Qian, « Safe feature screening for generalized lasso », *in*: *Ieee transactions on pattern analysis and machine intelligence* 40.*12* (2017), pp. 2992–3006.

[80] R. Tyrrell Rockafellar, *Convex analysis*, Princeton Mathematical Series, Princeton, N. J.: Princeton University Press, 1970.

[81] Guillaume Sagnol and Luc Pronzato, « Fast screening rules for optimal design via quadratic lasso reformulation », *in*: *Journal of machine learning research* 24.*307* (2023), pp. 1–32.

[82] Pan Shang and Lingchen Kong, « L1-norm quantile regression screening rule via the dual circumscribed sphere », *in*: *Ieee transactions on pattern analysis and machine intelligence* 44.*10* (2021), pp. 6254–6263.

[83] Mei Song, Andrea Montanari, and P Nguyen, « A mean field view of the landscape of two-layers neural networks », *in*: *Proceedings of the national academy of sciences* 115.*33* (2018), E7665–E7671.

[84] Yifan Sun and Francis Bach, « Safe screening for the generalized conditional gradient method », *in*: *Arxiv preprint arxiv:2002.09718* (2020).

[85] Robert Tibshirani, « Regression shrinkage and selection via the lasso », *in*: *Journal of the royal statistical society: series b (methodological)* 58.*1* (1996), pp. 267–288.

[86] Robert Tibshirani, Jacob Bien, Jerome Friedman, Trevor Hastie, Noah Simon, Jonathan Taylor, and Ryan J Tibshirani, « Strong rules for discarding predictors in lasso-type problems », *in*: *Journal of the royal statistical society: series b (statistical methodology)* 74.*2* (2012), pp. 245–266.

[87] Thu-Le Tran, Clément Elvira, Hong-Phuong Dang, and Cédric Herzet, « Beyond gap screening for lasso by exploiting new dual cutting half-spaces », *in*: *2022 30th european signal processing conference (eusipco)*, 2022, pp. 2056–2060, DOI: 10.23919/EUSIPCO55093.2022.9909943.

[88] Thu-Le Tran, Clément Elvira, Hong-Phuong Dang, and Cédric Herzet, *Beyond GAP screening for lasso by exploiting new dual cutting half-spaces with supplementary material*, arXiv:2203.00987, 2022, arXiv: 2203.00987 [cs.LG].

[89] Thu-Le Tran, Clément Elvira, Hong-Phuong Dang, and Cédric Herzet, « Une nouvelle méthode d'accélération pour lasso par élimination sûre de variables », *in*: *Cap 2022-conférence sur l'apprentissage automatique*, 2022, pp. 1–6.

[90] Yann Traonmilin, Jean-François Aujol, and Arthur Leclaire, « Projected gradient descent for non-convex sparse spike estimation », *in*: *Ieee signal processing letters* 27 (2020), pp. 1110–1114.

[91] Jie Wang, Wei Fan, and Jieping Ye, « Fused lasso screening rules via the monotonicity of subdifferentials », *in*: *Ieee transactions on pattern analysis and machine intelligence* 37.*9* (2015), pp. 1806–1820.

[92] Jie Wang, Peter Wonka, and Jieping Ye, « Lasso screening rules via dual polytope projection », *in*: *Journal of machine learning research* 16 (2015), pp. 1063–1101.

[93] Jie Wang, Jiayu Zhou, Jun Liu, Peter Wonka, and Jieping Ye, « A safe screening rule for sparse logistic regression », *in*: *Advances in neural information processing systems* 27 (2014).

[94] Albert Wilansky, *Modern methods in topological vector spaces*, Courier Corporation, 2013.

[95] Zhen Xiang, Hao Xu, and Peter J Ramadge, « Learning sparse representations of high dimensional data on large scale dictionaries », *in*: *Advances in neural information processing systems* 24 (2011).

[96] Zhen James Xiang and Peter J Ramadge, « Fast lasso screening tests based on correlations », *in*: *2012 ieee international conference on acoustics, speech and signal processing (icassp)*, IEEE, 2012, pp. 2137–2140.

[97] Zhen James Xiang, Yun Wang, and Peter J Ramadge, « Screening tests for lasso problems », *in*: *Ieee transactions on pattern analysis and machine intelligence* 39.*5* (2016), pp. 1008–1027.

[98] Yitian Xu, Ying Tian, Xianli Pan, and Hongmei Wang, « E-endpp: a safe feature selection rule for speeding up elastic net », *in*: *Applied intelligence* 49 (2019), pp. 592–604.

[99] Hiroaki Yamada and Makoto Yamada, « Dynamic sasvi: strong safe screening for norm-regularized least squares », *in*: *Advances in neural information processing systems* 34 (2021).

[100] Constantin Zalinescu, *Convex analysis in general vector spaces*, World scientific, 2002, DOI: 10.1142/5021.

COLLEGE DOCTORAL BRETAGNE
MATHS, TELECOMS
INFORMATIQUE, SIGNAL
SYSTEMES, ELECTRONIQUE

Université de Rennes

Titre : Quelques contributions dans la conception de “régions sûres” et “tests d’élagages sûrs” en optimisation convexe

Mot clés : Optimisation Convexe, Safe Regions, Safe Screening

Résumé : L’optimisation convexe est fréquente en apprentissage automatique, statistiques, signal et image. La résolution de problèmes d’optimisation en grande dimension reste difficile en raison de contraintes calculatoires et de stockage. La dernière décennie, les méthodes de “safe screening” sont devenues un outil puissant pour réduire la dimension de ces problèmes en se basant sur la connaissance d’une “safe region” contenant la solution optimale duale.

La première contribution de cette thèse est un cadre mathématique pour créer de nouvelles “safe region” tout en démontrant leur supériorité par rapport à l’état de l’art. Notre cadre offre également une manière élégante d’unifier les “safe regions” existantes. Cette contribution établit en particulier une base théorique pour les futures avancées dans l’étude des “safe region”.

La seconde contribution est une extension de la méthodologie de “safe screening” à des problèmes en dimension infinie. Nous montrons notamment que l’intégration de cette méthode dans un algorithme de l’état de l’art permet de réduire significativement sa complexité numérique tout en préservant sa propriété de convergence. Cette contribution met en évidence le potentiel du “safe screening” pour résoudre efficacement les défis calculatoires dans des contextes de dimension infinie.

Title: Some Contributions on Safe Regions and Safe Screening in Convex Optimization

Keywords: Convex Optimization, Safe Regions, Safe Screening

Abstract: Convex optimization is common in machine learning, statistics, signal, and image processing. Solving high-dimensional optimization problems remains challenging due to computational and storage constraints. In the last decade, the “safe screening” methods have become a powerful tool to reduce the dimension of these problems based on the knowledge of a “safe region” containing the dual optimal solution.

The first contribution of this thesis is a mathematical framework for creating new safe regions while demonstrating their superiority over the state-of-the-art. Our framework also provides an elegant way to unify existing safe regions. This contribution establishes a theoretical foundation for future advances in the study of safe regions.

The second contribution is an extension of the safe screening methodology to problems in infinite-dimensions. We show, in particular, that integrating this method into a state-of-the-art algorithm can significantly reduce its numerical complexity while preserving its convergence property. This contribution highlights the potential of safe screening to effectively address computational challenges in infinite-dimensional contexts.